85

CRANFIELD INSTITUTE OF TECHNOLOGY

SCHOOL OF MECHANICAL ENGINEERING

Ph. D. THESIS

Academic Year 1983-84

W.J. BATTY.

HEAT TRANSFER PROPERTIES OF POROUS MATERIALS AND INSULANTS

SUPERVISOR: Dr. P.W. O'CALLAGHAN.

March, 1984.

ACKNOWLEDGEMENTS

The author would like to express his thanks to all those who have contributed to this work. In particular thanks are due to Dr. P.W. O'Callaghan and Professor S.D. Probert for their influence and guidance aswell as the interest they have shown in the progress of the project.

Thanks are extended to the staff of the School of Mechanical Engineering, especially Charlies Chapman and Knight, and Brian Moffit, for their patience and advice.

The Science and Engineering Research Council are ackowledged for their financial support.

CONTENTS

FIGURES

CHAPTER 4

CHAPTER 6

TABLES

CHAPTER 6

INTRODUCTION

Buildings are complex thermally-dynamic structures serving aesthetic as well as utilitarian functions. It is essential that careful planning is undertaken if buildings are to be energy efficient and cheap to run throughout their expected life-spans. Although regulations have recently been introduced requiring the values of thermal transmittances (i.e. U-values) for walls and roofs of industrial and domestic buildings, to be less than specified limits, there is no guarantee that improved design will result.

Also condensation has increasingly become a problem, as natural ventilation has been reduced, because of the introduction of double-glazing and draught proofing.

The use of insulating materials to increase thermal efficiencies through the reduction of heat losses may also create problems in industrial plant and pipework. Metal structures covered with insulants are thereby hidden from view and so any ensuing corrosion, such as the general attack upon a low-alloy steel or stress-corrosion cracking of a stainless steel, may remain undetected until catastrophic failure occurs. It is, therefore, of utmost importance that the potential for and enhancement of corrosion due to the addition of insulants should be carefully considered. The ingress of water or water vapour into the insulant layer and subsequent leaching is the major cause of corrosion, and it is essential that steps are taken to prevent or reduce the likelihood of this occurring while ensuring that metal surfaces are adequately protected.

There is a need to ascertain the heat and mass transfer behaviours of building and insulating materials. Mathematical models require realistic data to simulate effectively conditions found in real structures. Too often in the past manufacturers' data for thermal properties, measured under laboratory conditions, have been used with little attempt to check on their validity or appropriateness to the conditions which are likely to be experienced. As desk-top computers become cheaper and more powerful

these dangers could well increase. The too prevalent trusting attitude that computer predictions are absolutely correct together with a potential lack of understanding of the concepts of heat transfer and moisture mitigation by the users could result in poorer, rather than better, designed buildings.

The thermal-probe technique for the measurement of the thermal conductivities of building structural materials has been assessed. This rapid transient and potentially cheap technique could be suited ideally to measurements in such materials. The theoretical basis for the method has been investigated and the accuracies and repeatabilities of thermal-probe instruments have been determined in measurements with paraffin wax. Determinations made with this technique, for masonry and structural components, were found to agree well with the manufacturer's thermal conductivity data. However, further developments need to be made to improve the usefulness of this technique for measuring the effective conductivities of fibrous insulants.

Also the thermal-probe technique has been assessed for use in moist materials. Initial investigations with wet-day specimens showed that the probe diameter had no significant effect on the indicated values of the apparent thermal conductivity. Tests to measure the apparent thermal conductivities of aerated concrete blocks, at various moisture contents, gave results that compared well with other published data.

Attempts to reduce national energy demands have led to increases in insulation thicknesses in roof spaces in Northern Europe and North America. It has generally been assumed that the apparent thermal conductivity of each material used has been a constant and equal to the value obtained in the testing laboratory. Examination of the temperature profiles through various horizontal thicknesses of loose-fill mineral wool insulants suggests that radiation effects and convection in the upper surface layers exposed to free air result in much larger apparent thermal conductivity values than those generally quoted in the literature, and the magnitudes of these effects also increase with the thickness of the

insulant layer. Heat transfer mechanisms have been examined to explain these phenomena.

Mathematical models of heat transfers through multi-phase materials have been examined. A model is proposed to describe the thermal conductivity of high-porosity cellular insulant which includes heat transfers by conduction through the solid and gaseous phases and by radiation. Predictions were found to agree well with experimental data for air-filled polystyrene foams and to be of the correct order of magnitude for air/fluorocarbon filled polyurethane foams.

CHAPTER 1

ENERGY AND CONDENSATION PROBLEMS IN BUILDINGS

HISTORICAL BACKGROUND

Both industry and the general public have during the last decade been made well aware of likely future energy shortages and the effect these will have on fuel prices. Much propaganda has been propogated through the advertising media in order to improve the thermal behaviour of the industrial and domestic building stock so as to reduce heat losses and improve comfort levels. The Building Regulations for England and Wales have, since June 1st 1979 (1), demanded much improved U-values for buildings other than dwellings and the Second Amendment Regulation (2) increased the required insulation levels and reduced permitted window area for new domestic buildings as from April 1982.

There are many who would argue that such regulations have been too long in coming. However it could also be suggested that the regulations have appeared in advance of adequate research having been completed with respect to the potential problems involved with introducing increased thermal isolation. For example, insufficient thought has been devoted to the advisability of using the U-valve, a steady-state concept, as the appropriate criterion when in practice buildings behave in a dynamic fashion.

MOISTURE PROBLEMS

In the long term, improvements in thermal insulation, the reduction of ventilation rates and isolation of buildings without due thought being given to the possible consequences, could result in very costly damage to their structures because of the consequent increased moisture levels therein. The introduction of double-glazing

and draught-proofing has drastically reduced natural ventilation through buildings. Many domestic buildings no longer have chimneys, and thus the ventilation of many modern dwellings is inadequate. Radon build up, from ancient rocks underground, is leading to increasing concern in modern thermally well insulated structures in South Wales and Cornwall because of the carcinogenic atmospheres in these dwellings. These problems can be overcome with the use of ventilating bricks, wall or window fans in kitchens and bathrooms, and dehumidifiers, but such measures rely on the good sense of the occupier to use them as and when necessary. Too often fans are not used and ventilation bricks are blocked up.

A recent survey carried out by the Building Research Establishment (3) concerning complaints received during a single week about dampness in five local authorities, found that 28% of privately-rented homes are likely to be severely damp, with a further 19% suffering from slight dampness, which compares with 5% of owner-occuped homes and 17% of council homes. When these figures are scaled up nationally, at least 2 million dwellings in England are probably very damp, rising to 2.5 million if Wales, Scotland and Northern Ireland are included. These problems seem to be greatest in homes built from the 1960's onwards.

CHOICE OF HEATING SYSTEM

Lack of proper consideration by architects and builders of the running costs of installed heating systems has aggravated condensation problems. Little is to be gained by berating the occupier for using water-releasing, inexpensive to run, paraffin or bottled-gas heaters

when he cannot afford to run, relatively cheaply installed, electrical underfloor or storage heater systems.

It can be seen from Table 1 that the installation costs, including labour and profits, for electrical heating systems is considerably less (for equal thermal outputs) than can be achieved with solid fuel, oil or gas systems. This comparison was obtained using Spon's Mechanical and Electrical Services Price Book 1979 (4) for the heating of six rooms plus hot-water service utilising a 13 kW boiler for various fuels, 10 kW of space heating plus hot water service for electrical under-floor heating and five 2 kW electrical storage heaters plus hot-water service. The running costs were calculated using price data since 1979, yearly tariff increases being averaged over each year to give an average price per gigajoule. It has been assumed that the annual energy usage for space heating was 50 GJ every year and that the efficiencies of the various forms of heating were - underfloor 100%, storage heaters 75% and boilers 40%.

ENERGY SOURCE	INSTALLATION COST IN 1979 (£)
SOLID FUEL	825
GAS	935
OIL	970
ELECTRICITY (UNDERFLOOR)	639
ELECTRICITY (STORAGE HEATERS)	655

Table 1. Estimated installation costs for various forms of space plus water heating, as estimated from Spon's Mechanical and Electrical Services Price Book 1979, (3).

It can be seen from figure 1 that, although the initial installation cost of electrical underfloor and storage heating is low compared with those using fossil fuels, this advantage is rapidly eroded due to the relatively high unit cost of electricity. The total cost of underfloor heating becomes greater than that for the fossil fuels within two heating seasons for electrical heating at domestic peak rates, and within three heating seasons for storage heaters at off-peak rates at an assumed efficiency of 75%. It has been suggested (5) that electrical storage heaters are only 25% efficient and under these circumstances they become even less competitive. These results are for a period when the percentage price increase per unit of gas have exceeded the corresponding rises in electricity unit prices, and an attempt made by the Electricity Boards to make "off-peak" electricity more competitive by keeping price increases 3% lower than for those for peak electricity.

Venning (5) concluded that the behaviour of buildings, in energy terms, should not be isolated from other "cost-in-use" considerations. It was also stated that re-current energy costs could not be reconciled with initial capital costs to produce precise predictions of a building's cost over its lifetime, but that such an exercise should be taken to facilitate the choice between alternative options. The fact that such exercises were not undertaken was thought to be due to the uncertainties of likely discount rates and the prediction of price inflation for periods in excess of 30 years (i.e. the expected lifetime of the heating system). The movements in the percentage domestic price increases for gas and electricity above the previous years price since 1974 are shown in Fig. 2., and illustrate how difficult it would be to make such predictions.

FIGURE 1

Comparison of total costs of alternative space heating systems.

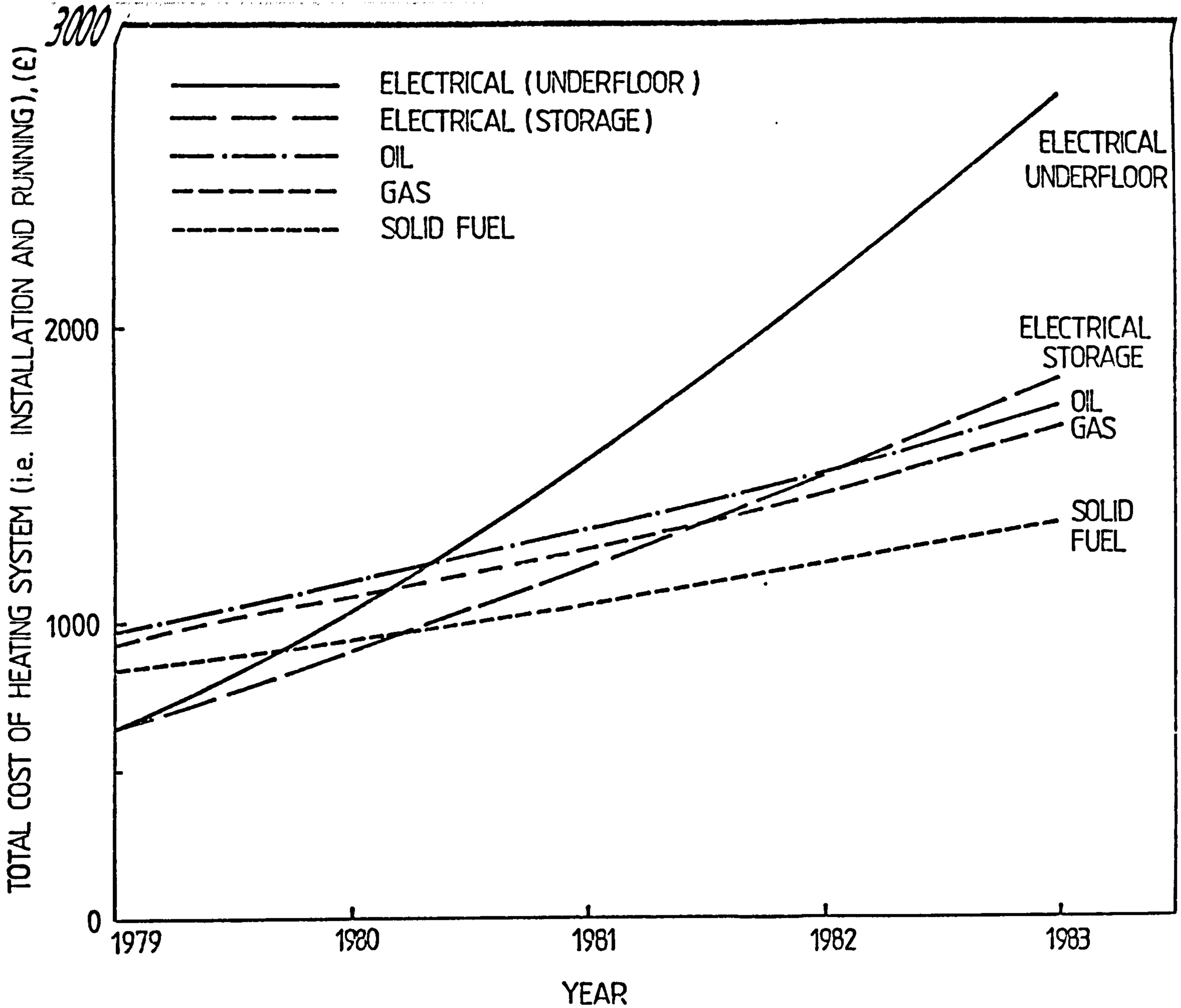
3000
2000
1000
0
TOTAL COST OF HEATING SYSTEM (i.e. INSTALLATION AND RUNNING), (£)
ELECTRICAL (UNDERFLOOR)
ELECTRICAL (STORAGE)
OIL
GAS
SOLID FUEL
ELECTRICAL UNDERFLOOR
ELECTRICAL STORAGE
OIL
GAS
SOLID FUEL
1979
1980
1981
1982
1983
YEAR

Recent statements by the Electricity Council's domestic marketing department (6) claim that space and water heating via electricity is cheaper than that obtained via North Sea gas in dwellings with heat losses up to about 5 kW, whereas gas systems are generally cheaper to run in dwellings with heat losses above 6 kW. The statements are made, however, on the assumption that 90% of the electricity used for space and water heating is on the night rate of the Economy 7 tariff. This presupposes that night-storage heaters are employed, but these are seldom reset and not always easy to control which is important when rapid and unforecast changes in weather occur.

The recent gas-price rises have not been due to "free" market forces but rather suprisingly to a Conservative Government's deliberate intervention policy. (Nevertheless to most energy-conservation engineers, the unit prices of all fuels has been too low for too long). It is not easy to predict how long such a situation will prevail.

If the annual quantity of electricity generated from nuclear fuels rises, then it will be increasingly to the advantage of the electricity industry to maintain a good off-peak load: domestic space and water heating based on Economy 7 tariff is one way of achieving this.

Heating systems that are expensive to run may lead the occupants of a building to choose paraffin or bottled-gas heaters (which are relatively cheap with respect to capital costs) in order

FIGURE 2

Lumped annual percentage price increases per unit for domestic gas and electricity supplies (i.e. excluding standing charges) between 1974 and 1982.

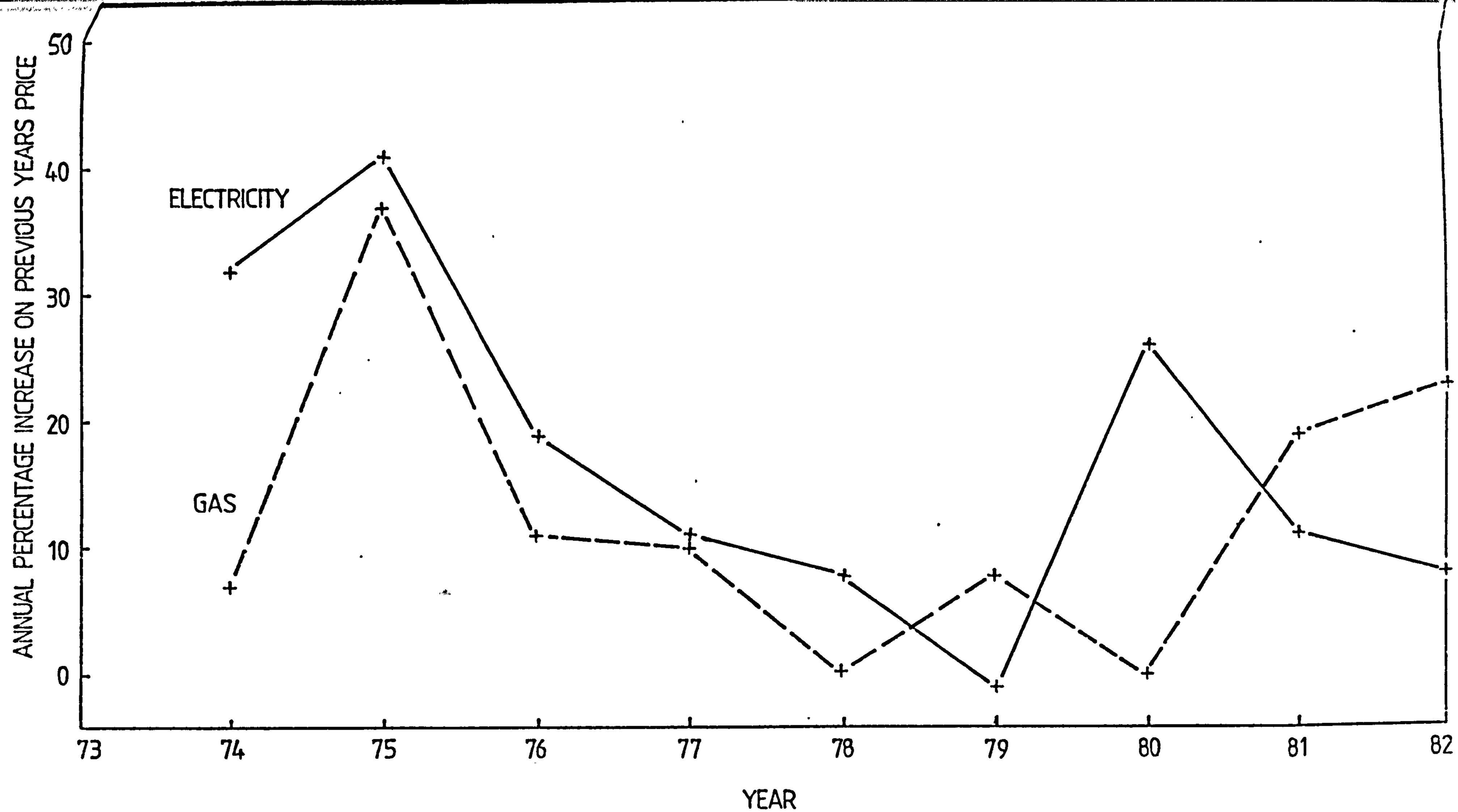
ELECTRICITY
GAS
ANNUAL PERCENTAGE INCREASE ON PREVIOUS YEARS PRICE
50
40
30
20
10
0
73
74
75
76
77
78
79
80
81
82
YEAR

to provide warmth in only a single room of the building. Although these methods of heating may be expensive in terms of cost per unit of fuel, their confined use results in reduced overall costs to the consumer. The building environment has, however, become less comfortable and, as will be discussed later, the unvented sources of water vapour from these heaters will probably result in increased condensation problems.

It is thus imperative that the long-term running costs of heating systems be considered before any decision is made as to which heating system option should be chosen.

EFFECTS OF INCREASED INSULATION ON INTERNAL ENVIRONMENTS

Increased roof and wall insulations usually lead to higher temperatures in buildings in winter in the U.K. (7) with the resulting greater ability for water vapour to be held by the air. A recent study (8) has shown that average domestic living-room temperatures during the evenings in the U.K. have risen at a rate of about $1^{o}C$ per decade since 1945. This is due to people's preference for wearing fewer clothes in a higher temperature rather than more clothes at a lower temperature. Mean temperatures over 24 hour periods were also shown to be rising particularly in centrally-heated houses, which were consistently $2^{o}C$ warmer than those containing coal fires or only partial central-heating.

Pimbert and Fishman (9) compared temperatures in 18 insulated and 15 uninsulated houses in London. The preferred temperatures in living rooms were not affected by outside temperature changes or by

alterations in the degree of insulation. However, bedroom temperatures were dependent upon external climatic conditions and were warmer in insulated homes.

Campbell (7) concluded that increased temperatures in halls and bedrooms of insulated houses compared with uninsulated houses of the same design led to an increase of 1.25^{o}C in whole house temperatures with an average outside environment temperature of 8.5^{o}C. This went some way to explain the disappointing heat savings resulting from enhancing the insulation : a reduction of space heating fuel consumption of 40% was expected but in fact the actual saving achieved was only about 22%. Additional insulation saved fuel only insofar as it allowed the same standard of comfort to be achieved in the rooms that people cared most about for less energy consumption. However if the insulation was added to the house without consideration of the existing heating system or controls, the result was likely to be a warmer house but the resulting fuel savings would be disappointingly small.

The performance of wet heating systems in present and future domestic buildings was considered by Pickup and Miles (10). It was stated that in conventional housing (i.e. those designed and built before the Second Amendment Regulation (2)) there were no clear indications that a decision to control space heating with a single thermostat or alternatively thermostatic radiator valves could be made without first determining the requirements and living habits of the occupier. However as the insulation level of the house is increased, the lower heat input requirement and uneven heating

demand throughout the house due to solar and incidental gains such as circulating pipe heat losses imply that individual room control may be essential.

The use of more efficient low-thermal mass boilers together with individual radiators fully controlled by thermostatic valves were thought to be the best system. However it was found that circulating pipe losses were frequently more than adequate to keep the house warm and that sometimes it was necessary to shut down the boiler and circulation completely. This was achieved by replacing the living room thermostatic radiator valve with an electrical room thermostat and to use a motorised valve in the hot-water circuit. It was considered that this was not an optimal mode of control and that there was scope for development.

MOISTURE SOURCES

Industrial and commercial buildings are, in general, occupied only intermittently; the degree of intermittency in domestic buildings being between 40% and 60% (11). Such occupation patterns can lead to condensation problems and to difficulties in rapidly attaining comfort conditions soon after the start of occupancy, unless the interior wall lining component is of a low thermal mass insulant.

Condensation has been a problem in domestic buildings for many years. In the past, surface condensation was the primary problem and was usually caused by the absence of low levels of heating in most rooms of a house, i.e. in those other than the living room. Water vapour from kitchens and bathrooms, evaporative gains from

surfaces, and metabolic gains from plants and occupants in heated rooms tended to condense on the cold surfaces in unheated bedrooms, landings and stairways leading to mould growth and the deterioration of structural timbers, decorations, furniture and clothes. However such conditions did not always ensue, and in general the presence of an open chimney provided an adequate means of ventilation.

The major sources of water vapour in a domestic building are generally found in the kitchen and bathroom. Cooking produces water vapour from the boiling of vegetables and from unvented gas cookers. Inspection of domestic gas bills over the Summer quarter, when the gas supplied is used only for cooking, suggests that at least 20 litres of gas per household are used daily for this purpose.

FIGURE 3.

ESTIMATED MAXIMUM DAILY WATER VAPOUR BALANCE FOR A TYPICAL THREE-BEDROOM HOUSE OCCUPIED BY FOUR ADULTS.

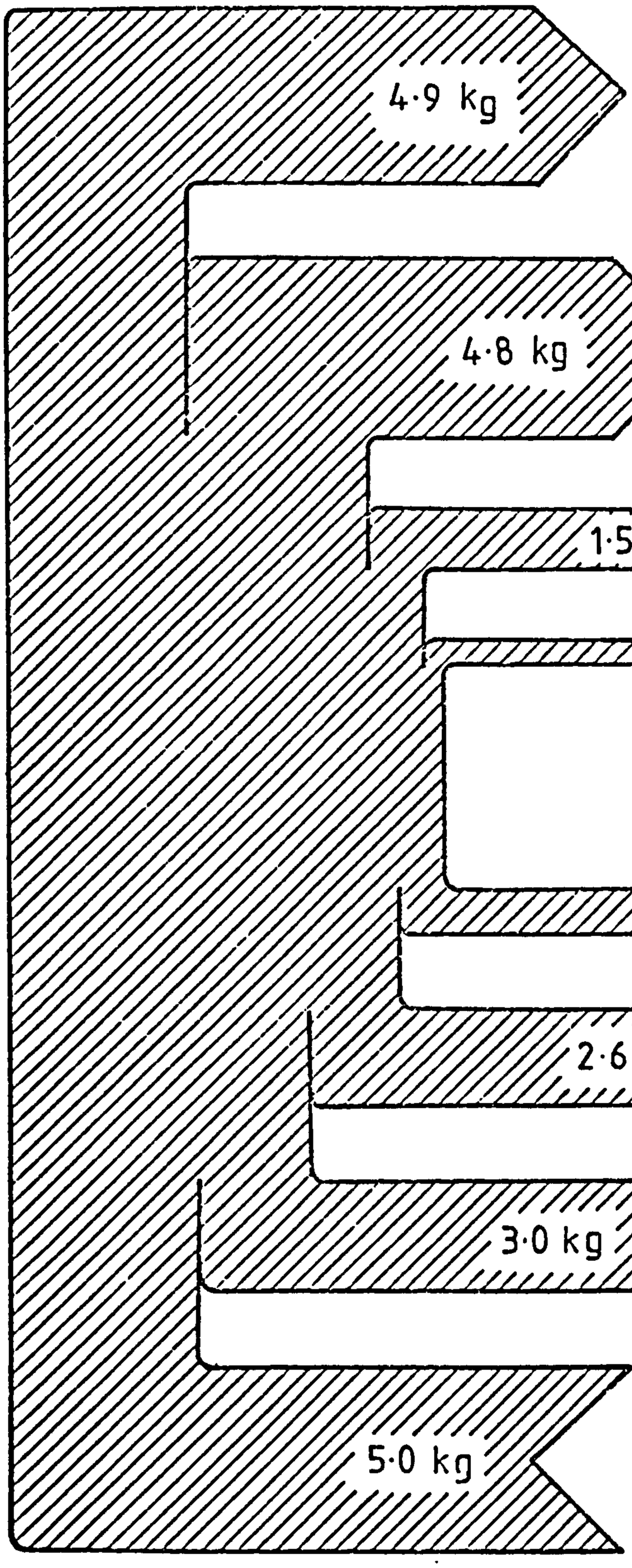

ADSORPTION BY STRUCTURE
INCREASE IN INFILTRATION
AIR HUMIDITY CONDENSATION

EXFILTRATION THROUGH
DOORS AND WINDOWS

TO LOFT SPACE, DIFFUSION
AND VENTILATION

DIFFUSION THROUGH WALLS

BATHS AND SINKS

COOKING

RESPIRATION

WASHING

This constitutes an addition of at least 0.13 kg of water vapour per day. If 80% of the energy input to a 2.4 kW kettle containing boiling water is actually used in boiling the water, then 0.05 kg of water vapour is released within one minute. Vigorously boiling water in open saucepans may thus add large quantities of water vapour to the kitchen atmosphere.

Bottled gas and paraffin heaters are often major contributors to condensation problems. Each kilogram of paraffin, when burnt, yields approximately 1.3 kg of water: and 1 m^3 of butane at ambient standard temperature and pressure (15^oC, 1 atm. pressure absolute) produces approximately 14.7 kg of water.

Estimates of evaporation rates from normal types of baths show that water vapour is released at the rate of 0.2 → 0.3 kg per hour. The increased surface area, higher temperature and movement of the water droplets issuing from showers ensures evaporation rates much higher than this. It has been estimated (12) that showers produce about four times as much water vapour as a bath.

The occupants of buildings also add water vapour to the atmosphere through respiration and perspiration which can range per person from 0.05 kg per hour when sleeping to 0.5 kg per hour when undertaking vigorous exercise.

Activities such as washing will also introduce water vapour to the atmosphere. In general, front-loading washing machines add little water vapour, the wash taking place within the drum and the hot waste water is removed rapidly, via plumbed-in systems, with little contact with the atmosphere. Tumble dryers, on the other hand, if

not vented directly to the environment external to the building, can result in large quantities of water vapour being allowed to escape into the airspace as does drying clothes over 'radiators' or in the bathroom.

Utilising these facts and experimental values for the amount of water contained in clothes, after they have been spun dry, the maximum daily water vapour input to the internal environment of a typical 4 person household was assessed to be ∿ 12 kg, as shown in fig.3. These data agree well with those of Sanders (13) and are within the values estimated in BS 5250 of 7 kg to 14 kg per day (14).

Such estimates point to the importance of having a relatively-dry infiltration air supply from the ambient environment to take up much of this water vapour and of exfiltration as means of removing internally-generated water vapour if effective draught-proofing is carried out. Economic thermal analyses show draught-stripping as an extremely effective method of reducing heat losses, giving very short pay-back periods of only months duration. However, too little attention is given to the condensation damage which may consequently occur.

Increased levels of insulation help to maintain internal air temperatures and those of internal surfaces. Double glazing performs the same function for windows. Surface condensation should have become less of a problem , but its place may well have been taken by the more insidious phenomenon of interstitial condensation (14). Vapour pressure gradients across the structure may result in condensation occurring on the inside surface of the outer leaf or within the insulant itself.

With present construction practice, about 20% to 30% of the air that enters a house leaves via the loft, when all the windows are closed. This occurs through holes in the ceiling of the upper floor such as the access hatch, around pipes connected to tanks in the loft and ceiling light roses (15). It has been estimated that for a typical two-storey house about 50g of water per hour enters the roof by this means (13). This figure is much larger than the amounts that diffuse through a ceiling which may be typically estimated to be about 10g.per hour.

Thermal insulation laid on the ceiling has the effect of reducing loft temperatures but generally, due to the insulants high porosity, it has little effect on the amount of water vapour transferred. Consequently, with the reduced temperatures, the relative humidity of the air increases giving rise to greater risks of condensation occurring in the loft. Even if condensation does not occur, the moisture content of hygroscopic materials such as wood is likely to increase with the any rise of relative humidity, allowing the spread of fungal growths.

Much of this problem can be overcome by the fairly simple expedient of reducing the flow of air from the building into the roof space by draughtproofing access hatches, filling holes around pipes with mastic and increasing roof ventilation. The effects of roof ventilation are clearly shown in fig.4. In many cases in practice, however, little attention will be paid to such details, particularly where retrofitting of insulation is carried out by the householder who may be completely ignorant of any of these risks.

FIGURE 4.

MOISTURE CONTENT OF ROOF TIMBERS

(— — —) NOT VENTILATED; (————)

VENTILATED TO BS. REQUIREMENTS. (C.H.

SANDERS, BRE SCOTTISH LABORATORY.

PRESENTED AT CIBS MEETING 15TH JULY

1981).

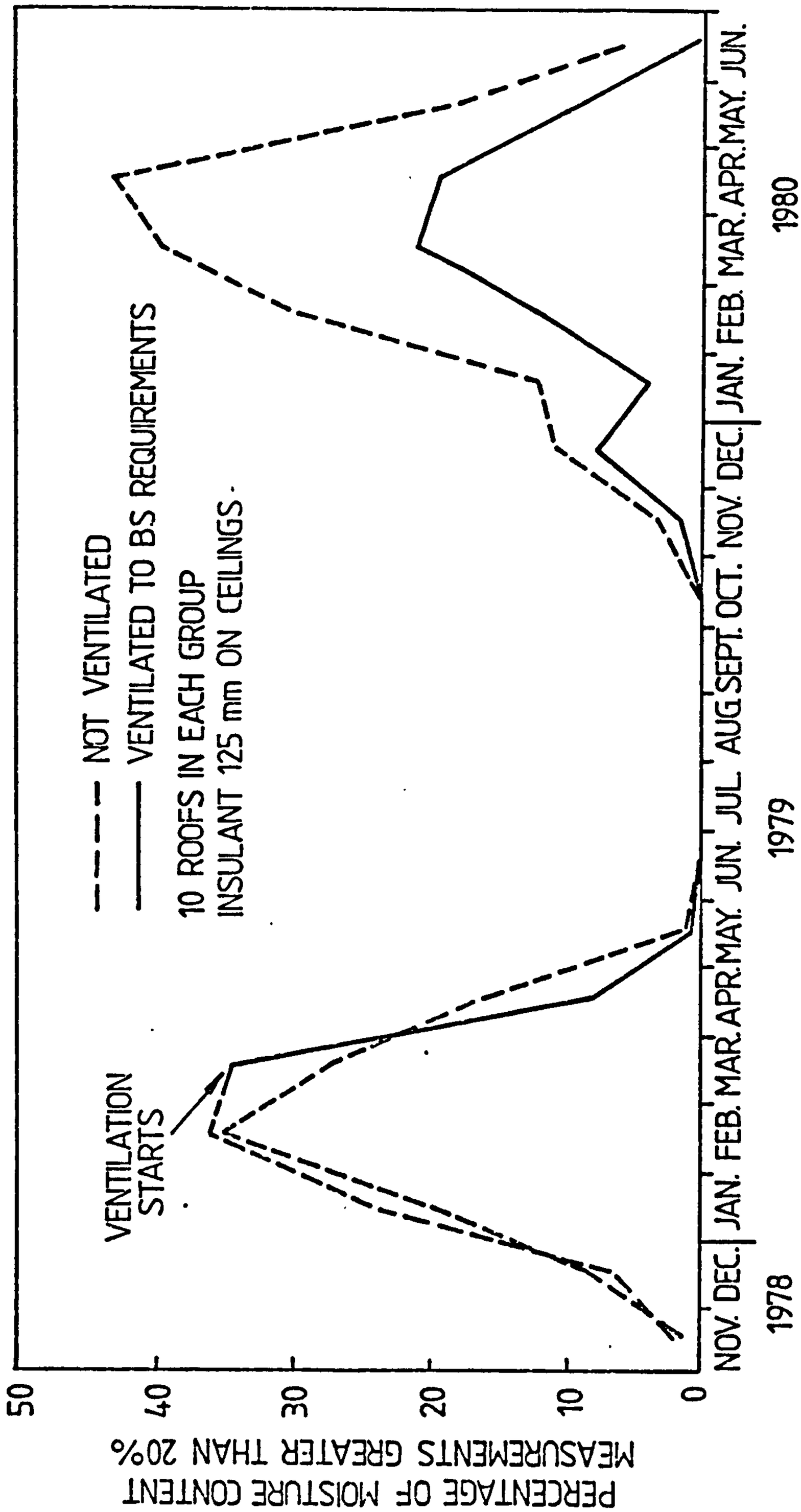
PERCENTAGE OF MOISTURE CONTENT
MEASUREMENTS GREATER THAN 20%
50
40
30
20
10
0
NOV. DEC.
1978
JAN. FEB. MAR. APR. MAY. JUN. JUL. AUG. SEPT. OCT. NOV. DEC.
1979
JAN. FEB. MAR. APR. MAY. JUN.
1980
VENTILATION STARTS
10 ROOFS IN EACH GROUP
INSULANT 125 mm ON CEILINGS
NOT VENTILATED
VENTILATED TO BS REQUIREMENTS

The introduction of insulants into the cavity has the effect of depressing the external leaf temperatures. Moist brickwork will thus more readily cool to temperatures below the freezing point of water. The result of this behaviour is a probable increase in the incidence of spalling, i.e. the breaking up of the external surface of the brick due to the expansion occurring when the trapped water freezes.

CONTEMPLATIONS

Many of these problems can be eradicated by thoughtful building design, but too often penny-pinching attitudes or a preponderance of attention to architectural features rather than engineering design results in structural problems that may subsequently lead to expensive repairs. In particular, great care needs to be shown when old buildings are up-graded, often by the blocking up of old chimneys or the addition of insulation to unventilated roof spaces.

Billington (16) emphasised that although structural insulation was an obvious way to reduce the rate of energy use in buildings, and that the Building Regulations help to achieve this aim, this only tackled part of the problem. It does not, for example, limit heat losses via other paths such as ventilation, excessive glazing or inappropriate building shape. Neither does it encourage designs which make the maximum use of heat from sunshine, lighting or equipment. Statutory regulations prescribe certain standards and so allow little flexibility to the designer.

It was stated (16) that a move comprehensive approach to building design was needed which was not only concerned with the quantity of energy delivered to the premises but also considered the degradation of the prime fuel used as well as losses in distribution. Such an approach would require close collaboration between architect and engineer at the design stage.

The preceding discussion suggests that a consideration of the U-value alone does not necessarily lead to improved design and may often be misleading. There is the danger that obtaining a building component with a U-value less than the prescribed value has become the sole criterion, to be achieved without due thought being given to basic engineering good practice. Building materials are usually damp to some degree,and interstitial condensation may lead to cavity wall insulants also being damp. The conductivities of these materials rise significantly with increasing moisture content, and thus calculated U-values using manufacturers' thermal conductivity values obtained under laboratory conditions for dry materials, can give rise to significant under-estimates of the actual U-value of the structure. Measurements of thermal conductivities carried out in-situ by Ashton (17) showed considerable excesses above normally quoted values. Blockwork in-situ, for example, had a measured thermal conductivity of 0.35 $Wm^{-1}K^{-1}$ which compares with a generally quoted value of 0.18 $Wm^{-1}K^{-1}$, and brickwork was found to have values of 1.0 → 1.47 $Wm^{-1}K^{-1}$ which compares with a value of approximately 0.66 $Wm^{-1}K^{-1}$ for dry facing bricks of density 1600 → 1700 kg m^{-3}. Also up to 20% of the heat transfer area of a typical brick or block wall consists of mortar, which exhibits different thermal properties from those of the bricks or blocks, but this is rarely considered in the heat transfer calculations.

Heating strategies and boiler sizes may thus be under-designed, so leading to the further use of portable, water-vapour producing butane or paraffin heaters in extremely cold weather conditions when condensation is more likely to occur.

Building design procedures need careful consideration if changes are to be made from well-tried traditions. Data on the actual performance of the components of building structures are needed to ascertain the extent to which potential problems will in fact occur.

The U-value should only be regarded as a limited guide-line and will provide no indication of the time response of a building to variable heat gains or losses. If higher levels of insulation are to become mandatory then it would be wise to obtain the most cost effective use of the capital investment involved in its installation. In order that this may be achieved, the functions undertaken in the building together with the occupancy patterns need careful assessment.

There has been no attempt in the Building Regulations (1,2) to arrive at the recommended U-values through a cost-optimisation process. There are many industrial activities that require extremely high ventilation rates to provide some measure of cooling and to remove unwanted products from processes and personnel. The savings made by the reduction of heat losses through the building fabric may, under such circumstances, be completely overshadowed by ventilation losses. In some casesthe reduction of heat losses can compound

already difficult cooling problems. A much broader outlook needs to be encouraged. A reduction in the U-value of the building component in many cases would only become economic if heat recovery from the ventilating air is achieved, and this low-grade energy utilised to preheat the incoming air or to drive heat pumps to provide cooling (18) where heat production of processes exceeds space heating requirements.

There is a need to ascertain the heat and mass transfer behaviours of building materials, in particular those that affect the prediction of the transient behaviour. Mathematical models may then effectively simulate conditions found in real buildings. Too often, in the past, manufacturer's values for the thermal conductivity or diffusivity have been used with little attempt to check on their validity. Information regarding the transient behaviour such as the thermal diffusivity have been, at the least, somewhat esoteric. $\alpha = \left(\frac{\rho C_p}{k}\right)^{-1}$

As desk top computers become cheaper and more powerful, these dangers could well increase. The too prevelent, trusting attitude that computer predictions are absolutely correct together with a potential lack of understanding of the concept of heat transfer and moisture migration by the users could result in poorer rather than better designed buildings.

It is essential that the lowest initial capital cost does not become the sole criterion for building design. Efforts should be made by the government and the energy supply industries to educate the public so that the real choices available when purchasing new houses, are generally appreciated. Greater attempts should also be made to ensure that the vast amount of pretinent research information is more repidly disseminated and utilised in the design of heating systems.

REFERENCES

1). B.S.1. "The Building (First Amendment) Regulations Part F.F. No.723" 1978, British Standards Institution, London, 1978.

2). B.S. I. "The Building (Second Amendment)Regulations 1981 Part F. No.1338, British Standards Institution, London, 1981.

3). BRE Report No. "Dampness: One Weeks Complaints in Five Local Authorities in England and Wales" Building Research Establishment, HMSO, 1982.

4). Davis, Belfield & Everest, Chartered Quantity Surveyors (Editors) "Spon's Mechanical and Electrical Services", Price Book 1979, 10th Edition. E. and F.N. Spon Ltd., London, 1978.

5). P.C. Venning "The economics of energy use and conservation", pp. 27-42, in Experience of Energy Conservation in Buildings, (Edited by A.F.C. Sherratt) Construction Press, London, 1981.

6). Anonymous "Economic turning point for electric heating", Building Services & Environmental Engineer, Vol.5, No.2, pp. 11-12 October 1982.

7). P.M. Campbell "Experience with insulating existing houses", The Heating & Ventilating Engineer, pp. 10-12, October, 1980.

8). D.R.G. Hunt & M.R. Steele "Domestic temperature trends", The Heating & Ventilating Engineer, 54, No.626, pp. 5-15, April 1980.

9). S. Pimbert & D. Fishman — "How warm do people run their homes?" Building Services & Environmental Engineer, Vol.5, No.2, pp. 5-7 October, 1982.

10) G.A. Pickup & A.J. Miles — "The performance of domestic wet heating systems in contemporary and future housing", Communication 1041 The Institution of Gas Engineers, 43rd Autumn Meeting, London, November, 1977.

11). R.A. Desson — "Energy Conservation : the intermittent occupation of dwellings and domestic energy consumption" (CP 37/76). BRE Building Research Series, Energy, Heating and Thermal Comfort, pp.65-74, The Construction Press, London, 1978.

12). U.S. Department of Energy — Residential Energy Audit Manual, The Fairmont Press, Inc., Atlanta, U.S.A., ISBN 0-915586-53-3.

13). Sanders C.H. — "Condensation and its Treatment" Building Technology and Management, 18, 11, pp. 35-8, Dec. 1980.

14). B.S. 5250 — Code of : Basic data for the design of buildings : the control of condensation. British Standards Institution, London, 1975.

15). TIL 59 — "Condensation in domestic tiled pitch roofs - advice to householders" Building Research Advisory Service Technical Information Leaflet, Building Research Establishment, Department of the Environment, 1978.

16). N.S. Billington — "Commercial and domestic heating - preparing for the future." Chartered Mechanical Engineer, Vol. 26, No.2, pp. 57-59, February 1979.

17). D.F. Ashton — "Test to measure the thermal properties of the external fabric. of six test houses", Electricity Council Research Centre report ECRC/N724, 1974.

18). R.M. Hamner — "An alternative source of cooling: the ejector compressor heat pump" ASHRAE Journal, 22, 7, pp.62-66, July 1980.

CHAPTER 2.

CORROSION UNDER INSULANTS.

The Corrosion Problem

The petrochemical and food-processing industries make use of insulants for both plant and pipework. The reduction of heat losses is not always the prime concern when insulants are applied to a system but rather the maintenance of the optimal temperature for the process, ensuring that the safe-touch temperatures for the external cladding with respect to personnel is not exceeded, or extending the escape period in the event of a fire by delaying buckling or cracking under elevated temperatures of the structural members. Any cracking occurring in pipelines could result in the release of volatile, noxious or highly inflammabel products.

The growing awareness of the cost of heat losses, as unit fuel costs have increased, has meant that more consideration has been devoted to the proper insulation of pipework and other plant. However, the insulation of such systems (e.g. vats) has often led to problems due to the subsequent ingress of water and water vapour, giving rise to corrosion under the lagging. A Government Committee reporting in 1971 estimated that the cost of all corrosion in the U.K. was approximately £1.4 x 10^9 per annum, i.e. 3.5% of the gross national product at that time. More recently, 1982, Hope (1) has stated that in excess of £4 x 10^9 per annum is wasted in the U.K. as a result of corrosion.

Visual observations of moisture ingress and corrosion under lagging is difficult without major removal of the insulant: as yet no satisfactory non-destructive test method has been developed to detect and locate exactly this form of corrosion. Unless regular and careful inspection of the components, with the insulant claddings removed is carried out, then such insidious developments may unknowingly reach hazardous proportions. It has been stated (2) that stress corrosion cracking can occur in austenitic stainless steels in less than two years at temperatures of $\sim 90^{0}C$. Thus any financial savings made over these two years as a result of the presence of the insulant leading to reduced energy losses would then probably be more than off-set by the expense incurred in replacing the large and expensive equipment such as storage tanks and vats. The expenditures so incurred may not only include the replacement of the corroded articles but also compensation payments for injured personnel, loss of production and reduction of operating efficiency. Although vats for brewing and food processes were usually manufactured from copper, this metal has been largely superseded by stainless steel. Bearing this in mind, only the corrosion of steel will be considered in this paper.

Corrosion Processes

Most metals exist in the Earth's crust in the form of stable compounds such as oxides, sulphides and carbonates. Metals in their pure and many of their alloyed states, are chemically unstable and will, under suitable conditions, revert to their more stable compounds.

Corrosion involves the loss of electrons from the metal's surface to the environment: this process usually requires the presence of water and oxygen. Corrosion products, which are generally insoluble in water, form a protective skin on the metal thus reducing the rate of corrosion. However in the case of mild steel, the products of corrosion are loose and so do not prevent further chemical degradation.

A galvanic cell, as illustrated in figure 1, involves an electrolyte, an electrode which losses electrons, the anode and the cathode i.e. an electrode which receives the electrons. Corrosion is an electrochemical process and requires an electrial potential difference in order that electrons might flow. By the loss of electrons the metal anode is converted to its compounds and thus corrodes while the cathode remains intact. The cathode may be another metal in electrical contact with the anode or part of the same metal surface but with a different composition. For the latter electrical potential differences exist across the crystal boundaries, causing some areas to become cathodes with other areas anodes (as illustrated in figure 2) and thus liable to suffer corrosion.

The corrosion process is initiated when iron atoms leave a steel surface and dissolve in the water to form ferrous ions, so releasing two electrons, see figure 3.

$$Fe = Fe^{2+} + 2e^{-} \quad \ldots\ldots (1)$$

These electrons flow to the cathode region where they react with the water and its dissolved oxygen to form hydroxyl ions

$$2e^{-} + H_2O + (O) = 2OH^{-} \quad \ldots\ldots (2)$$

FIGURE 1

BASIC GALVINIC CELL ACTION.

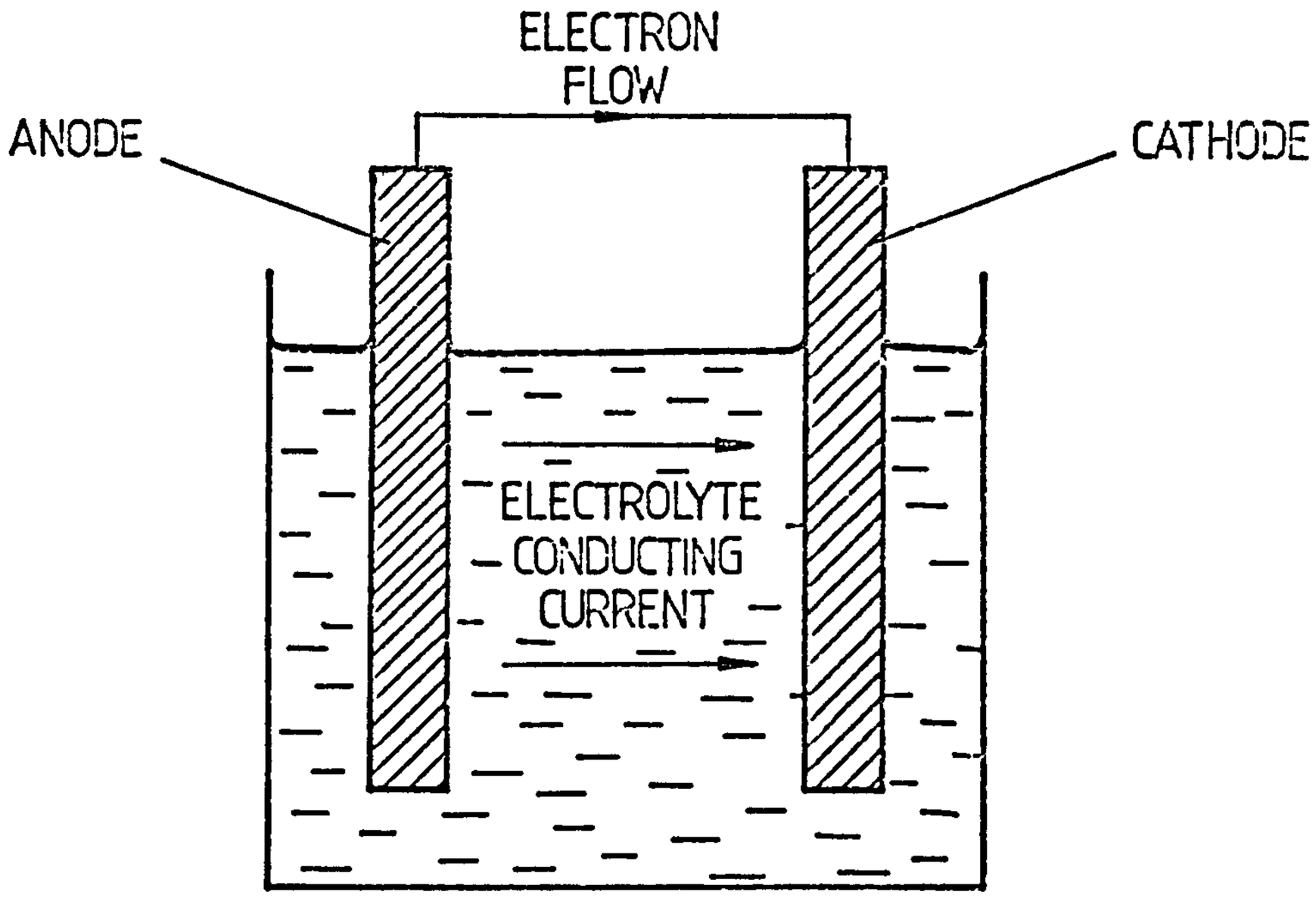
ELECTRON
FLOW
ANODE
CATHODE
ELECTROLYTE
CONDUCTING
CURRENT

FIGURE 2

CORROSION CELLS ON A METAL'S SURFACE:
THEY ARE PRESENT DUE TO THE INHOMOGENEITY
OF THE CONSTITUENT PHASES OR VARIATIONS
OF THE SURFACE FINISH.

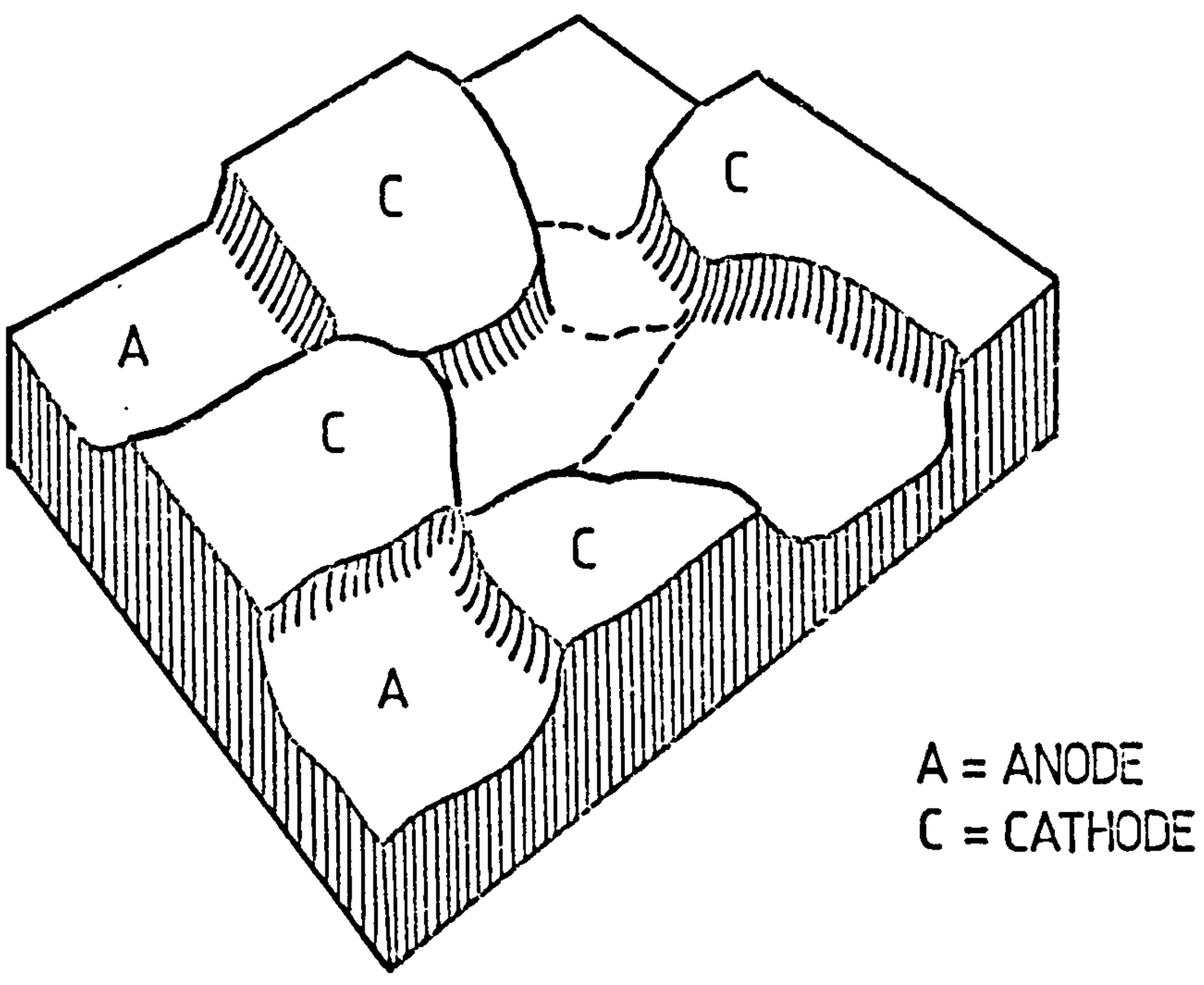
C
C
A
C
C
C
A
A = ANODE
C = CATHODE

As the electrons are taken up by this reaction, more iron dissolves to maintain the supply and thus the anode corrodes. The hydroxyl ions produced at the cathode move towards the anode and the ferrous ions towards the cathode. Subsequently, these ions react to form ferrous hydroxide, i.e.

$$Fe^{2+} + 2OH^{-} = Fe^{2+}(OH^{-})_2 \quad \ldots\ldots (3)$$

Further reactions ensue with the dissolved oxygen in the aqueous electrolyte resulting in hydrated ferrous oxide, viz:-

$$2Fe(OH)_2 + (O) \rightarrow Fe_2O_3\ H_2O + H_2O \quad \ldots\ldots (4)$$

Rust is formed slightly away from the surface and thus fails to protect it from further degradation.

"Atmospheric" corrosion of metals can occur at ambient temperatures in polluted atmospheres of high humidity. Passivating thin oxide films on metals and alloys (i.e. films that are chemically stable in the presence of the electrolyte) usually attain a limiting thickness, but under polluted atmosphere conditions the film growth may continue. When the atmospheric humidity is sufficiently high for condensation to occur on the metal surface, the rate of atmospheric corrosion increases considerably.

Should hygroscopic materials be present on the metal surface, then aqueous corrosion conditions will occur at relative humidities greater than approximately 60%.

FIGURE 3

THE CORROSION REACTION OCCURING AT THE CRYSTAL GRAIN BOUNDARIES WITHIN MILD STEEL.

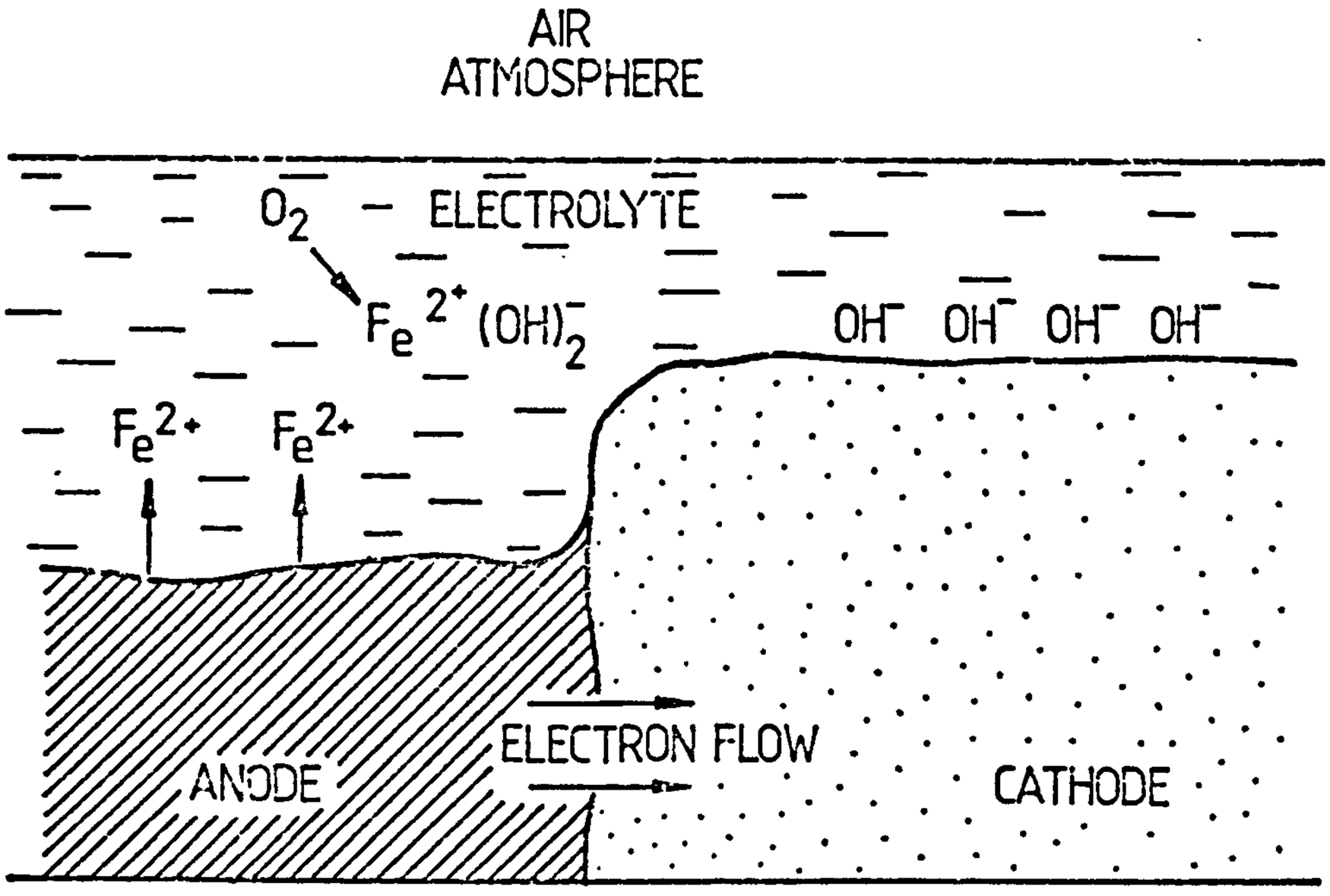
AIR
ATMOSPHERE
O_2
ELECTROLYTE
$Fe^{2+}(OH)_2^-$
OH^- OH^- OH^- OH^-
Fe^{2+} Fe^{2+}
$2e^-$ $2e^-$
ELECTRON FLOW
ANODE
CATHODE

Corrosion is a complex process and is often the result of both physical and chemical activities occurring simultaneously. Physical processes may result in the production of potential corrosion sites, for example cavitation in a liquid near the solid-liquid interface can cause erosion of protective films or severe deformations of a surface. Erosion, due to the impingement of fluids and any abrasive materials they may carry, can break through corrosion scale and dissolve the metal. Stress corrosion cracking is due to the combination of high surface tensile stresses, which may be residual or applied, and a corrosive environment. This list indicates some of the many processes that can lead to corrosion.

Generally, plant and pipework to be lagged is constructed of carbon and low-alloy steels. These steels are cheaper than the more corrosion resistant stainless-steels, which should be used in more aggressive environments.

Carbon and low-alloy steels tend to suffer from general attack in acid or hot moist environments. During general corrosion, no distinguishable area of metal is solely anodic or cathodic and a general wasting away of the surface occurs. Such corrosion is normally found where the metal is in contact with an acid or a salt solution. If aqueous solutions of nitrates or caustics, or sea water are trapped under thermal insulation lagging, corrosion cracking may occur. Stress corrosion cracking is the phenomenon of stress alloy failures that occur by the propagation of cracks in corrosive environments. The cracks form and propagate at right angles to the direction of the tensile stress, at stress levels much lower than those required to fracture the material in the absence of the corrodent.

The corrosion occurs at a faster rate than would occur if either the stress or the chemical corrodent were acting independently.

Stainless steels are generally used in corrosive environments because of their relatively high resistances to corrosion: they are however susceptible to stress corrosion cracking in the presence of soluble inorganic chlorides, oxygen and water. It is important that this phenomenon be put into perspective. Sedricks (3) stated that, in 1970, those industries reporting significant numbers of stress corrosion failures consumed only 20% of stainless steel production. The industries concerned however, tend to be those where any failure would be highly expensive and potentially very dangerous. e.g. in the petrochemical or power industries.

Any failure that occurs is usually the result of a complex interaction dependent upon alloy composition, chloride and oxygen concentrations and temperature. Problems were considered, by Nicholson (4), to predominate for systems within the temperature range 70°C to 200°C and for plant which was cycled between 0°C and 100°C in agressive environments. It is also stated in BS 5970 (5) that stress corrosion cracking is not likely to occur below 70°C and will be most severe in the range from 70°C to 105°C.

In order that the frequency of stress corrosion cracking may be reduced any prospective sources of chloride ions need to be identified and their migration to the metal surface prevented. Insulants may contain leachable chlorides or other halogen ions. These are present either as a result of the manufacturing process of the insulant, its chemical composition or the addition of fire retardants. These chlorides may be leached out by free water (if the insulant ever becomes wet), and tend to become concentrated at

the junction between the insulant and the metal surface. Delahunt (6) stated that in laboratory tests where commercial fibrous insulants were leached using distilled water, alkaline solutions having 7 < ph < 11 resulted. Such solutions are non-corrosive and lead to passivation of the metal surface, thus providing some protection against corrosion. Similar tests with foamed insulants indicated pH values of between 6 and 3, i.e. acid solutions for polyurethane and phenolic foams. It was considered that phenolic foams were the more corrosive.

Many petrochemical plants are situated near the coast or on estauries, where salt water becomes the major source of chloride ions. Sea water is often used for cooling purposes in such areas so resulting in the drift of salt water spray across the plant. Rain then washes these salts into the insulant, through cracks and defects in the external cladding, with the resulting enhanced corrosion risk.

Reduction of Corrosion

Insulants themselves do not cause corrosion. In nearly every case corrosion is caused by the ingress of water either directly through cracks in the cladding or by interstitial condensation of water vapour in low temperature (i.e. usually $15^{0}C$) systems. Therefore it is essential that care be used in insulating the often difficult shapes of many plant structures and to avoid obvious moisture traps and thermal bridges, the presence of the latter enhancing the probability of interstitial condensation occurring.

The presence of water is essential to form an electrolyte if corrosion, other than that due to high temperature oxidation, is to ensue. It is thus

essential that moisture ingress, in the form of water or through vapour migration, into the insulated structure is prevented. Unfortunately most plant experiences temperature cycling causing expansion and contraction stresses on any external waterproofing or vapour-barrier layer. Ideally mechanical integrity and thermal insulation design should be undertaken simultaneously. However, insulation contractors are sometimes placed in difficult situations if changes in specifications or design occur after a contract has begun. Materials cut to specifications will no longer fit but may well be made to, thereby resulting in potential future problems due to badly or uninsulated areas of pipe or plant. Insulants should be properly stored in dry conditions on site and exposed insulants should be covered over-night to protect them from rain, condensation and spray. The prevention of water penetration into an insulated system is achievable with good planning and goods site supervision. However, the prevention of moisture ingress due to vapour migration is considered by many to be an almost impossible task. The phenomenon occurs when the water vapour pressure at some point in the insulant or at the structure's surface is less than that of the external environment. If the temperature within the insulated system falls below the dewpoint temperature of the air/water vapour mixture, then condensation will occur. Unfortunately plant maintenance sometimes leads to the damage of weatherproofing and vapour barriers, and thus water vapour ingress occurs.

Corrosion of carbon steels may be controlled by the use of:-

Electrical methods, such as cathodic protection where an external electric current is applied with the structure itself becoming the cathode, or by the use of a sacrificial anode, e.g. of aluminium, which will corrode in preference to the structure which needs protection.

Protective coatings, which may be metallic such as zinc on galvanised steel, inorganic coatings such as vitreous enamels, or organic coatings in the form of paint systems or bituminous compounds.

It is important that the surfaces to be protected are firstly properly cleaned and prepared. Paint performance is very depenent upon the type and standard of surface preparation: wire brushing results in protection durations of two years whereas blast cleaning extends this to ten years (7). Surface preparation of the underlying metal is also important where foamed insulants are to be used, if full advantage is to be made of their excellent adhesive properties.

The protection of stainless steel also requires great care. A secondary barrier of aluminium foil (> 0.6 mm thickness) can be applied to the stainless steel surface with the insulant applied over the foil (2,5). The foil should overlap at the joints by at least 50 mm. A service temperature limitation of 500°C is recommended in BS 5970 (5) for this technique. Delahunt (6) considers that inorganic zinc-rich coatings should not be applied, and in BS 5970 (5) it is considered that such paints should not be used where temperatures exceed 350°C.

SUMMARY

It is clear that thermally-insulating plant or pipework hides and sometimes enhances the corrosion of these structures. Economics gained by the use of insulants to reduce the rates of heat loss may be totally eradicated if corrosion is accelerated. The proper insulation of these structures thus is a complex and difficult task both from the view of design and impliment-ation. It is essential that expert advice from specialists in other fields is utilised at the design stage and that any alterations to specifications are agreed upon by all involved parties before being undertaken. Insulants themselves do not cause corrosion, but ill-designed and poorly maintained systems may produce conditions leading to corrosion.

REFERENCES

(1) K. HOPE — "Where to place your protection money", Process Engineering, pp. 57-59, November 1982.

(2) M.E.D. Turner — "Precautions against stress corrosion cracking under lagging", Paper presented at Institute of Corrosion Science and Technology Conference - Corrosion Under Lagging, Newcastle, November 1980.

(3) A.J. Sedricks — "Corrosion of Stainless Steels", John Wiley & Sons, New York, 1979.

(4) J. Nickolson — "Thermal Insulation. Specifications and materials application to stainless-steel surfaces", Paper presented at Institute of Corrosion Science & Technology Conference - Corrosion Under Lagging, Newcastle, November 1980.

(5) B.S.I. — BS 5970 Code of Practice for: Thermal insulation of pipework and equipment (in the temperature range -100°C to + 870°C), British Standards Institution, London, 1981.

(6) J.F. Delahunt — "Corrosion control under thermal insulation and fireproofing", Insulation pp. 10-18, February 1982.

(7) Anonymous — Controlling Corrosion: (1) Methods, H.M.S.O. London, 1976.

CHAPTER 3.

WATER VAPOUR DIFFUSION THROUGH FIBROUS THERMAL INSULANTS.

Nomenclature

A	Area of material exposed to the environment	(m^2)
a,b	Arbitrary factors in equation 3	
C_v	Concentration of water vapour	($kg\ m^{-3}$)
D	Diffusion coefficient	($m^2\ s^{-1}$)
$\dot{G}_v$	Vapour flow per unit surface area	($kg\ m^{-2}\ s^{-1}$)
h*	Surface mass transfer coefficient	($m\ s^{-1}$)
k	Thermal conductivity of the considered material	($Wm^{-1}\ K^{-1}$)
k*	Water vapour permeability of a material	($kg\ m\ N^{-1}\ s^{-}$
k^*_a	Water vapour permeability through air	($kg\ m\ N^{-1}\ s^{-}$
M_v	Mass of water vapour present	(kg)
P_{sat}	Saturation vapour pressure of the fluid at the surface temperature	($N\ m^{-2}$)
P_v	Vapour pressure in the bulk fluid	($N\ m^{-2}$)
$\dot{Q}$	Rate of heat flow through the material	(W)
R^*_{12}	External air layer resistance to the passage of water vapour	($N\ s\ kg^{-1}$)
R^*_{23}	Resistance of the insulant to the flow of water vapour	($N\ s\ kg^{-1}$)
R^*_{34}	Internal air layer resistance to the passage of water vapour	($N\ s\ kg^{-1}$)
R^*_o	Overall resistance to the transmission of water vapour	($N\ s\ kg^{-1}$)
R_v	Characteristic gas constant for water vapour(=461 $Jkg^{-1}K^{-1}$)	
T	Temperature	(K)
T_m	Mean absolute temperature	(K)
t	Time	(s)
V	Considered volume of gas containing water vapour	(m^3)
V_a	Volume of air within the insulant	(m^3)
V_b	Total volume of the insulant bulk	(m^3)
V_v	Volume voidage $(= \frac{V_a}{V_b} \times 100\%)$	(%)
S	Thickness of a material	(m)
$\Delta(\ )$	Difference between two values of the parameter ( )	

κ	Dimensionless diffusion resistance factor $(=k_a^* / k^*)$	
ρ_a	Density of dry air under normal ambient conditions	$(kg\ m^{-3})$
ρ_b	Bulk density of the insulant	$(kg\ m^{-3})$
ρ_g	Density of insulant fibre	$(kg\ m^{-3})$

THE PROBLEM

Although vapour diffusion and condensation in insulants are much discussed topics (1,2,3), as yet the phenomena cannot be predicted accurately. Changes in occupants' patterns of usage of buildings, or in building technology, such as are inevitable due to rapidly inflating fuel prices, while solving one set of problems, may produce others. In recent years, concern about condensation has been directed predominantly towards surface condensation. The less immediately obvious problem of interstitial condensation is now on the increase and is probably, in the long-term, more harmful.

Financial and other pressures on occupants to employ thermal isolation techniques, such as draught-proofing, have led to the reduced natural ventilation of buildings and thus to the increased likelihood that moisture egress will try to occur by diffusion through building structures. It may be asserted that such problems will not ensue in properly designed buildings using vapour barriers, and forced ventilation systems with heat recovery. However it is stated in the I.H.V.E. guide (4) that "it is unsafe to rely completely on vapour barriers because these are rarely perfect and are often penetrated by fittings such as light pendants". Also ventilation systems incur extra initial capital costs thereby making their introduction less likely and they may be easily switched off at the often perverse whims of occupiers.

Apart from buildings, the most extensive use of thermal insulants is for industrial pipework often located in the open and unprotected from the external environment. Vapour barriers used to seal these pipes against water, and water vapour ingress, often split at the joining seals, due to the cyclic nature of the temperature imposed upon the pipe. Any penetrating moisture, once trapped within the insulant, causes increased heat dissipation from, and possibly even corrosion of, the metal pipe (5).

The unwanted presence of moisture will probably remain a problem in walls, and, as insulation standards improve, the frequency and severity of the condensation arising will increase. Consequently there is an urgent need to have reliable data available, concerning the heat and moisture transfer properties (6-12) through insulants and structural materials over the ranges of humidity conditions commonly encountered in building practice within the U.K. Computer aided design predictions and optimisations of building systems and services will then improve because the imput data will be more realistic.

The application of fibrous, thermal insulants to the warm surface of a structure will lower the temperature elsewhere in the wall. But, because of the low resistance to vapour diffusion through such insulants, the vapour-pressure distribution may not be significantly affected. A knowledge of the temperatures and vapour pressures on either side of the wall together with the respective resistances of the wall components enables the temperature and vapour-pressure gradients to be predicted (3). The basic equation which describes the vapour-pressure gradient acting across a wall namely Fick's 'law', is analogous in form to that describing the associated temperature gradients (12), namely Fourier's 'law'. Fick's law can be expressed as

$$\dot{G}_v = \frac{k^*}{\delta} \Delta P_v \qquad \ldots\ldots (1)$$

and Fourier's law as

$$\dot{Q} = \frac{kA}{\delta} \Delta T \qquad \ldots\ldots (2)$$

If the relationship between the water-vapour permeability of a material, its bulk density and its volume voidage is considered, then it is reasonable to expect that

$$k^* = o \quad \text{if} \quad \rho_b = \infty$$

$$k^* = k_a^* \quad \text{if} \quad \rho_b = \rho_a$$

Further if the permeability of a vacuum is considered then

$k^* = \infty$ at $\rho_b = 0$

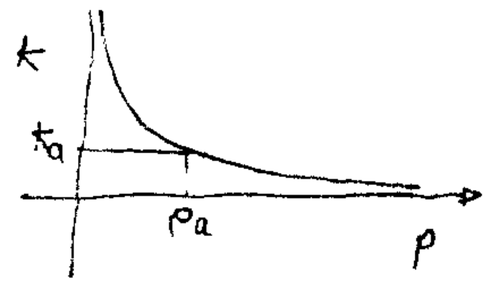

These criteria suggest an exponential relationship between the water-vapour permeability of the material and its bulk density. Similarly if the volume of the voids is considered in relation to the volume of the bulk of the material, then it is anticipated that

when $V_a = V_b$, the k* measured is that of still air k_a^*

$V_a = o$, the k* measured is that of the bulk material.

Because the volume of the voids cannot exceed the volume of the bulk material, values of $V_a > V_b$ have no physical meaning. If the relationship

$$\frac{k^*}{k_a^*} = ab^{\left(\frac{V_b}{V_a}\right)} \qquad \ldots\ldots (3)$$

is considered, then if $V_a = V_b$

$$\frac{k^*}{k_a^*} = ab = 1$$

and if $V_a = o$

$$\frac{k^*}{k_a^*} = \infty$$

The expression V_b/V_a equals $1/V_v$ where V_v is the volume voidage of the material.

THE EXPERIMENTAL INVESTIGATION

The water-vapour permeability of fibrous insulants has been measured both under compression and in the normal (as received) uncompressed state. Results from the two traditional methods — the dry-cup (B.S. 4370) (14) and the wet-cup (15) methods — were compared with the compression rig, using rigid glass-fibre slab.

EXPERIMENTAL PROCEDURE

The vapour permeability versus loading experiments were undertaken for two specimens (see table 1) over test periods each of 8 hours. The increase in weight of the absorber was recorded at hourly intervals (13). Prior to each experimental run, the thermal insulant under the test load was placed in an environmental test chamber together with an absorber (anhydrous calcium chloride) to allow the vapour diffusion rate to stabilise overnight. The silica gel absorber was dried at 99.8 ($\pm$0.1) ^{o}C in the laboratory oven before commencement of the stabilisation period. All tests were carried out in an environmental cabinet under the controlled conditions of 20^{o}C and 50% R.H. with the specimens under various compressive loadings, each test being repeated at least once. The weight increase of the absorber box plus silica gel was determined to 10^{-4} grams using a Nivoc Aperiodic balance, and the average rate of water vapour transmission for each hour of the experimental run then deduced. These values were used to estimate the overall average rate of water-vapour transmission for the complete 8 hours. The rate of vapour diffusion through the material could then be used to calculate the vapour resistance permeability of the insulant.

The dry-cup method (14) involved the desiccant being placed in four empty beakers and then a bung of the insulant under test inserted into each beaker: paraffin wax was used to achieve a good seal between the curved surface of the container and the insulant. A 5 mm air gap was left between the lower specimen surface and the absorber.

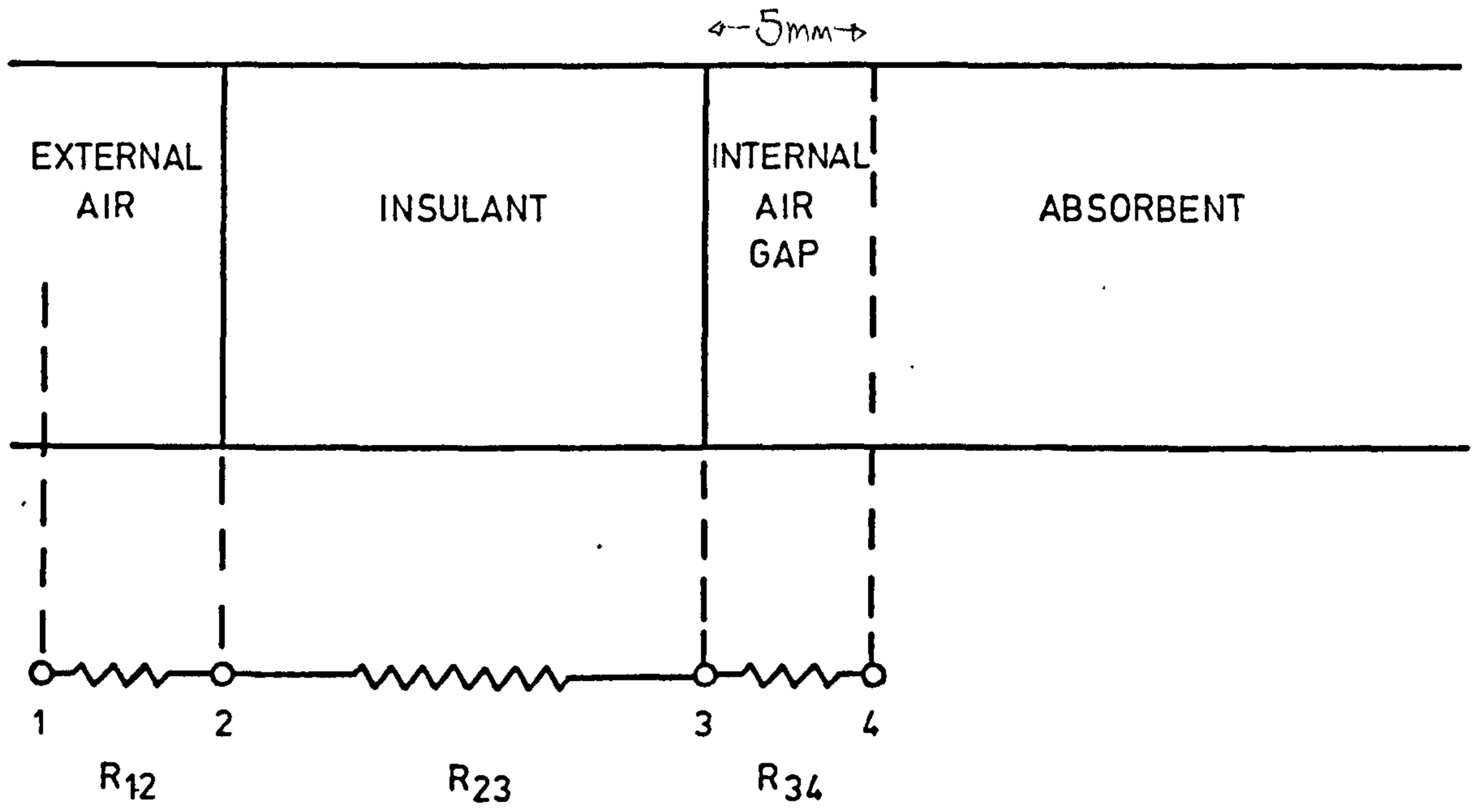

FIG. 1. REPRESENTATION OF THE SEQUENCE OF THE RESISTANCES TO THE FLOW OF WATER-VAPOUR THROUGH THE EXPERIMENTAL ASSEMBLY

The assemblies were then weighed and placed in the environmental chamber at 20°C and 50%R.H. An overall water vapour permeability could then be determined using equation (1) as recommended in B.S. 4370, but such an equation neglects the resistance of the adjacent air-layer. Therefore the water-vapour permeability needs to be calculated using the resistance method outlined in the following section.

A similar treatment was applied to the beaker test 'wet-cup' condition, except that the desiccant was replaced by water in order to maintain the air beneath the specimen at 100% R.H. The vapour pressure difference was 1165 Nm^{-2} when the environmental conditions were maintained at 20°C and 50% R.H. The results of these tests are given in Table 2.

Calculation of the water vapour permeability (Fig.1)

In order to evaluate the water-vapour permeability, k*, of the insulant under test, its water vapour resistance, R^*_{23}, must be measured. Then k* may be deduced because

$$k^* = \frac{\delta}{R^*_{23}} \qquad \ldots\ldots \quad (4)$$

The overall resistance to water-vapour flow through the rig, R^*_o, equals the sum of the component resistances, i.e.

$$R^*_o = R^*_{12} + R^*_{23} + R^*_{34} \qquad \ldots\ldots \quad (5)$$

But R^*_o can also be obtained directly from the experimental measurements, viz.,

$$R^*_o = \frac{\Delta p_v}{G_v} \qquad \ldots\ldots, \quad (6)$$

Thus a knowledge of R^*_{12}, R^*_{34}, the external and internal air layer water-vapour resistances respectively enables R^*_{23}, the insulant resistance, to be evaluated. From Fick's law the total amount of water transferred per unit area by

the diffusion process is given by

$$\dot{G}_v = D \frac{\Delta C_v}{\delta} \qquad \ldots\ldots (7)$$

where D is the diffusion coefficient ($m^2\ s^{-1}$)

The concentration C_v can be expressed in terms of the partial pressure p_v, viz

$$C_v = \frac{M_v}{V} = \frac{p_v}{R_v T_m} \qquad \ldots\ldots (8)$$

With this, Fick's law becomes

$$\dot{G}_v = \frac{D}{\delta} \frac{\Delta p_v}{R_v T_m}$$

$$= \frac{h^*}{R_v T_m} (p_v - p_{sat}) \qquad \ldots\ldots (9)$$

where h* is a surface mass-transfer coefficient. It is then possible to calculate h^*_{12} and thus R^*_{12} from

$$R^*_{12} = \frac{R_v T_m}{h^*_{12}} \qquad \ldots\ldots (10)$$

R^*_{34} can be determined from

$$R^*_{34} = \frac{\delta}{k^*_a} \qquad \ldots\ldots (11)$$

where k^*_a is the water-vapour permeability through air at atmospheric pressure and is taken as 20×10^{-11} kg m $N^{-1}\ s^{-1}$.

But

$$R_{23} = R_o - R_{12} - R_{34}$$

The water vapour permeability k* of the specimen under test can thus be calculated from equation (4).

RESULTS

The measured values of the water-vapour permeability and water-vapour resistance of the specimens at various bulk densities are presented in Table 1 and shown graphically in figures 2 and 3. Figures 4 and 5 showing $\ell n\ k^*/k_a^*$ plotted against ρ_a/ρ_b and $^1/V_v$ respectively were derived from Table 3.

INSULANT SAMPLE	BULK DENSITY ($kg\ m^{-3}$)	APPLIED LOAD ($N\ m^{-2}$)	COMPRESSION (%)	WATER VAPOUR PERMEABILITY $\bar{U}(10^{-11}$ kg m N^{-1} $s^{-1})$	WATER VAPOUR RESISTANCE $R\ (10^{8}\ N\ s\ kg^{-1})$
GLASSWOOL	104.10	0	0	15.4	1.62
	110.74	38.8	6	15.1	1.66
	140.68	106.4	26	14.7	1.70
	173.50	174.1	40	13.7	1.83
	185.89	309.4	44	12.6	1.99
	236.59	444.7	56	11.6	2.15
ROCKWOOL	136.19	0	0	13.1	1.91
	158.36	38.8	14	12.8	1.96
	206.35	106.4	34	11.7	2.14
	212.80	174.1	36	11.5	2.17
	252.20	309.4	46	11.4	2.20
	296.06	444.7	54	10.7	2.33

TABLE 1

The effects of compression on the specimens of glasswool and rockwool. Each of the tested specimens consisted of non-hygroscopic, loosely bonded, short thin ($\leqslant$ 10 μm), inorganic fibres.

METHOD OF TEST	WATER-VAPOUR PERMEABILITY (10^{-11} kg m N^{-1} s^{-1})
Vapour permeability and loading rig (13)	8.63
Dry Cup (BS 4370) (14)	9.38
Wet Cup (15)	10.33

TABLE 2 Typical vapour permeability data measured for the glass-fibre slab (loose bonded) under 'no-load' condition, using the three different methods. (Insulant thickness 25 mm, bulk density 129.9 kgm^{-3}).

Material	$\frac{k^*}{k_a^*}$	$\frac{\rho_a}{\rho_b}(x10^3)$	$\frac{1}{V_v}$
Glass Wool	0.77	11.6	1.043
	0.76	10.9	1.046
	0.74	8.6	1.059
	0.69	6.9	1.074
	0.63	6.5	1.080
	0.58	5.1	1.104
Rock Wool	0.66	8.8	1.046
	0.64	7.6	1.054
	0.59	5.8	1.071
	0.58	5.7	1.073
	0.57	4.8	1.088
	0.54	4.1	1.105

TABLE 3 Dimensionless parameters describing the tested specimens.

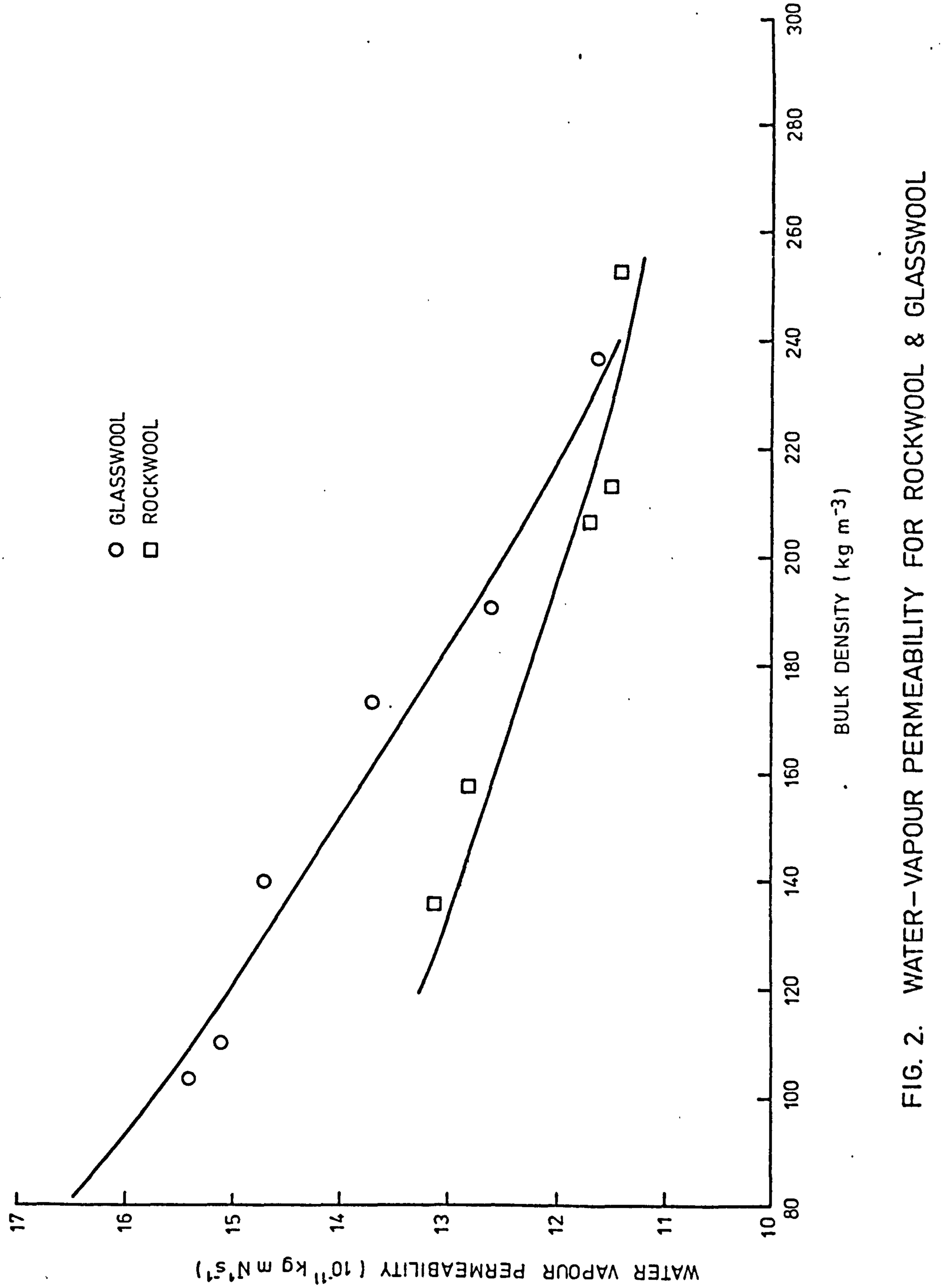

FIG. 2. WATER-VAPOUR PERMEABILITY FOR ROCKWOOL & GLASSWOOL

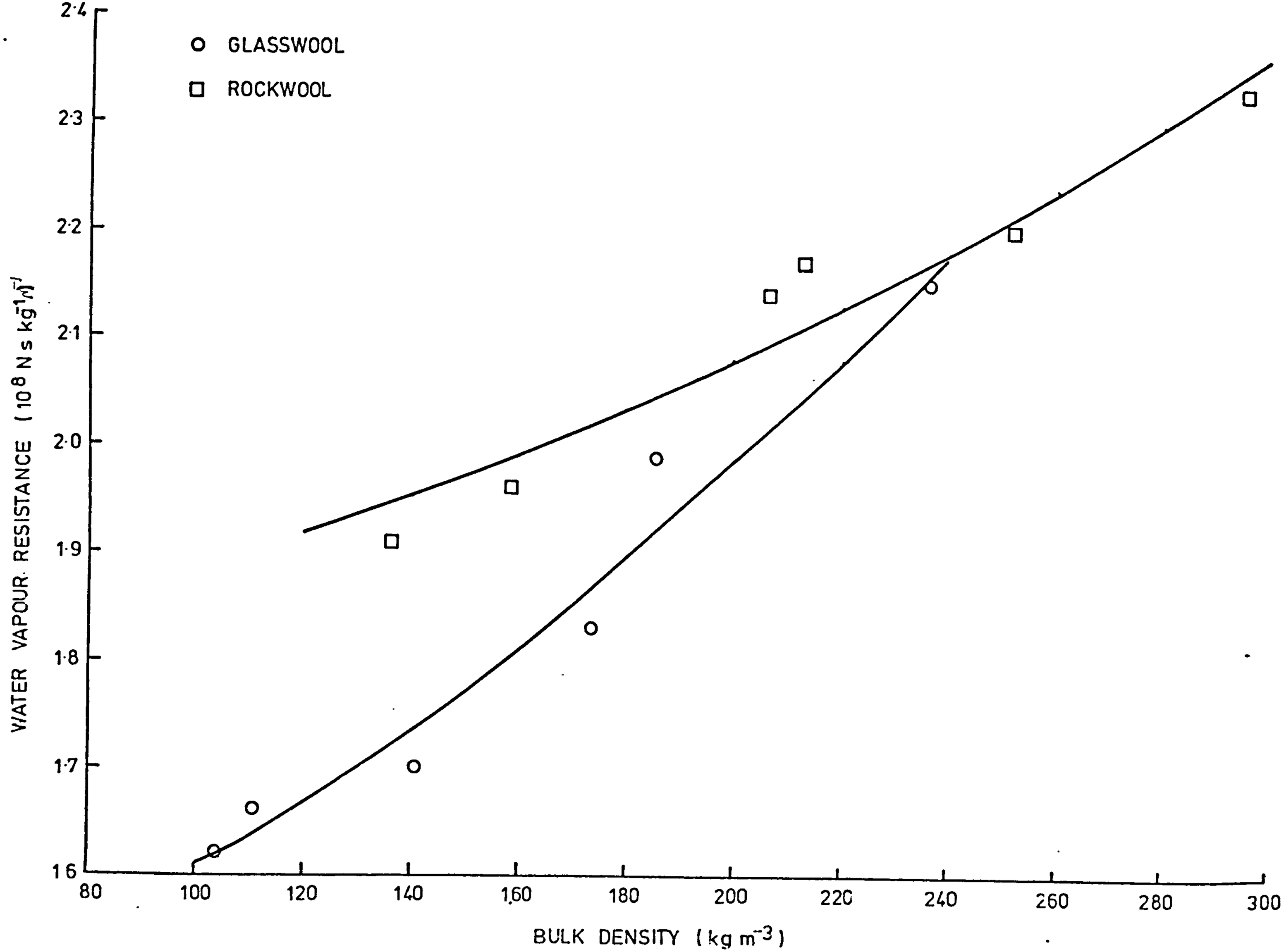

FIG. 3. VARIATION OF WATER VAPOUR RESISTANCE WITH BULK DENSITY FOR ROCKWOOL & GLASSWOOL

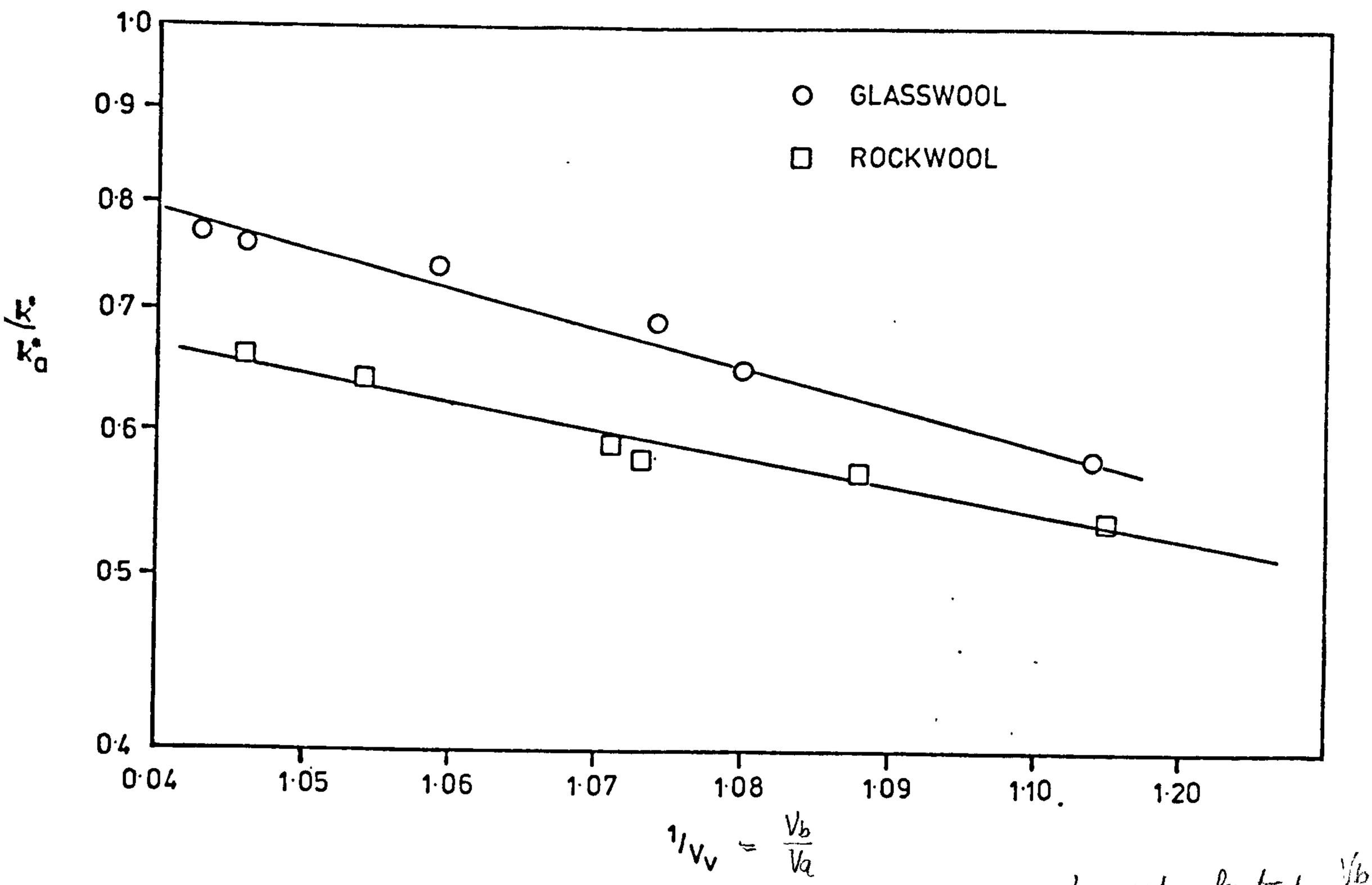

FIG. 4 GRAPH OF $\ln k^*/k_a^*$ AGAINST $1/V_v$

$$\frac{k^*}{k_a^*} = ab^{\left(\frac{V_b}{V_a}\right)} \qquad -(3)$$

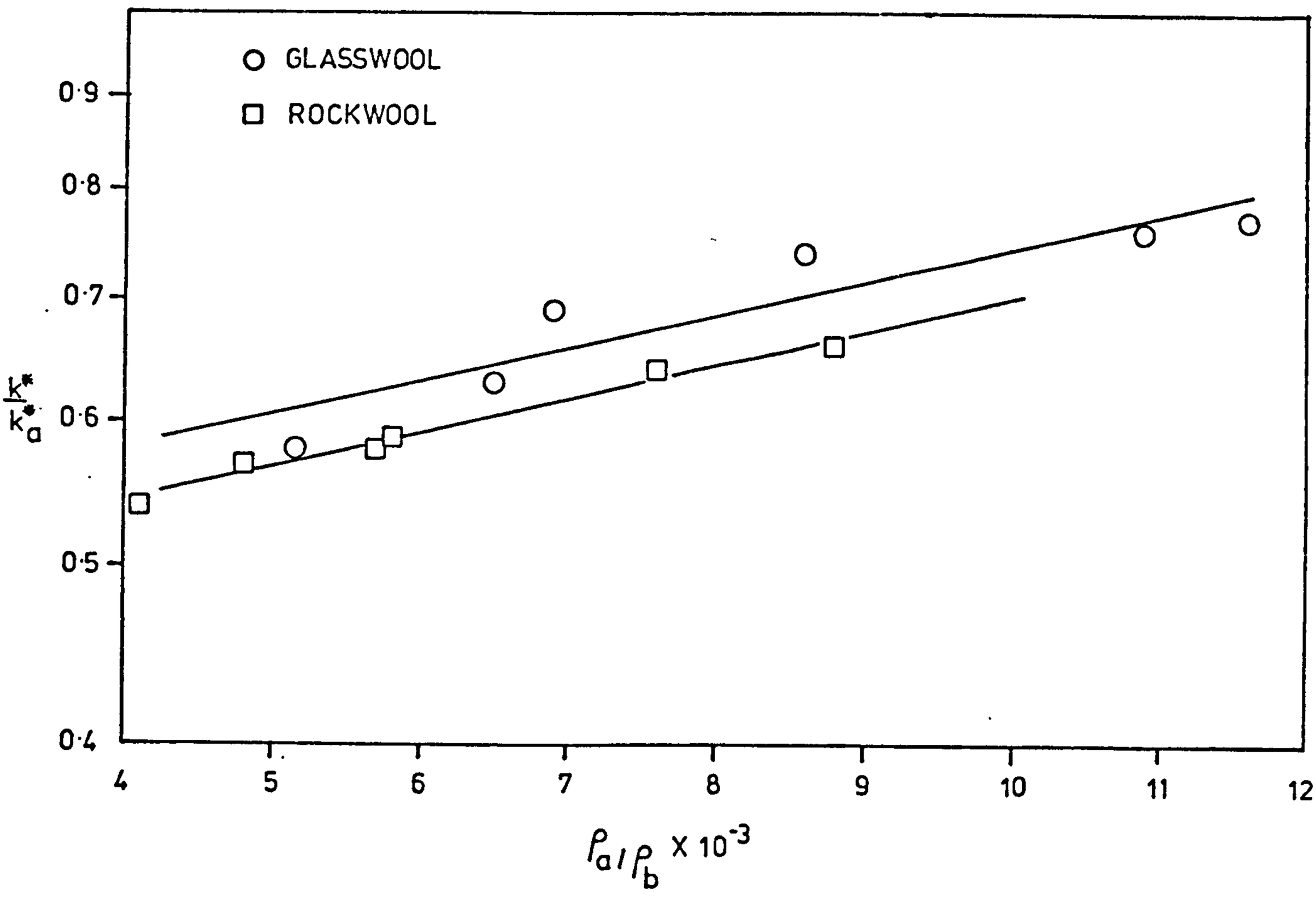

FIG. 5. GRAPH OF $\ln k^*/k_a^*$ AGAINST ρ_a/ρ_b

DISCUSSION

It can be seen from Table 2 that the method of measurement appears to affect the nominally similar specimens, and so great care is needed when using water-vapour permeability data. The discrepancies between the results from the dry and wet-cup methods could be due to a reduction in the absorptive ability of the desiccant as the water vapour is taken up. This would lead to changes in vapour-pressure difference and consequently in water-vapour permeability.

The water-vapour permeability of a material can be defined by the expression

$$k^* = \frac{k_a^*}{\kappa} \qquad \text{..... (14)}$$

where κ is a dimensionless diffusion resistance factor. The Chartered Institute of Building Services (I.H.V.E.) 1970 Guide gives a dimensionless diffusion resistance factor for mineral wool of 1.03, whereas Billington (16) suggested a value of 1.1.

If the water-vapour permeability of air is taken as 20×10^{-11} kg m N^{-1} s^{-1} (3) then such diffusion resistance factors give water-vapour permeabilities of 19.4×10^{-11} and 18.2×10^{-11} kg m N^{-1} s^{-1} respectively for glass wool and rockwool. The values obtained in the present investigation using specimens under no-load conditions gave values of 15.4×10^{-11} kg m N^{-1} s^{-1} for glass-wool with a bulk density of 104.1 kg m^{-3} and 13.1×10^{-11} kg m N^{-1} s^{-1} for rock-wool with a bulk density of 136.2 kg m^{-3}. The values in the Guide are presented irrespective of bulk density.

It can be seen from figure 4 that the relationship between the water-vapour permeability and the volume voidage conform closely to the conditions set for equation (3). The 'least squares' method for fitting curves reveals:-

for glass wool $$\frac{k^*}{k^*_a} = 118\ (0.0081)^{1/V_v} \quad \ldots\ldots (14)$$

for rock wool $$\frac{k^*}{k^*_a} = 22.3\ (0.34)^{1/V_v} \quad \ldots\ldots (15)$$

The product of 'ab' for glass wool is 0.96 and approximates closely to the condition that ab = 1, whereas that for rock wool is 0.76. This latter discrepancy could well be due to the difficulty found in determining the density of the fibres. This was achieved by using the method of Huggins and Sun (17) from a knowledge of the chemical composition of the fibres. The fibres of the glass wool were assumed to have the density of soda glass. The volume voidage was calculated using the density method (18) as in equation (16):

$$V_v = \frac{1}{1 + \frac{(\rho_b - \rho_a)}{(\rho_g - \rho_b)}} \quad \ldots\ldots (16)$$

The relationship between the vapour permeability and the bulk density of the materials, Figure 5, was more difficult to define but over the range of densities considered conforms to exponential relation. Changes in the bulk density affect the volume voidage, the size of the individual voids and the fibre distributions. The shape of the fibre-void matrix also affects the vapour permeability (19) and it is thus difficult, theoretically, to relate the vapour permeability changes to those of the bulk density. If the range of bulk densities over which the vapour permeability measurements were taken was extended then the relationship should become more definite.

CONCLUSIONS

Increases in the bulk density of fibrous insulants cause decreases in their water-vapour permeabilities and increases in water-vapour resistances. The water-vapour permeability values for uncompressed insulants measured with the experimental rig compared within experimental error with those from the B.S. 4370 dry-cup method of test but it was found that the wet-cup method produced somewhat higher results.

ACKNOWLEDGEMENT

The authors wish to thank the Science Research Council for financial support of this project.

REFERENCES

1. N.S. Billington, "Commercial and domestic heating", Chartered Mechanical Engineer, Vol.26, 57-59, 1979.

2. R.M.E. Diamant, "Condensation in buildings" Heating & Air Conditioning Journal, Feb. - May 1979.

3 P.W. O'Callaghan, "Building for energy conservation", Pergamon Press, 1978.

4. I.H.V.E. Guide Book A, Institute of Heating & Ventilating Engineer London, 1970.

5. C. Bankvall, "Heat transfer in fibrous materials", J. of Testing & Evaluation, 1,3, 235-243. 1973.

6. D.R. Bates, Esso Chemicals Ltd., Private Communication.

7. P.J. Serada & N.B. Hutcheon, "Moisture equilibrium and migration in building materials", ASTM Special Technical Publication, No. 385, 1965.

8. A.H. Woodcock, "Moisture transfer in textile systems". Text. Res. J. 32, 1, 628-633, 1962.

9. H.E. Beckett, "Effect of moisture content on the thermal resistance of insulating wallboard", J.I.H.V.E. 4, 87, 1936.

10. A.V. Korsgaard & M.R. Byberg, "Driving rain tests with cavity-filled brick walls", Symp. RILEM/CIB, 'Moisture problems in buildings', Helsinki, 1965.

11. A.V. Korsgaard & T.L. Madson, "The thermal insulation of some typical Danish outer walls exposed to the natural climate", J.H.I.V.E., 35, 3, 106-118, 1967.

12. J.D. Babbitt, The diffusion of water vapour through various building materials, Canadian Journal of Research, Vol. 17, part 2, 15-32, 1939.

13. S. Gregory, Vapour diffusion and condensation in thermal insulants. M.Sc. Thesis, Cranfield Institute of Technology, 1978.

14. B.S. 4370, Methods of test for rigid cellular materials, B.S.I., London, part 2, pp. 10-13, 1973.

15. F. Levy, Vapour diffusion and vapour sealing, Insulation Journal, Vol. 5, part 112, pp. 53-55, 1962.

16. N.S. Billington, 'Thermal Properties of Buildings' Cleaver-Hume, London, 1952.

17. M.L. Huggins & K. Sun, "Calculation of density and optical constants of a glass from its composition in weight percentage", J. Am. Ceram. Soc. 26, 4, 1943.

18. W.J. Batty, "The effect of compression on the heat and mass transport properties of thermal insulants", M.Sc. Thesis, Cranfield Institute of Technology, 1979.

19. D.A. Rose, "Water movement in porous materials: Part 1 - isothermal vapour transfer. Brit. J. Appl. Phys., Vol. 14, pp. 256-262, 1963.

PAGE NUMBERING AS ORIGINAL

CHAPTER 4.

ASSESSMENT OF THE THERMAL-PROBE TECHNIQUE FOR RAPID, ACCURATE MEASUREMENTS OF EFFECTIVE THERMAL CONDUCTIVITIES.

N O M E N C L A T U R E

A, B, C, D	parameters in equation (5)	
a	accuracy, as defined by equation (10)	
b	smallest distance between probe and the specimen boundary	m
c	specific heat capacity of the probe	$Jkg^{-1}\ K^{-1}$
d	'instrument' discrepancy	%
$\bar{d}$	mean 'instrument' discrepancy	%
H	thermal contact conductance	$Wm^{-2}\ K^{-1}$
k	thermal conductivity of the material under test	$Wm^{-1}\ K^{-1}$
$\bar{k}$	mean of measured thermal conductivities	$Wm^{-1}\ K^{-1}$
L	probe or hot-wire length	m
M	mass per unit length of probe	$kg\ m^{-1}$
n	number of data points in a single sample	
p	the digitised label for the particular probe being used	
$\dot{Q}$	power dissipated per unit length of probe	Wm^{-1}

R	Repeatability (≡ half-range random uncertainty)	
r_o	probe radius	m
S	a parameter defined by equation (8)	
S_i	component systematic uncertainty	
T	temperature	K
t	t-statistic, as defined by equation (9)	
t_ℓ	length of period of heating	s
x_c	reading of a 'calibrator'	
x_i	reading of an instrument	
$\bar{x}_i$	sample mean	
α	thermal diffusivity of the material under test $(= k/\rho c)$	$m^2\ s^{-1}$
δ	thickness of probe sheath material	m
ε	the ratio k_p/k	
γ	Euler's constant = 0.5772	
λ	probe length-to-diameter ratio	
η	$k_p\alpha/k\alpha_p$	
ρ	density of the material under test	$kg\ m^{-3}$

σ	aspect ratio
σ_d	standard deviation of the instrument's discrepancy
σ_s	sample standard deviation

Subscripts

B	for the brick
BL	for the aerated concrete block
c	of the copper
i	of the insulant
p	for the probe
s	of the stainless steel

Prefixes

$( )_0$	a relatively small term of the order of whatever is contained within the bracket.
Δ_R	relative error in Q due to axial heat flows.

THE THERMAL-PROBE TECHNIQUE

The line-source probe usually consists of a heater constructed from a cylinder, of radius r_o, with a linear heater wire at its axis. A thermo-junction is attached to the heater wire at the mid-length of the probe, so that excellent thermal contact between the two ensues. The probe, when fitted into a specimen of the material to be tested, should exude a time invariant heat flow per unit length.

The theory of the transient heat-flow method using a line source was developed in Carslaw and Jaeger (1), which for long heating periods gave the solution

$$T = \frac{\dot{Q}}{4\pi k}\left[\left(\ln \frac{4\alpha t_\ell}{r_o^2}\right) - \gamma\right] \qquad \ldots (1)$$

and consequently

$$T_2 - T_1 = \frac{\dot{Q}}{4\pi k} \ln \frac{t_{\ell 2}}{t_{\ell 1}} \qquad \ldots (2)$$

for a perfectly-conducting line source of infinite length, surrounded by an infinite medium. Equation (1) is valid for large times i.e. when $\alpha t_\ell / r_o^2 \gg 1$, where r_o is the radius of the probe and α is the thermal diffusivity of the material being tested.

A curve of temperature versus the natural logarithm of t_ℓ has a linear asymptote of slope $\dot{Q}/4\pi k$. So if $\dot{Q}$, the power dissipated per unit length, is measured then k may be determined easily.

If the probe technique is to be utilised under real engineering conditions, rather than merely in controlled laboratory situations, then the effects of departures from ideal conditions on the accuracy of thermal

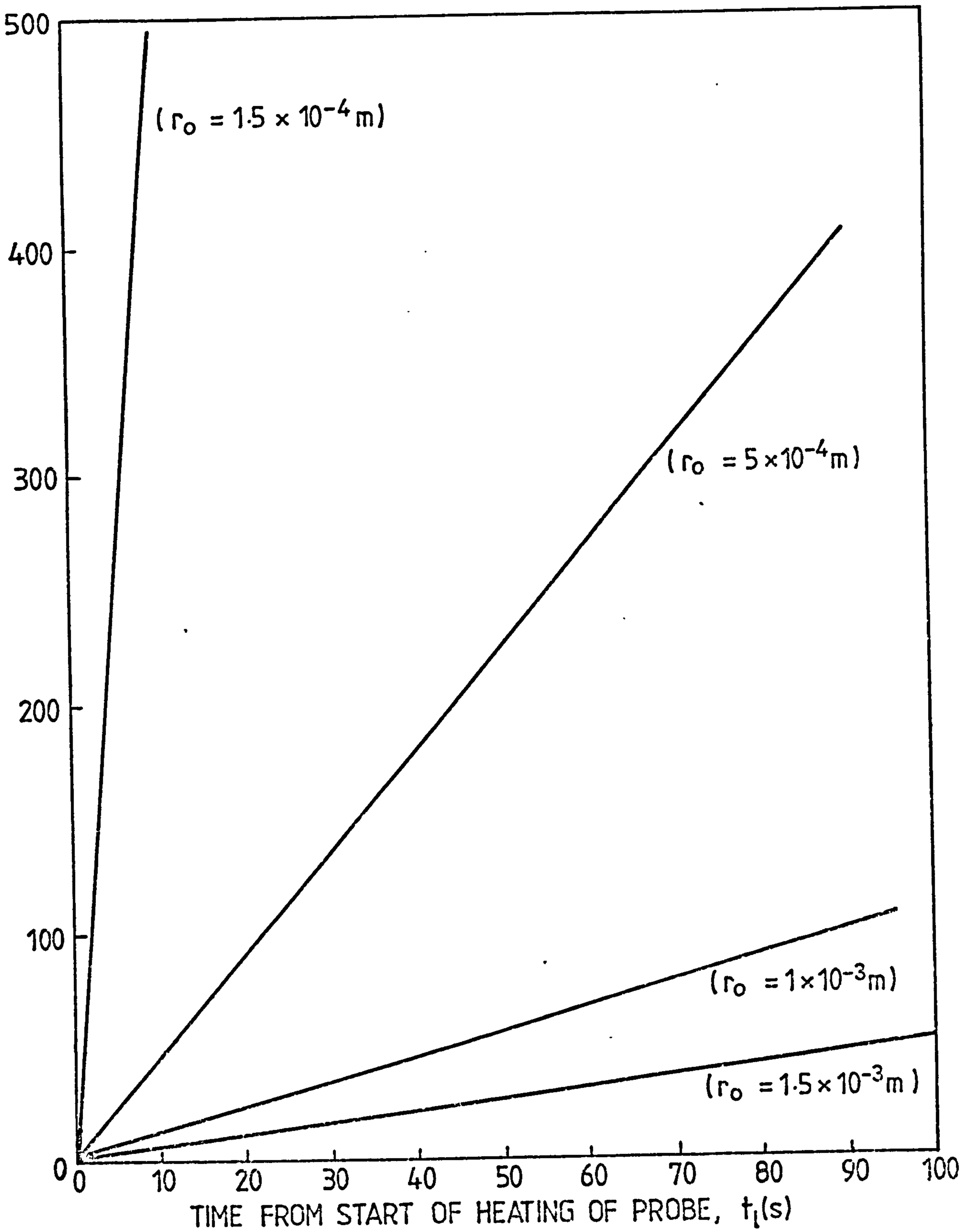

FIG. 1 THE r_o EFFECT FOR GLASS WOOL WITH A BINDER
($\alpha = 2.8 \times 10^{-7} m^2 s^1$)

conductivity determinations must be assessed. For instance the effects of the finite radius of the probe and the finite dimensions of the specimen have been considered by Vos (2). It was concluded that the temperature versus ln t_ℓ can within experimental error only be taken as a straight line if $4\alpha t_\ell / r_o^2 > 50$. The influences of these factors can be seen in Figures 1 and 2.

Equation (1) only holds true for an infinite medium, i.e. if there are no disturbances due to the presence of boundaries of the test sample with other materials. According to Vos (2), the boundary effects become significant if

$$4\alpha t_\ell / b^2 > 0.6 \qquad \ldots (3)$$

where b represents the shortest distance between the heater wire and the nearest boundary of the test specimen. Anderson and Bäckström (3) used the theoretical derivations of Carslaw and Jaeger (1) for heat flows through a semi-infinite solid, with varying surface temperatures, to obtain an estimate of the influence of the outer boundary of the finite medium. It was concluded that the effect of the test sample being finite in extent on the probe temperature was less than 0.1% when $4\alpha t_\ell / b^2 < 1$, which is very similar to the condition stated by Vos (2). The thermal properties of the medium beyond the boundary will affect the rate of transference of the heat pulse, and thus influence the temperature at the probe. The phase of the disturbance will depend upon the time taken for the pulse to travel twice the distance between the probe and the boundary in the media under consideration.

It can be seen from Figures 1 and 2 that the periods required before the temperature versus ln (t_ℓ) curve may be described by its asymptote are highly dependent upon the radius of the probe and the thermal diffusivity of the material under test. Thus careful consideration must be devoted to these two effects before an appropriate probe is designed for use with specimens of limited dimensions.

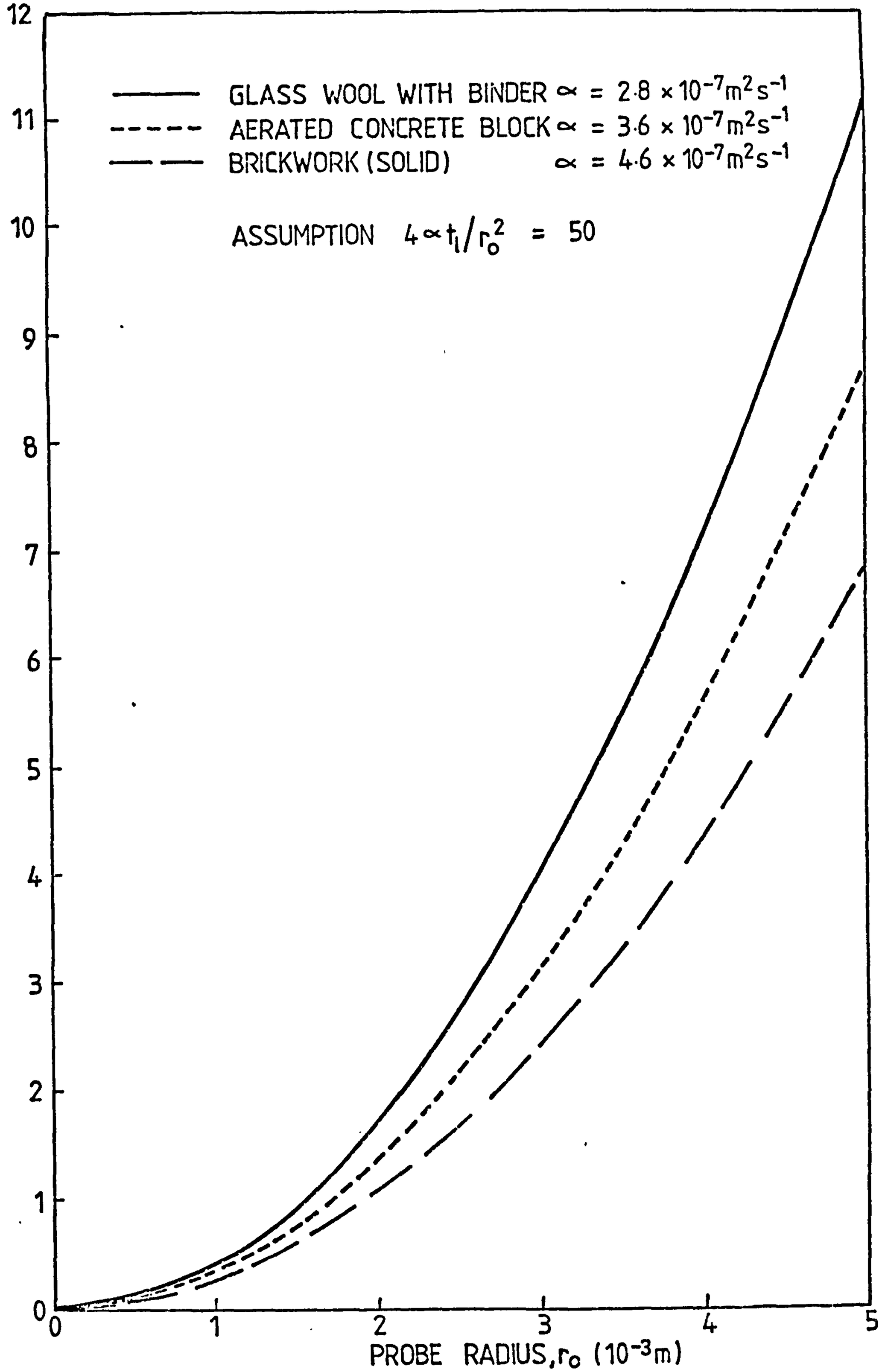

FIG. 2 PERIOD OF TIME ELAPSED FROM COMMENCEMENT OF HEATING VERSES PROBE RADIUS (r_o) FOR GLASS WOOL WITH A BINDER, BRICK AND AERATED CONCRETE BLOCK

Blackwell (4) contended that basic inadequacies in the mathematical analyses and in the treatment of experimental data occurred in using the probe technique. He suggested that the theory should be revised completely in view of the following:-

(i) It had been assumed, to a first approximation, that the behaviour of the probe can be represented theoretically as a continuous line source of heat. The correction for the probe's finite diameter (applied by van der Held and van Drunen (5),who proposed that the presence of the probe in the test material was equivalent to heat being released before the start of the measured period) was considered to be of dubious validity.

(ii) Thermal contact resistance at the boundary between the probe and its surrounding medium was assumed to be zero. Blackwell held that this was not true. Large contact resistances often ensue in geophysical applications where the use of long drills results in loosely-fitting probes.

(iii) Only semi-intuitive estimates had been made of the minimum acceptable lengths for the probe.

In consequence, Blackwell refined the theoretical method. For instance the inclusion of contact resistance at the probe boundary complicated the long-time solutions used by previous workers. Also it was deemed desirable to determine the contact resistance independently. A solution subject to the same boundary conditions, but valid for short heating periods, facilitated this determination. Calculations were made to determine the miminum probe length for the radial flow assumption to be reasonably accurate for real applications.

The expression derived for the temperature in the considered specimen, is, as a function of time

$$T(t) \simeq \frac{\dot{Q}}{4\pi k}\left\{\ln\left(\frac{4\alpha t_\ell}{r_o^2}\right)-\gamma+\frac{2k}{r_o H}+\frac{r_o^2}{8\alpha t_\ell}\left[\ln\left(\frac{4\alpha t_\ell}{r_o^2}\right)-\gamma+1-\frac{\alpha M_p\, c_p}{\pi r_o^2\, k}\left(\ln\left(\frac{4\alpha t_\ell}{r_o^2}\right)-\gamma+\frac{2k}{r_o H}\right)\right]+O\left(\frac{r_o^2}{\alpha t_\ell}\right)^2\right\} \quad \ldots (4)$$

which reduces to:-

$$T(t) \simeq A\left[\ln(t_\ell)+B+\frac{1}{t_\ell}\left(C\ln(t_\ell)+D\right)\right] \quad \ldots (5)$$

where

$$A = \frac{\dot{Q}}{4\pi k}$$

$$B = \frac{\dot{Q}}{4\pi k}\left[\ln\left(\frac{4\alpha}{r_o^2}\right)-\gamma+\frac{2k}{r_o H}\right]$$

$$C = \frac{r_o^2}{2\alpha}\left[1-\frac{\alpha M_p c_p}{\pi r_o^2 k}\right]$$

$$D = \frac{r_o^2}{2\alpha}\left[\ln\left(\frac{4\alpha}{r_o^2}\right)-\alpha+1-\frac{M_p c_p \alpha B}{\pi r_o^2 k}\right]+O\left(\frac{1}{t_\ell^2}\right)$$

For long-period solutions, i.e. when $\frac{\alpha t_\ell}{r_o^2} >> 1$, the contribution of the $\frac{1}{t_\ell}$ terms of equation (5) become negligible. Under this condition, the

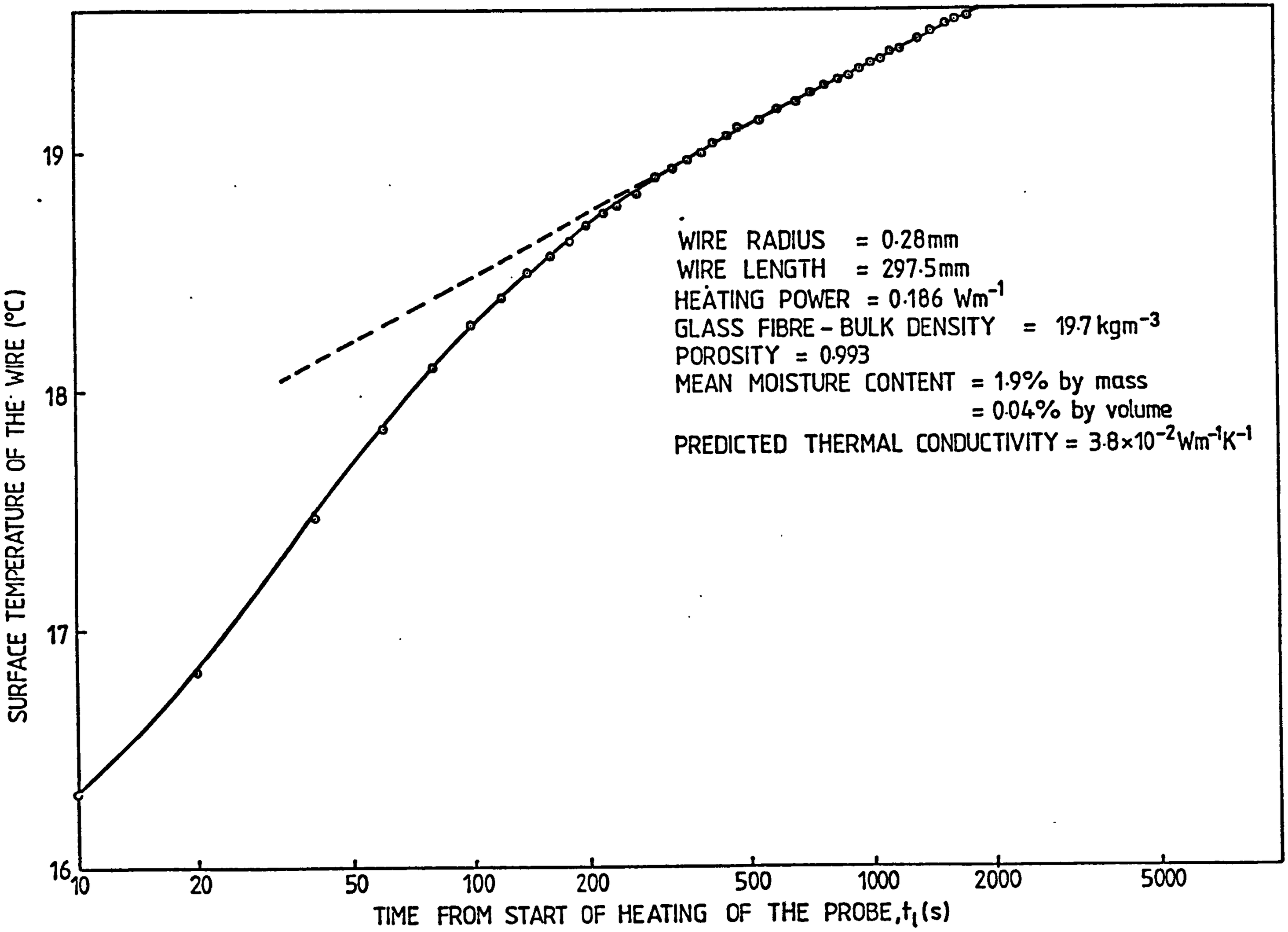

FIG.3. TEMPERATURE VS. TIME CURVE FOR A HOT-WIRE IN A SAMPLE OF GLASS FIBRE INSULANT.

fitting of equation (5) to experimental data yields the thermal conductivity of the surrounding medium directly from parameter A. The value of B may be used to assess the thermal diffusivity of the measured medium if $2k/r_oH$ is negligible (i.e. the outer surface conductance H is very large) or if the value of H is known. A procedure for assessing the value of H, by utilising a 'short time' solution, was derived by Blackwell (4). It is important that the nature of the material, whose behaviour is being observed, should be considered. The thermal conductivity of an inhomogeneous material depends upon the region within the specimen where the temperature indications are being observed, and the radius vector of the radial direction from the probes axis through the thermojunction. Measurements of short duration, utilising transient techniques satisfying the condition that $\alpha t_\ell/r_o^2 \gg 1$, can yield values for the apparent thermal conductivity that may not be representative of the whole specimen, because they refer only to the localised volume around the probe. Measurements taken over much longer periods are more likely to provide an average value of the apparent thermal conductivity pertinent to the whole volume of the test specimen. This is illustrated in figure 3, which shows the temperature versus ln t_ℓ curve for a hot wire in a sample of glass fibres. In this specimen, for $\alpha t_\ell/r_o^2$ to become much greater than unity, say equal to 50 with $r_o = 2.8 \times 10^{-4}$m and $\alpha = 2.8 \times 10^{-7}m^2s^{-1}$, then this condition can be satisfied after 14 seconds. Examination of figure 3, however, shows that a linear relationship between temperature and ln t_ℓ does not ensue until at least 300 seconds after the start of the test.

A method for determining the thermal diffusivity of a medium, utilising long-time solutions for which equation (1) is valid rather than short-time solutions, was derived by Sandberg et al (6).

The final accuracy of determining the thermal conductivity was considered to depend mainly upon the accuracy of data fitting (4). The assumption of a straight-line relationship over the range where ΔT versus $\ln(t_\ell)$ plot becomes asymptotic could introduce significant errors unless a high minimum value of $\alpha t_\ell/r_o^2$ was used, so corroborating the conclusion of Vos (2).

If the entire equation (4) could be utilised via the 'least-squares' method to fit the experimental data, then much smaller values of $\alpha t_\ell/r_o^2$, could be tolerated and shorter measuring periods employed. Equation (4), however, contains terms in $\ln t_\ell$ and $1/t_\ell$.

To avoid significant errors due to axial heat losses, Blackwell (4) derived a condition for the minimum probe length-to-radius ratio, namely

$$\frac{L}{r_o} \geqslant \left(\frac{\alpha t_\ell}{0.0632\ r_o^2}\right)^{\frac{1}{2}} \qquad \ldots (6)$$

for errors in the value of k due to axial flows to be less than ½ percent.

Blackwell gave further consideration to the uncertainties arising from axial heat flow errors (7, 8). For a specified length-to-radius ratio, an expression for the relative error due to the presence of an axial heat flow was deduced (8), namely

$$\Delta R = \pi^{-\frac{1}{2}} \exp\left[-\left(\frac{L}{r_o}\right)^2 \Big/ \left(\frac{4\alpha t_\ell}{r_o^2}\right)\left[\left(\frac{4\alpha t_\ell}{r_o^2}\right)^{\frac{1}{2}} \Big/ \left(\frac{L}{r_o}\right) + 2\sigma \frac{LS}{r_o}(\varepsilon - n)\left(\frac{4\alpha t_\ell}{r_o^2}\right)^{-\frac{3}{2}}\right]\right]$$

.... (7)

where $\varepsilon = \dfrac{k_p}{k}$

$\eta = \dfrac{k_p \alpha}{k \alpha_p}$

$\sigma = \dfrac{2\delta}{r_o}\left(1 - \dfrac{\delta}{2r_o}\right) \simeq \dfrac{2\delta}{r_o}$ for a thin-walled hollow probe

$\sigma = 1$ for a solid probe

and $S = \ln\left(\dfrac{4\alpha t_\ell}{r_o^2}\right) - \gamma + \dfrac{2k}{r_o H}$ ... (8)

The error in the measured effective conductivity arising from axial heat leaks increases with the duration of the heating period, so that the times used

in this expression should be those at which the measurement is completed. It is possible, by making assumptions for the minimum values of H, to assess the minimum required length-to-radius ratios for the probes.

There is a fundamental difference of approach inherent in equations (6) and (7). The first considers the effects of the probe radius and thermal diffusivity of the surrounding medium only, whereas equation (7) makes due allowances for the conductivities and diffusivities of both the surrounding medium and the probe. The latter would appear to be the wiser procedure to adopt because this gives some allowance for the effects of the material used in the probe construction. Such considerations suggest that larger probe length-to-radius ratios would be required for probes constructed of good conductors,which would provide an easier heat flow path along the probe length. It is also apparent that the thermal diffusivities of the materials involved, for both the medium and the probe, will affect the minimum length-to-radius ratio.

The graphs in figures 4 → 8 illustrate the changes in the influential parameters with respect to probe length-to-radius ratios. An axial heat flow which was 50% of the total rate of heat released from the probe would,for example,result in apparent thermal conductivities one half of the actual values, the corresponding ΔR being unity. As the probe length is reduced from this value and tends to zero, the error ΔR approaches infinity. The contact resistance of the glass-fibre insulant with the probe was considered to be relatively small compared with the thermal resistances provided by the insulant. Such materials have porosities $\geqslant$ 90% . The probability of probe contact with the local fibres is relatively high because the probe is pushed into such an insulant i.e. creating its own 'bore hole' by slightly pushing aside the fibres. Fibre/probe contacts should be better than those between fibres.

For the purpose of comparison, contact resistance has been neglected for brickwork and aerated concrete block in figure.6, but the effect of surface conductance can be clearly seen in figure 7.

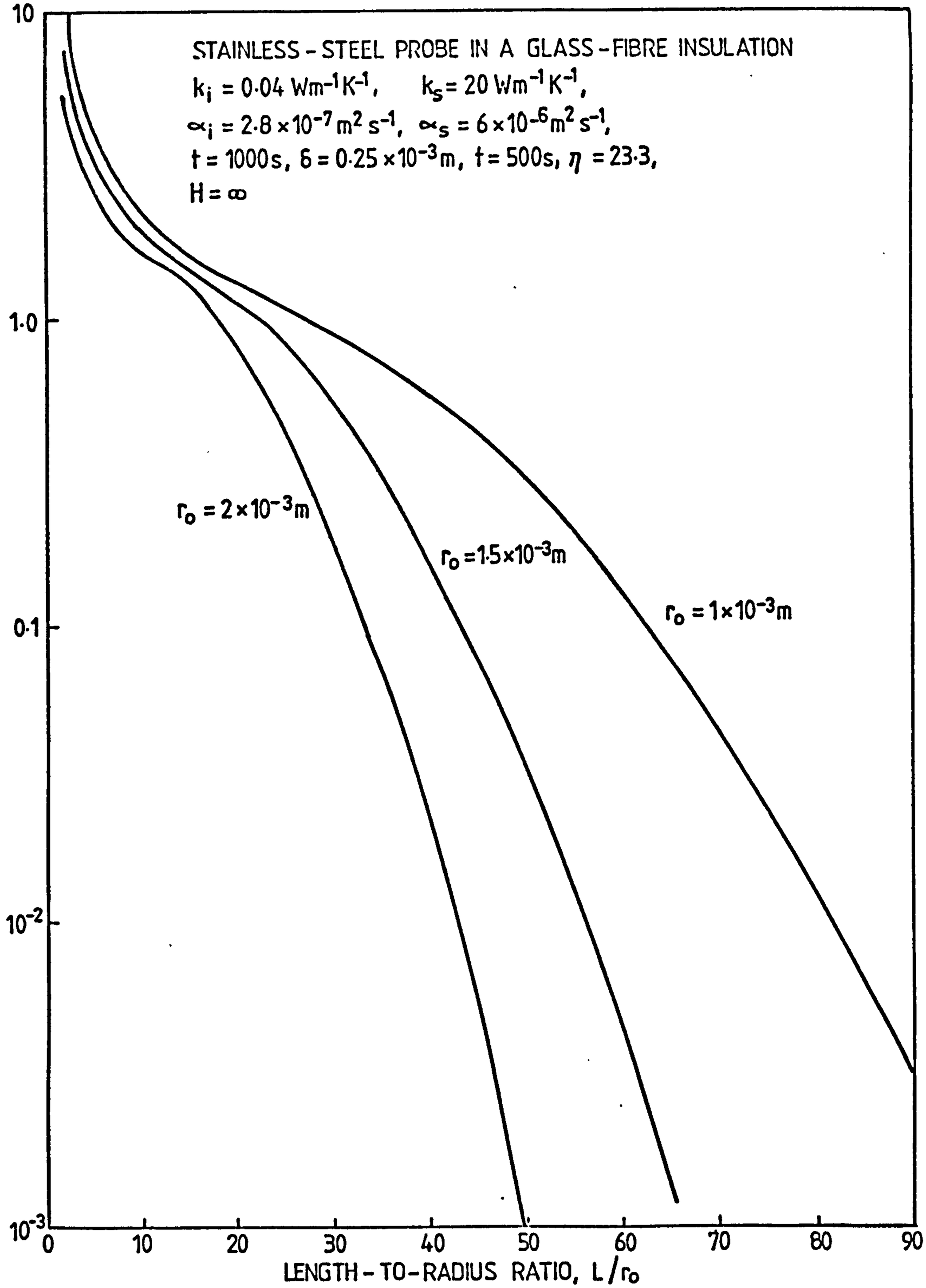

FIG. 4 EFFECT OF PROBE RADIUS ON THE VALUE OF RELATIVE AXIAL FLOW ERROR ΔR

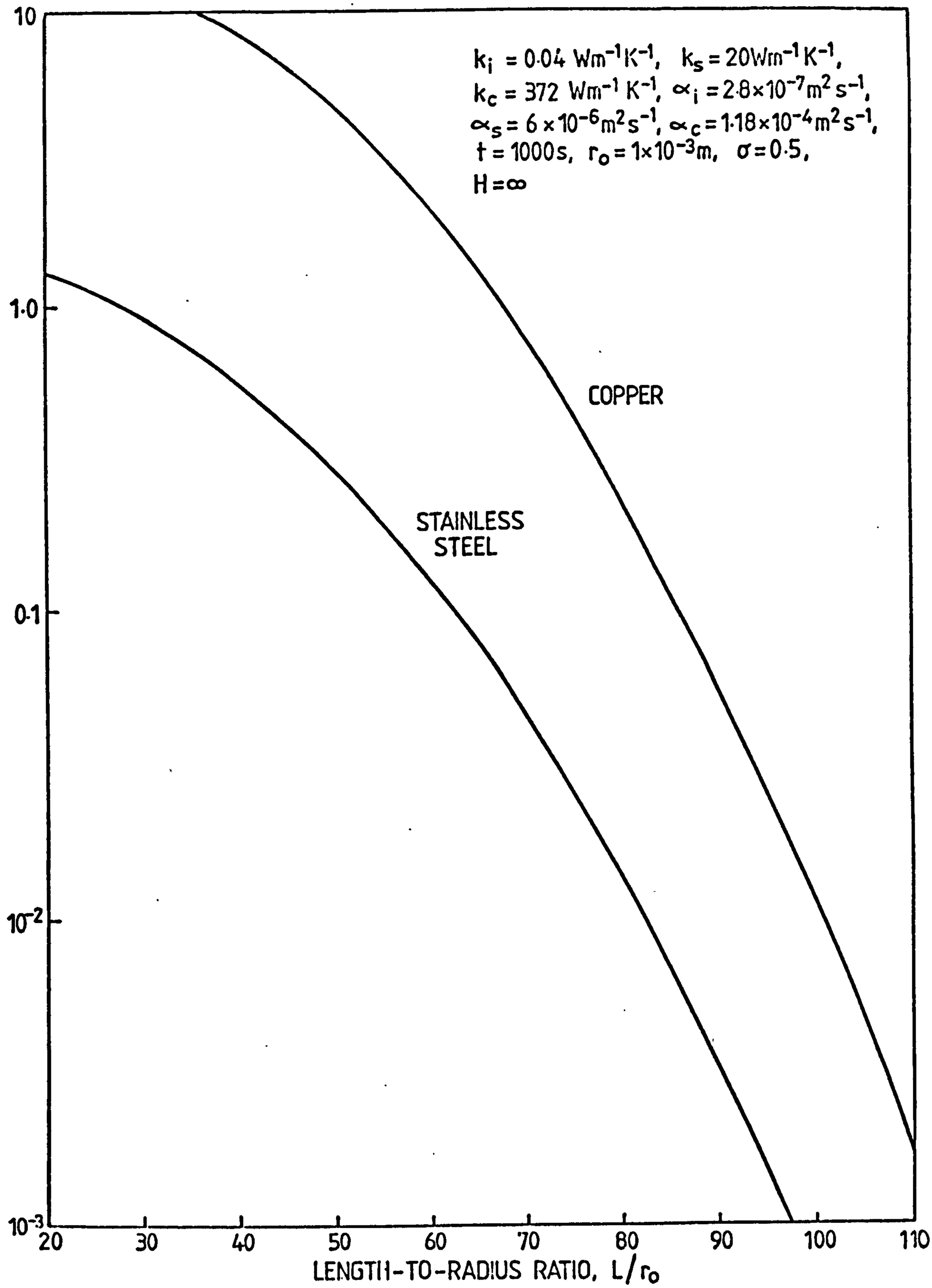

FIG. 5 COMPARISON OF THE RELATIVE ERRORS DUE TO THE AXIAL FLOW WITH LENGTH-TO-RADIUS RATIO FOR COPPER OR STAINLESS-STEEL PROBES IN A GLASS-FIBRE INSULANT

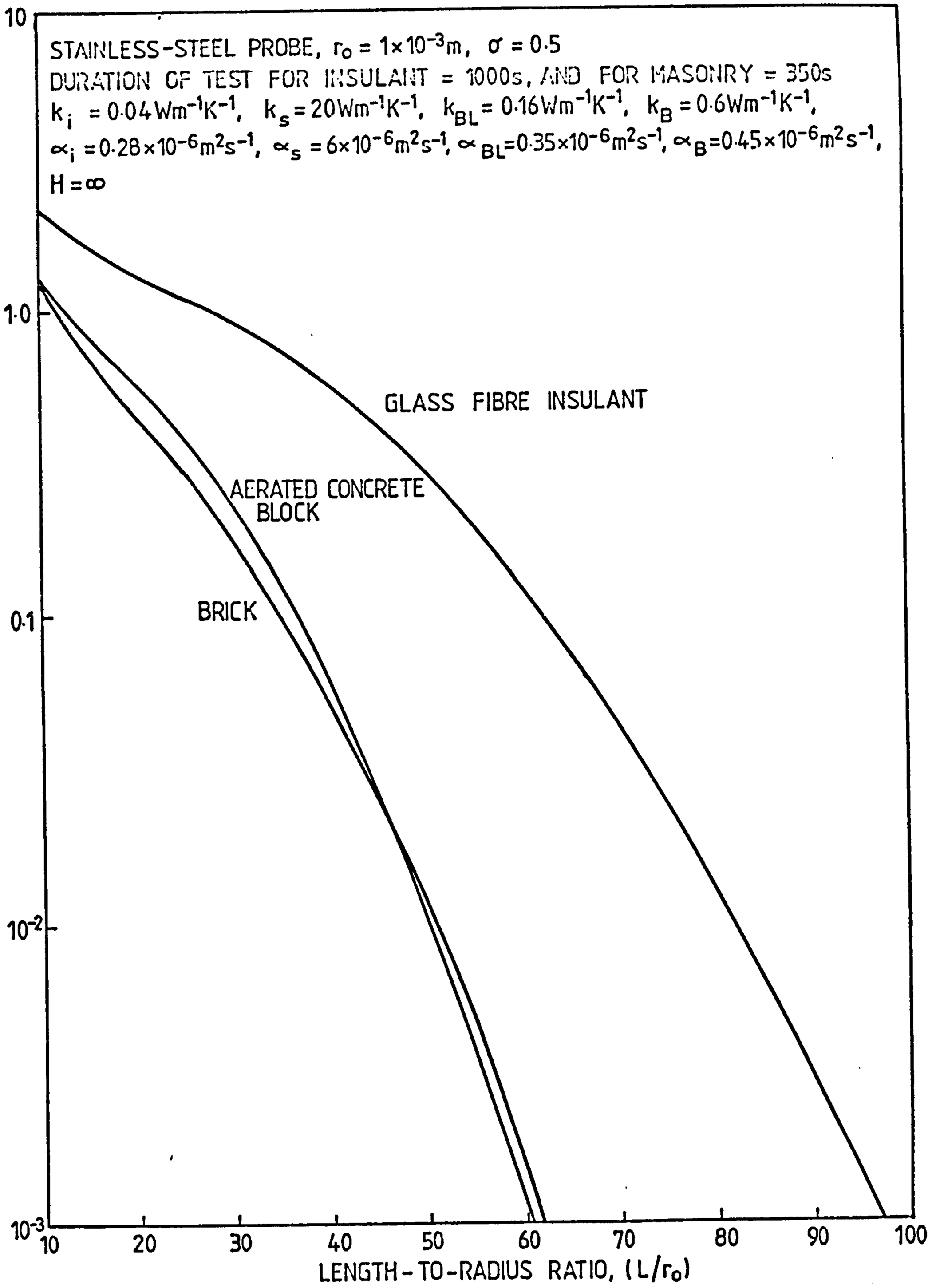

FIG.6 EFECTS OF THE THERMAL PARAMETERS OF THE MEASURED MEDIA UPON THE RELATIVE ERROR DUE TO AXIAL FLOWS FOR VARIOUS LENGTH-TO-RADIUS RATIOS OF THE PROBE.

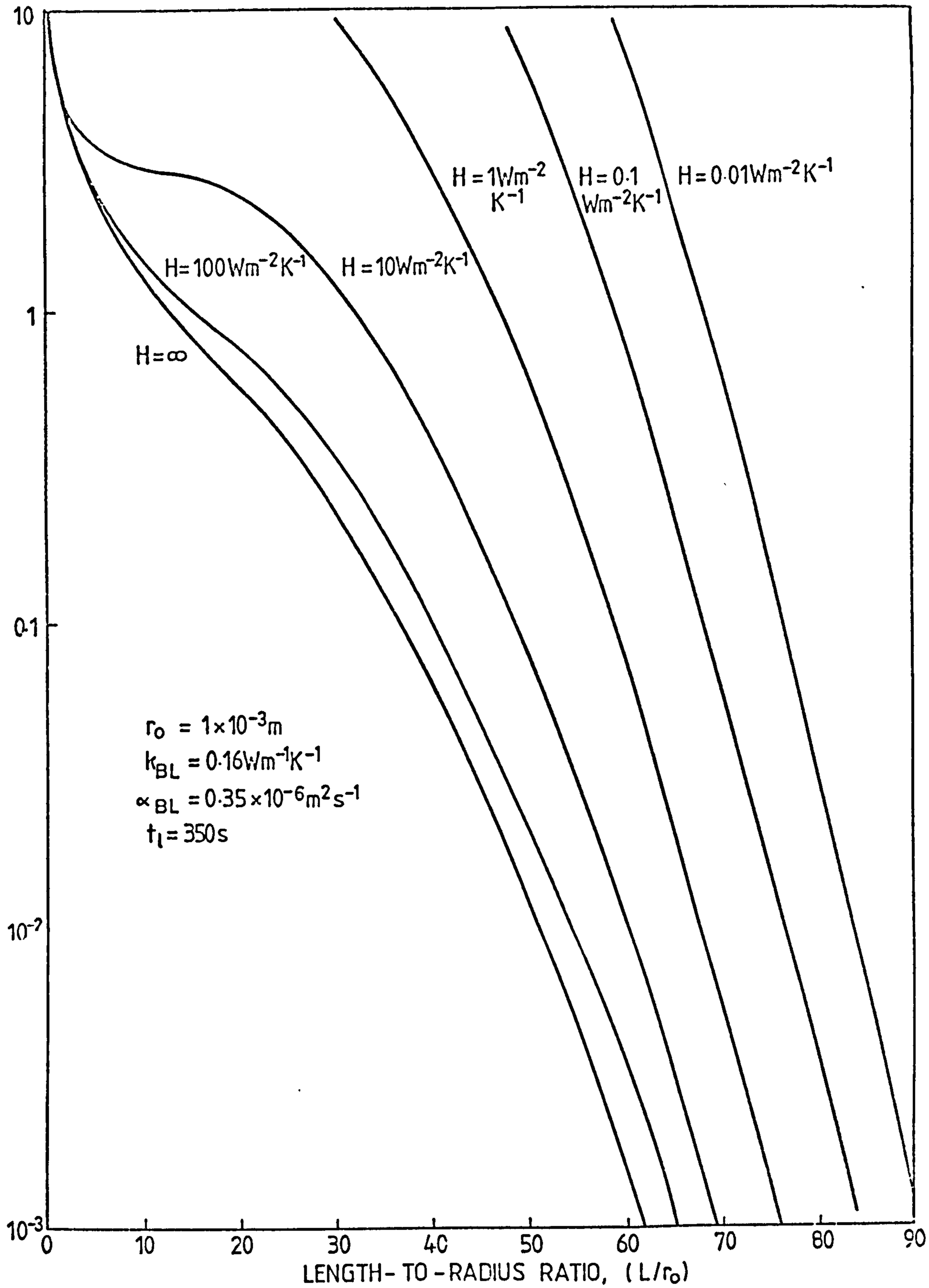

FIG.7. EFFECTS OF SURFACE CONDUCTANCE BETWEEN PROBE AND SPECIMEN ON THE RELATIVE ERROR DUE TO AXIAL FLOWS FOR VARIOUS LENGTH-TO-RADIUS RATIOS FOR STAINLESS-STEEL PROBES IN AERATED CONCRETE BLOCK.

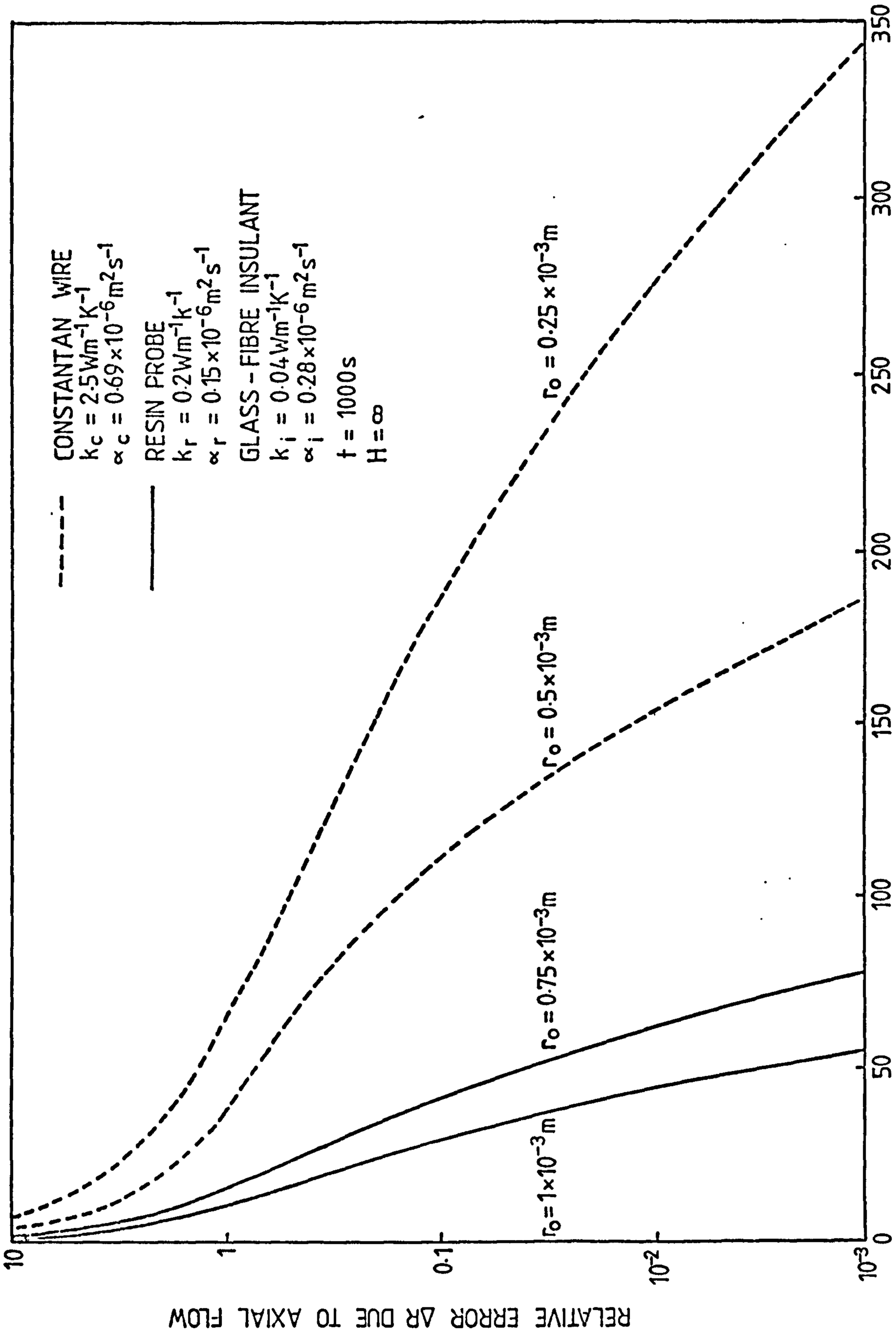

FIG.8. EFFECTS OF THE RADIUS OF THE PROBE ON THE AXIAL FLOW ERROR FOR RESIN PROBES AND CONSTANTAN HOT WIRES IN A GLASS-FIBRE INSULANT.

Accurate thermal conductance data for pressed contacts in air at atmospheric pressures are rare; most of the reliable contact measurements being carried out under high vacuum - a more universally achievable common condition. A guide to the magnitudes of contact conductances may be obtained from Ozisik and Hughes (9) who found values of 1900 $Wm^{-2}K^{-1}$ for a contact between stainless steel surfaces of 0.2 μm and 1 μm r.m.s. roughnesses at a mean interfacial temperature of 167°C, the actual contact area was 0.25 percent of the nominal contact area at an interfacial loading of 7 atmospheres. Holman (10) gave values of 1890 $Wm^{-2}K^{-1}$ for the contact between nominally identical "flat" stainless steel surfaces of 1.14 μm r.m.s. roughness at 20°C under a loading of 55 atmospheres, and 3790 $Wm^{-2}K^{-1}$ for stainless steel surfaces of 2.54 μm r.m.s. roughness at an interfacial temperature of 145°C and contact loading of 14 atmospheres. These data suggest that an assumption of contact conductances of the order of 100 $Wm^{-2}K^{-1}$ for the calculation of acceptable length to radius ratios would be reasonable when considering metal-sheath probes, of roughness ≃ 1 μm, making tight fits in drilled holes in masonry materials.

Before the probe designs were finalised, consideration was given to several other constraints, not least of which were the abrasive materials into which the probes needed to be placed, and the finite sizes of the specimens tested.

It was decided to follow the example of Blackwell (4) and aim to achieve axial-flow errors of 0.5 percent (or less) in the measured probe power when deciding on the length-to-radius ratio. This consideration led to probes of stainless steel and copper of radii 1.00 and 1.15 mm respectively with length-to-radius ratios of 60 and 64 respectively for insertion into masonry materials. Probes for use in insulants require sheath materials of much lower thermal conductivities so that the probes can be made sufficiently small to fit into these specimens, which in many applications are of limited dimensions. Stainless steel probes for use in thermal insulants would need ratios of 90 and 70 for probe radii of 10^{-3}m and 1.5×10^{-3}m, so leading to probe lengths of 0.090m and 0.105 m respectively. After a fruitless search for low conductivity materials available commercially in the required diameters, it was decided to mould an epoxy directly around the probe heater. The epoxy material possessed acceptable machanical properties for use in thermal insulants up to 100°C.

The epoxy resin's thermal conductivity of 0.19 → 0.21 $Wm^{-1}K^{-1}$ resulted in probe lengths of 0.050 and 0.047 m respectively for probes of this construction with radii 0.75 x 10^{-3}m and 10^{-3}m.

Initially it was believed desirable to test the probes in paraffin wax. This material possesses the advantage that it can be moulded around the probes, thereby reducing the contact resistance. It also exhibits a low thermal diffusivity, due to its large specific heat capacity, which means that probes designed for masonry or insulants should have more than twice the required length-to-radius ratios than those for use in the wax.

The tests in paraffin wax were used to ascertain the accuracy of the probes and the repeatabilities that could be achieved.

ACCURACY AND REPEATABILITY OF OBSERVATIONS WITH THE THERMAL CONDUCTIVITY PROBES

Unfortunately, at present, there is no accepted standard procedure for evaluating the accuracy of an instrument's indications. It is therefore proposed that the procedures laid down by Hayward (11) be followed.

Repeatability

By definition (12), repeatability is the ability of a measuring instrument to give identical indications or responses for repeated applications of the same value of the measured quantity under stated conditions of use. However, a more quantitative definition is needed if repeatability is to be quoted as a number or percentage.

Hayward (11) considered that the repeatability of an instrument is the half-range random uncertainty of a typical measurement made with the instrument under specified conditions of operation.

If a number of readings of an instrument are taken, they will differ due to various factors (beyond the control of the individual undertaking the experiment), such as small fluctuations in temperature, random electrical

effects in electronic equipment, vibrations or air currents within the laboratories. Because of these factors, each individual reading is subject to a random uncertainty. The greater the scatter of the observations about their mean value, the greater is the random uncertainty attaching to each observation. It should be noted that the mean value will also be subject to a random uncertainty, but this will be considerably less than that attached to the individual values.

If an infinite number of readings were taken, the random uncertainty of the mean would become zero. A limit, of say $\pm$ R, could be set on either side of this mean so as to encompass 95 percent of all values. Thus $\pm$ R would become a quantitative definition of the random uncertainty of all the measurements in this set.

This approach to the specification of random uncertainty relies upon a large number of repeat measurements. It was considered by Book (13) that, for all practical purposes, a large number of data points is 30 or more. Frequently, however, it is not possible or economically feasible to use a large sample. Nevertheless, small samples (of < 30 data points) can be dealt with, if it is assumed that these data points come from a Gaussian distributed population. Then for all samples of size n, no matter how large or small, the data numbers exhibit a t-distribution and t is defined(13) by

$$t = \frac{1}{\sqrt{n}} \quad \frac{(\bar{x} - \mu)}{\sigma_s} \qquad \ldots (9)$$

where $\bar{x}$ = sample mean,

μ = true mean of the population,

σ_s = sample standard deviation,

and n = number of data points in the sample.

Systematic uncertainties may also occur, which have the effect of weighting each measurement equally by the same amount and in the same direction. There is nothing random about such effects. For example, an apparently 1 kg mass that was in fact 0.005 kg overmass would result in all measurements being in error by that amount. When a systematic effect has been recognised and quantified, it is no longer an uncertainty, because the experimenter knows that it exists and can often take remedial action. In general, however, there will remain a small systematic effect which is undetectable with equipment at the investigators' disposal. As with random uncertainties, all one can hope to achieve is to try to set boundaries within which the residual systematic effect is 95 percent certain to occur.

Accuracy

Accuracy is a measure of an instrument's ability to tell the truth, whereas repeatability is a measure of its ability to tell the same story. Thus good repeatability is no guarantee of accuracy.

Hayward (11) asserted that to obtain a value for the accuracy of an instrument, its repeatability has to be combined with the half-range systematic uncertainty of its measurements. Whilst admitting that the manner in which these parameters may be combined is a matter of controversy, he suggests

$$\text{Accuracy} = \sqrt{\{(\text{repeatability})^2 + (\text{Half-range systematic uncertainty})^2)\}}$$

$$\text{i.e.} \quad a = (R^2 + S_1{}^2)^{\frac{1}{2}} \qquad \ldots (10)$$

Measuring the repeatability of an instrument

The experimental procedure by which repeatability may be assessed depends on the nature of the measurement made with the instrument. Parameters such as mass or thermal conductivity of a specimen under a given set of conditions may be considered as "static", whereas parameters such as time, wind velocity or electrical current are "transient" in nature. The thermal-conductivity probe may be considered as measuring a static quantity if the

conditions of temperature and humidity remain invariant throughout a series of tests. Repeated measurements should be made on the same sample with the instrument maintaining identical applied conditions. The standard deviation σ_s is then defined by:-

$$\sigma_s = \sqrt{\frac{1}{n-1} \sum_{j=1}^{n} (x_{ij} - \bar{x}_{ij})^2} \qquad \ldots (11)$$

This quantity, multiplied by the appropriate value of the t-distribution for the sample size at the 95 percent confidence level, gives the repeatability (11): namely

$$R = t\sigma_s \qquad \ldots (12)$$

Assessing the systematic uncertainty

The performance of the uncalibrated instrument should be compared with that of a calibrator, which must be at least four times as accurate as the instrument being calibrated. The use of a calibrator of this accuracy means that its own small uncertainty may be neglected when evaluating the uncertainty of the instrument.

If the reading x_i of the instrument being tested is compared with the reading x_c obtained from the calibrator, under identical conditions, then the results of the calibration can be expressed in terms of a percentage instrument discrepancy d, defined by:

$$\frac{x_c}{x_i} = 1 + \left(\frac{d}{100}\right) \qquad \ldots (13)$$

The value of d for all the measurements being considered is calculated and the mean discrepancy $\bar{d}$ and estimated standard deviation σ_d are assessed. The half-range systematic uncertainty of the instrument is then given by:

$$S_1 = \bar{d} + t\,\sigma_d \qquad \ldots (14)$$

where t is the appropriate value from the t-distribution for the sample size at the 95 percent confidence level.

Assessment of the repeatability and accuracy of the probes for measuring the thermal conductivity of paraffin wax

Five probes of each type were constructed and coded in the manner:-

MATERIAL/HEATER WIRE FORMAT/DIAMETER(in mm)/LENGTH:DIAMETER RATIO/PROBE NUMBER p

The materials were designated by the symbols

SS - stainless steel

Cu - copper

and the wire heater configuration by

S - single wire

D - double wire

Thus SS/D/2.05/30/1 is a stainless steel probe with a double wire heater of diameter 2.05 mm and a length-to-diameter ratio of 30.

Although most theoretical analyses are based on the length-to-radius ratio of the thermal probe, in practice because the diameter is the more direct measurement to obtain, the length-to-diameter ratio, is normally the chosen parameter for experimental investigations.

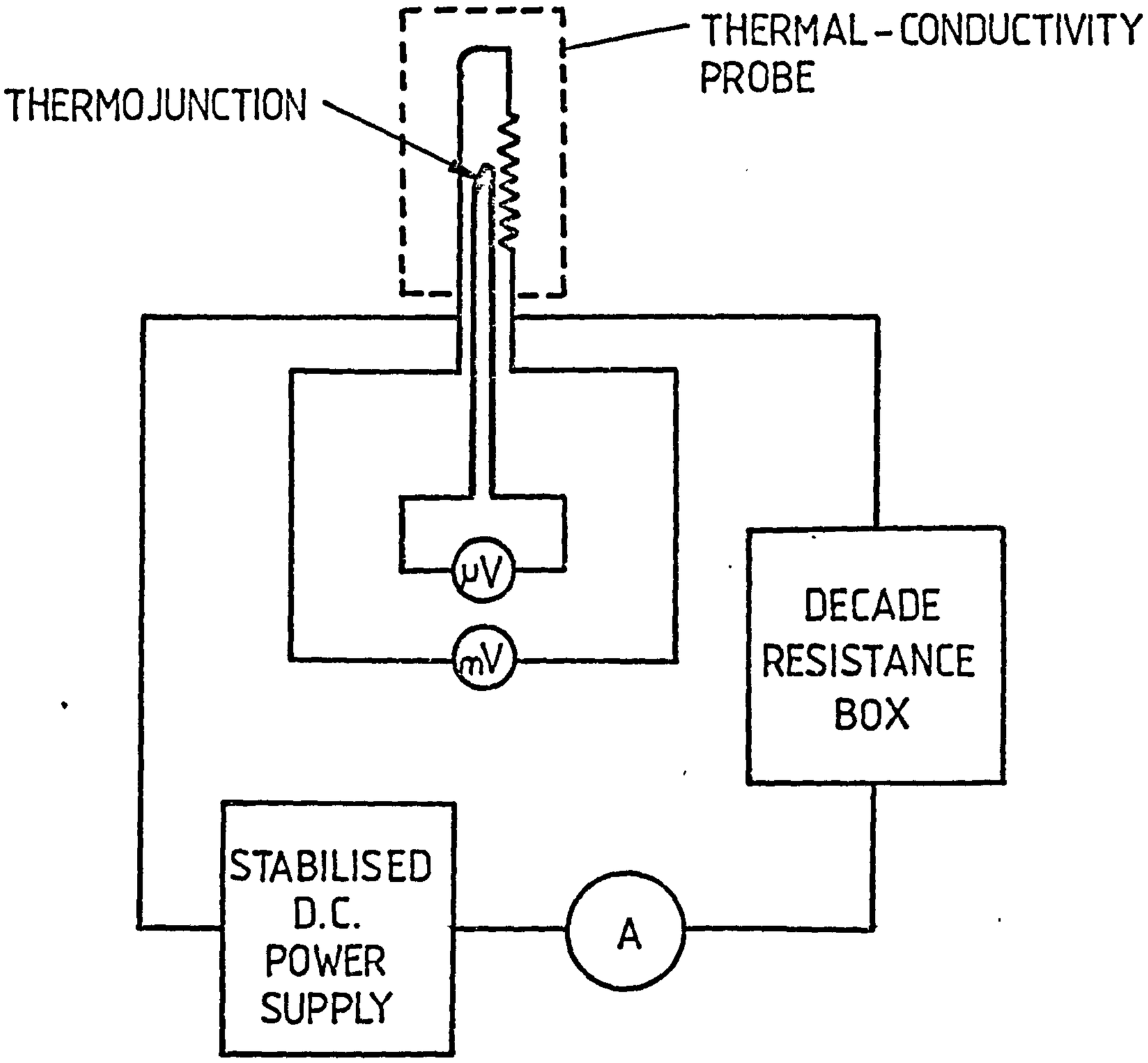

FIG.9. SCHEMETIC DIAGRAM OF THE PROBES ELECTRICAL CIRCUIT.

The probes were immersed in paraffin wax (of melting point 49°C, and density 898 kg m^{-3}), held in metal containers of sufficiently large size so as to cause no problems due to boundary effects. The containers were well insulated with expanded polystyrene and placed in an environmental chamber which maintained the air temperature at 15 ($\pm$ 0.5)°C. Temperature fluctuations in the chamber, caused by temperature control limitations, were reduced to an undetectable level (for an instrumentation resolution of 1 μV) by the surrounding insulation. The samples were allowed twenty-four hours to settle to the chamber temperature before any measurements were undertaken.

Each probe (see fig.9) was switched on, in turn, and its temperature recorded after prescribed time intervals, together with the power dissipation per metre length of probe.

The electrical current was set for each test and the potential difference across the probe heater measured using a digital voltmeter having a 0.1 mV resolution.

A regression analysis was made of the linear section of the probe temperature versus ln t_ℓ graph, and the thermal conductivity of the material under test deduced using equation (2). This procedure was repeated 15 times for each probe.

The repeatability for each probe was then assessed using the procedure outlined, the results being shown in Tables 1, 2 and 3 for various probe constructions. The presented results were obtained by manual reading of the thermocouple e.m.f's using a digital voltmeter after time intervals measured with a stopwatch. In order that the accuracy of the probes could be assessed, the thermal conductivity of the paraffin wax was also measured using the plain hot-plate technique. Slabs of paraffin wax, each of 300 ($\pm$ 1) mm linear dimension, were each machined using a flycutter to a thickness of 28 ($\pm$ 0.2) mm. Five thermojunctions were positioned on each face of the slabs; the leads being set in grooves cut in the respective surface of each slab. The temperature difference between the hot and cold faces of the wax slabs was maintained at 17°C, with the mean temperature of the wax equal to 18°C. The thermal conductivity of the wax as measured by this standard technique was 0.251 $Wm^{-1}K^{-1}$. This value has been used to assess the accuracy of the probes.

PROBE Cu/D/2·3/30/4
REPEATABILITY LIMIT AND MEAN VALUE ARE TAKEN FROM REPEATABILITY ASSESMENTS SHOWN IN TABLE 1.

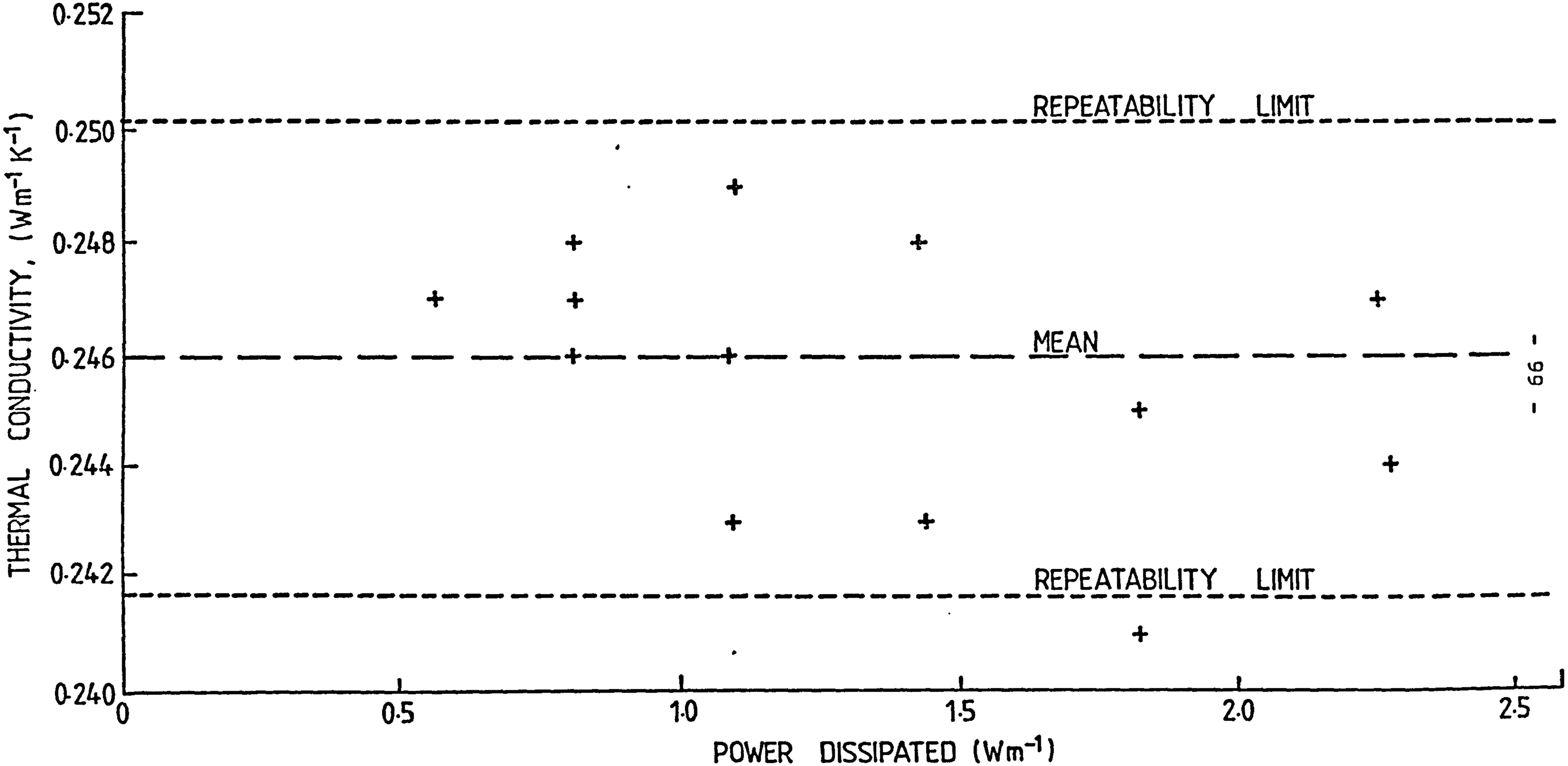

FIG.10. EFFECT OF POWER DISSIPATED ALONG THE LENGTH OF THE PROBE ON THE THERMAL CONDUCTIVITY VALUES OBTAINED FOR PARAFFIN WAX (MELTING POINT 49 C).

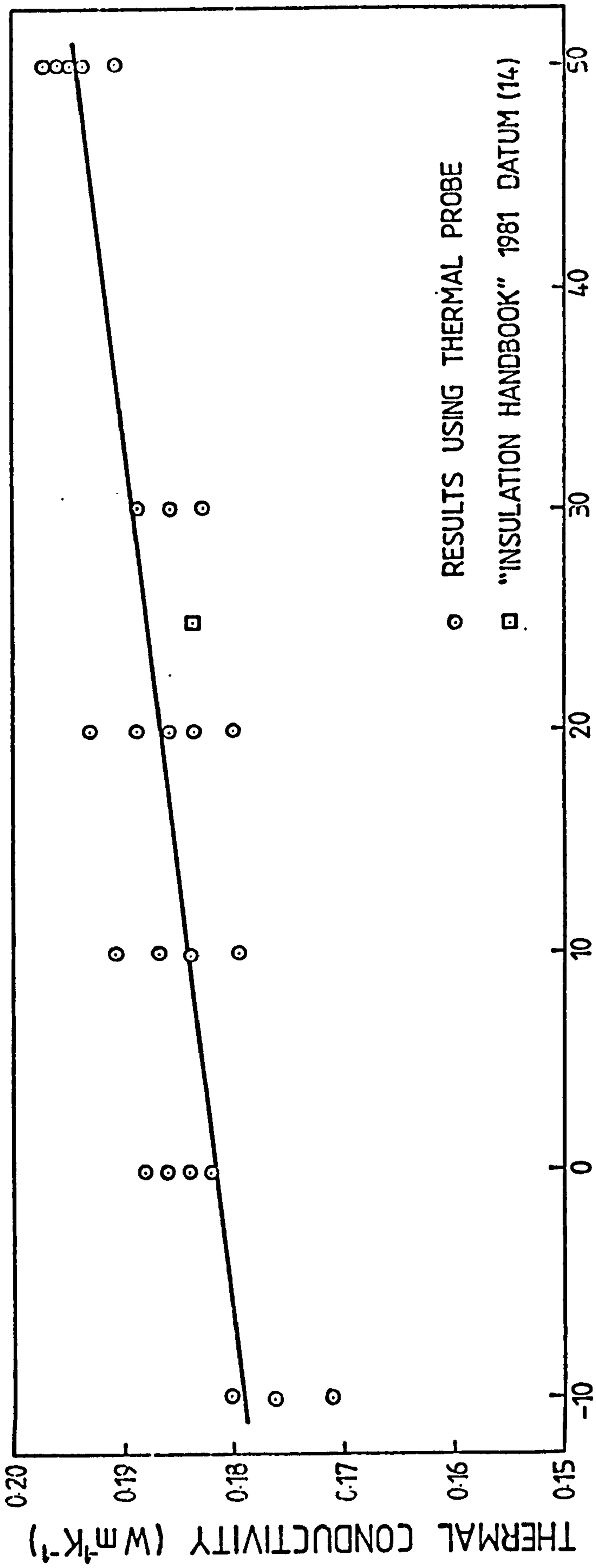

VARIATION OF THE THERMAL CONDUCTIVITY OF AN AERATED CONCRETE BLOCK
(DENSITY = 750 kg m^{-3}) WITH TEMPERATURE USING THE THERMAL PROBE TECHNIQUE.

FIG.11.

Effect of the power input per unit length of probe on the thermal conductivity measurements.

In order that the influence of the power dissipated per unit length of the probe could be assessed, the circuit current was adjusted to give a variety of constant value $\dot{Q}$ power inputs. For each such value, the temperature was recorded after regular time intervals and a linear regression analysis undertaken to allow the deduction of the thermal conductivity.

The probe used during these experiments was the one which gave the best repeatability. This it was hoped would reduce random effects on the deduced value for the thermal conductivity to a minimum. The environment's temperature was maintained at 15 ($\pm$ 0.5)^{o}C. The results are shown in figure 10.

Effect of length-to-diameter ratio of the probe on the accuracy of the thermal conductivity measurements

Stainless-steel probes of 2.05 mm diameter were constructed with a double-wire heater and length-to-diameter ratios of 15, 20, 25 and 50 successively to compare with the results obtained from probes with ratios of 30. An identical procedure to that adopted in our previous experiments was followed with the tested specimen in an ambient environment at a controlled temperature of 15 ($\pm$ 0.5)^{o}C. The ratio of 30 was derived from equation (7) to give an error due to axial flow of 0.5% for masonry materials. It would be expected from figure 6 that the choice of a (L/d) ratio of 25 would lead to an increase in the errors in the thermal conductivity of masonry materials to about 1%, whereas the ratios of 20 would increase these axial errors to 5 → 6%. For paraffin wax, it would be expected that no measurable reduction in accuracy would occur at length-to-diameter ratio of 15. Although very little effect was expected with paraffin wax, it was considered that this exercise should be undertaken for comparison with later results. The data are shown in Table 4.

Measurements of the thermal conductivities of dry bricks and aerated concrete blocks

The brick and aerated concrete block samples were dried to a steady mass using an oven temperature setting of 120^{o}C. Thermal probes were inserted into the samples which were then placed in metal cylinders, containing dried calcium chloride. Each cylinder was sealed to prevent the ingress of water

vapour, and placed in an environmental chamber. The two brick samples were held at a temperature of 15 ($\pm$ 0.5)^{o}C, fifteen thermal conductivity measurements made for each sample and the probe repeatabilities calculated as shown in Table 5.

The thermal conductivity of the aerated concrete block was measured at increments of 10^{o}C between -10^{o}C and 50^{o}C, as can be seen in Figure 11.

Measurements of the thermal conductivities of glass-fibre insulant using a hot-wire

To determine accurately the effective thermal conductivities of fibrous insulants of high porosity is difficult with the hot-wire/probe technique. Insulant thicknesses in wall structures and in operational plant are generally such that boundary effects occur towards the ends of the inherently longer testing periods required for these inhomogenous materials. Fibrous insulants, in particular, have different structures in the heat flow and the isothermal planes. This leads to differences of effective conductivity with direction of heat flow through the material. It is thus essential that such directional effects are investigated in order to ascertain the magnitudes of their influence on the measured thermal conductivities.

The thermal conductivities of glass fibre insulants were measured using a hot-wire of length-to-diameter ratio exceeding 500 thereby effectively eliminating errors due to axial heat flows at the wire mid-length (see fig.8). Changes in the bulk density of the glass fibres were achieved by compressing the material, always ensuring that sufficient thickness was present to prevent the onsett of boundary effects within the measurement period. The results of this investigation are shown in figure 12.

DISCUSSION

With the probes as presently constructed, repeatabilities as low as 2% and accuracies of 4.6% may be achieved for individual instruments. However if all the probes tested are considered as a group, then the mean repeatability

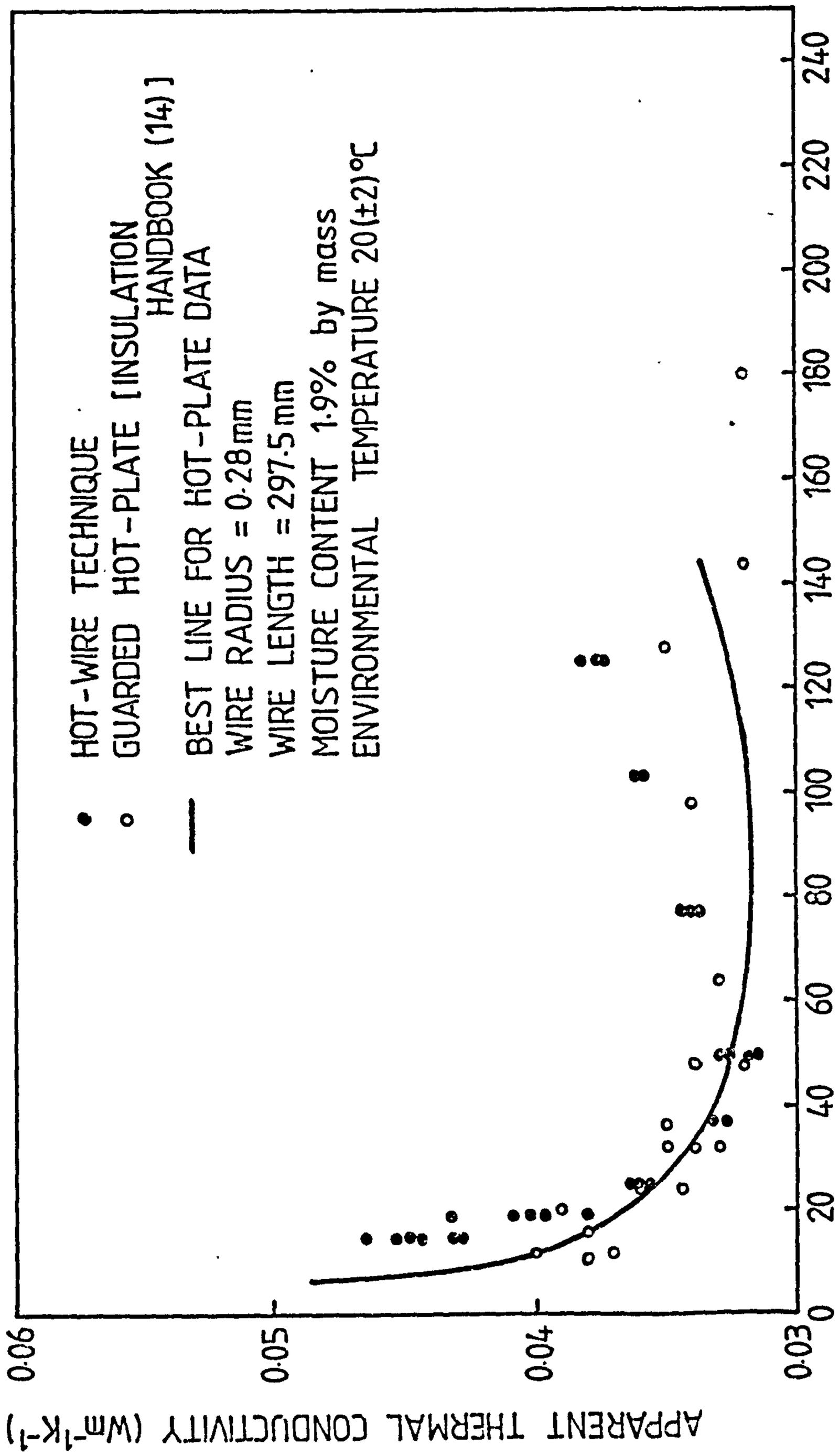

FIG.12. COMPARISON OF THE CHANGES IN THE APPARENT THERMAL CONDUCTIVITY OF GLASS-FIBRE WITH BULK DENSITY AS MEASURED BY THE HOT-WIRE AND GUARDED HOT-PLATE TECHNIQUES.

	PROBE Cu/D/2.3/30/p				
p	1	2	3	4	5
Observed values of the thermal conductivity, k measured under identical conditions,($Wm^{-1}K^{-1}$)	0.256	0.248	0.245	0.239	0.228
	0.238	0.242	0.241	0.251	0.243
	0.252	0.231	0.245	0.247	0.245
	0.262	0.239	0.247	0.242	0.251
	0.263	0.248	0.249	0.253	0.250
	0.258	0.240	0.234	0.242	0.232
	0.252	0.235	0.247	0.244	0.243
	0.254	0.242	0.247	0.248	0.251
	0.255	0.239	0.242	0.244	0.244
	0.251	0.235	0.247	0.246	0.242
	0.261	0.229	0.249	0.242	0.242
	0.254	0.240	0.254	0.248	0.250
	0.256	0.241	0.246	0.243	0.243
	0.255	0.243	0.248	0.253	0.242
	0.255	0.233	0.246	0.247	0.242
Σk	3.822	3.585	3.687	3.689	3.648
$\bar{k}$	0.255	0.239	0.246	0.246	0.243
σ_s	5.66×10^{-3}	5.57×10^{-3}	4.45×10^{-3}	4.20×10^{-3}	6.44×10^{-3}
R	0.012	0.012	9.5×10^{-3}	0.009	0.014
R (%)	4.7	5.0	3.9	3.7	5.7
$\bar{d}$	1.56	5.07	2.15	2.09	3.28
σ_d	2.47	2.46	1.88	1.74	2.81
S_1	6.86	10.34	6.19	5.81	9.30
a(%)	8.32	11.50	7.31	6.90	10.90

Table 1. Repeatability and accuracy of copper sheathed probes immersed in solid paraffin wax.

	PROBE SS/D/2.05/30/p				
p	1	2	3	4	5
Observed values of the thermal conductivity k measured under identical conditions, ($Wm^{-1}K^{-1}$)	0.273	0.249	0.264	0.252	0.229
	0.266	0.252	0.259	0.254	0.231
	0.265	0.254	0.262	0.252	0.230
	0.272	0.251	0.265	0.252	0.231
	0.274	0.258	0.263	0.254	0.236
	0.263	0.254	0.265	0.255	0.230
	0.267	0.251	0.263	0.250	0.229
	0.276	0.246	0.263	0.257	0.232
	0.263	0.252	0.269	0.259	0.230
	0.270	0.253	0.271	0.257	0.233
	0.277	0.249	0.267	0.255	0.233
	0.266	0.260	0.262	0.252	0.235
	0.263	0.251	0.266	0.255	0.231
	0.273	0.256	0.264	0.255	0.234
	0.268	0.255	0.265	0.251	0.229
$\sum k$	4.036	3.791	3.968	2.820	3.473
$\bar{k}$	0.269	0.253	0.265	0.255	0.232
σ_s	4.8×10^{-3}	3.6×10^{-3}	2.9×10^{-3}	3.0×10^{-3}	2.3×10^{-3}
R	10^{-2}	7.8×10^{-3}	6.2×10^{-3}	6.4×10^{-3}	4.9×10^{-3}
R (%)	3.9	3.1	2.3	2.5	2.1
$\bar{d}$	6.69	0.667	5.10	1.48	8.57
σ_d	1.66	1.42	1.05	1.10	1.19
S_1	10.26	3.71	7.36	3.84	11.10
a(%)	11.00	4.84	7.71	4.58	11.30

Table 2. Repeatability and accuracy of stainless-steel sheathed probes immersed in solid paraffin wax.

PROBE Cu/D/2.3/30/4		PROBE POWER (Wm^{-1})
Observed values of the thermal conductivity k measured under identical ambient conditions, ($Wm^{-1}K^{-1}$)	0.242	2.25
	0.241	1.82
	0.234	1.09
	0.246	0.80
	0.243	1.44
	0.247	2.25
	0.245	1.82
	0.248	1.43
	0.245	1.09
	0.247	0.81
	0.248	0.81
	0.247	0.56
	0.249	1.10
	0.244	2.27
$\sum k$	3.436	
$\bar{k}$	0.245	
σ_s	2.51×10^{-3}	
R	5.42×10^{-3}	
R (%)	2.2	
$\bar{d}$	2.65	
σ_d	1.75	
S_1	6.41	
a(%)	6.77	

Table 3. Effects of variation of probe power generation on the accuracy and repeatability of thermal conductivity measurements obtained with a copper sheathed-probe immersed in paraffin wax.

	PROBE SS/D/2.05/λ/1			
λ	20/1	25/1	15/1	50/1
Observed values of the thermal conductivity k measured under identical conditions, ($Wm^{-1}K^{-1}$)	0.242	0.238	0.260	0.244
	0.239	0.238	0.253	0.239
	0.241	0.243	0.257	0.246
	0.240	0.239	0.256	0.246
	0.242	0.235	0.254	0.255
	0.244	0.234	0.247	0.242
	0.239	0.235	0.255	0.243
	0.241	0.236	0.253	0.248
	0.241	0.235	0.255	0.245
	0.239	0.234	0.256	0.243
	0.245	0.237	0.261	0.248
	0.238	0.235	0.260	0.245
	0.241	0.236	0.257	0.253
	0.245	0.238	0.256	0.246
	0.241	0.237	0.256	0.248
$\sum k$	3.618	3.55	3.836	3.691
$\bar{k}$	0.241	0.237	0.256	0.246
σ_s	2.16×10^{-3}	2.38×10^{-3}	3.42×10^{-3}	4.06×10^{-3}
R	4.62×10^{-3}	5.10×10^{-3}	7.34×10^{-3}	8.71×10^{-3}
R (%)	1.9	2.2	2.9	3.5
$\bar{d}$	4.07	6.07	1.83	2.03
σ_d	0.922	1.04	1.32	1.67
S_1	6.05	8.30	4.67	5.61
a(%)	6.34	8.60	5.50	6.61

Table 4. Effects of changes of length-to-diameter ratio on the accuracy and repeatability of thermal conductivity measurements obtained with stainless-steel probes immersed in solid paraffin wax.

PROBE SS/D/2.05/30/p		
p	3	4
Observed values of the thermal conductivity k measured under identical conditions, ($Wm^{-1}K^{-1}$)	0.631	0.425
	0.612	0.411
	0.629	0.434
	0.630	0.425
	0.646	0.439
	0.610	0.446
	0.618	0.436
	0.646	0.455
	0.613	0.430
	0.616	0.443
	0.611	0.441
	0.590	0.434
	0.642	0.441
	0.641	0.424
$\sum k$	9.380	6.514
$\bar{x}$	0.625	0.434
σ_s	0.017	0.011
R	0.036	0.023
R (%)	5.8	5.3
Brick Density ($kg\ m^{-3}$)	1660	1613

Table 5. Thermal conductivities and probe repeatabilities of dry samples of two different bricks.

in paraffin wax was 3.3% and the overall accuracy 10.6%. Improved techniques of probe construction should enable probe performances nearer to the best values experienced during this investigation to be obtained consistently. The results indicate that, for paraffin wax, the probe sheath material has little effect on the obtainable accuracy.

The power input to the probe made no significant differences to the results obtained, all of which fell within the 95% repeatability limit for the probe at one given input. The greatest power per unit length used was five times the least.

Woodside (18) measured the thermal conductivity of dry silica aerogel with different power inputs to the hearer wire giving the results shown in Table 6.

INPUT POWER (Wm^{-})	SPECIMEN'S MEAN TEMPERATURE (Wm^{-} K^{-})	APPARENT THERMAL CONDUCTIVITY (^{o}C)
0.012	21.4	0.0238
0.021	21.7	0.0243
0.046	22.3	0.0266
0.096	23.4	0.0268
0.170	25.2	0.0274

Table 6. Variation of measured apparent thermal conductivity of dry silica aerogel (ρ = 88 kgm^{-3}) with power input (18).

A four-fold increase in power resulted in a definite increase in apparent thermal conductivity. Measurements made using the guarded hot-plate technique gave a value of 0.0241 Wm^{-} K^{-} for the thermal conductivity of dry silica aerogel (18) indicating that the lower probe powers gave more accurate results. The data for paraffin wax, however, showed no significant correlation between indicated thermal conductivity and power input.

It was considered (18) that the increases for silica aerogel were too great to be attributed to the increases in mean temperature. The studies of Van der Held (19,20) were cited to explain this increase. Van der Held observed that materials of high porosity, and thus easily penetrated by thermal radiation, appeared to possess higher thermal conductivities when measured by transient methods than those by steady-state methods. If the surface of a 'transparent' material is subjected to higher temperatures than its surroundings, a radiation field will be immediately produced. This radiation field will heat the material at a distance from the heated surface long before pure conduction could produce the effect. When high probe powers are used in insulating materials then high temperature gradients occur at the probe surface, so increasing this radiation effect.

Such a phenomenon would not be expected to be significant in solid paraffin wax: it would, however, be expected that glass-fibre insulants of porisities exceeding 0.975 would exhibit such behaviour. The radiation component of the apparent thermal conductivity of fibrous materials becomes dominant at these porosities for the ambient temperatures considered. It can be seen from figure 12, that the results obtained with the hot-wire techniques were 13% →15% higher than those revealed using a guarded hot-plate technique for bulk densities below 25 kg m^{-3} (i.e. porosities > 0.99). The probe power used to obtain these results was approximately 0.2 Wm^{-1}. It can be seen from Table 6, that for similar probe powers Woodside (18) obtained a value 14% higher than the guarded hot-plate technique. The choice of probe power was not arbitrary but designed to give changes of readings of at least 1 μv for the time interval chosen using chromel-constantan thermocouples. If lower powers are used, then the thermocouple signals will need to be amplified. Further investigation is required to verify that the technique may be used for insulants of such high porosities.

Figure 12 also shows that the values of the effective thermal conductivities obtained for high bulk-density specimens (> 60 kgm^{-3}), using the hot-wire technique, were greater than those for the steady-state technique. It was considered that this may be due to the layered structure of the material giving rise to increased thermal conduction in the planes parallel to the fibre layers. The steady-state technique usually assumes that heat flows predominantly across these planes whereas the hot-wire loses heat radially.

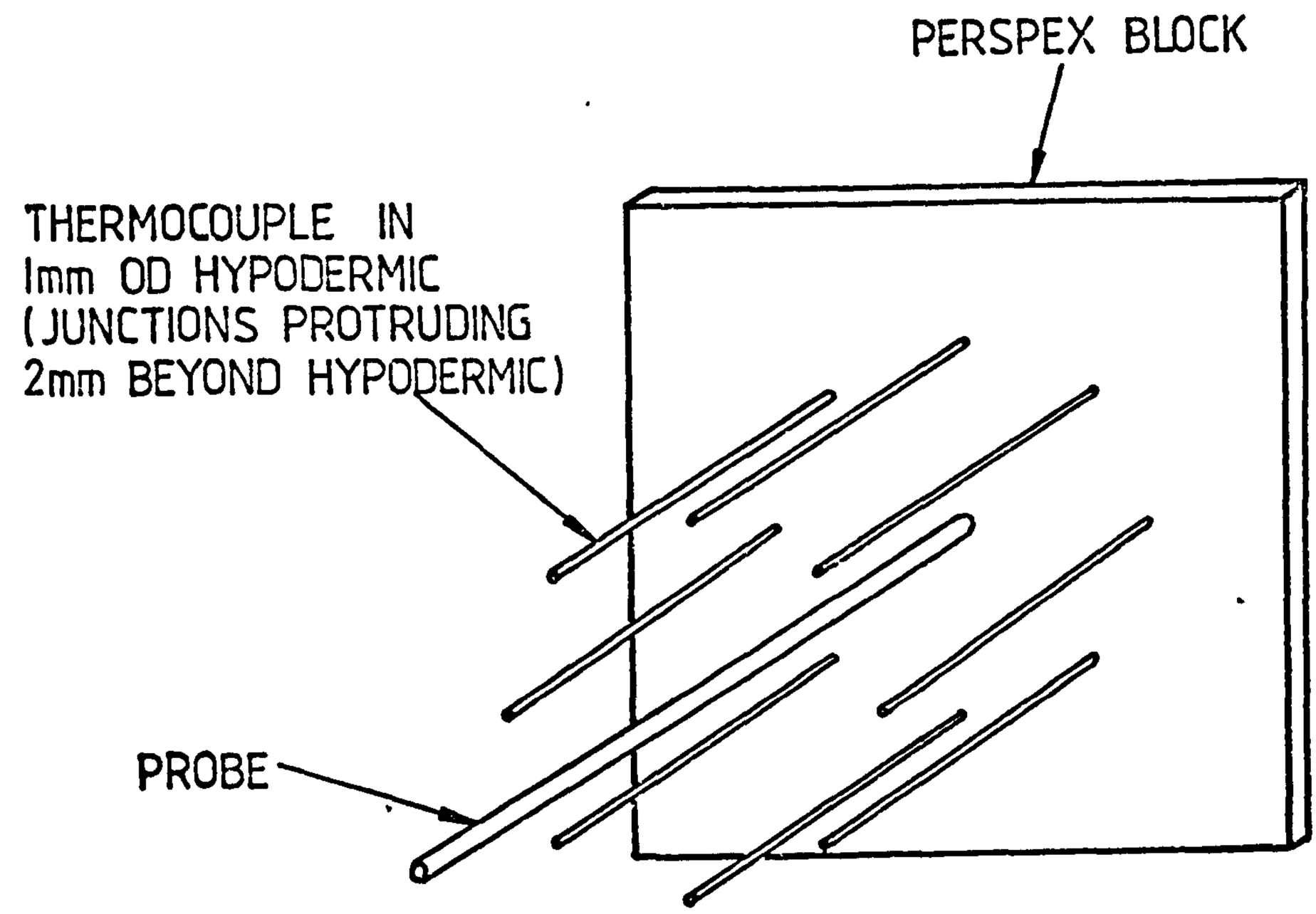

FIG.13. SCHEMATIC ARRANGEMENT OF THE THERMOCOUPLES FOR MEASURING THE TEMPERATURE DISTRIBUTION AROUND A THERMAL-PROBE WHEN INSERTED IN FIBROUS MATERIAL.

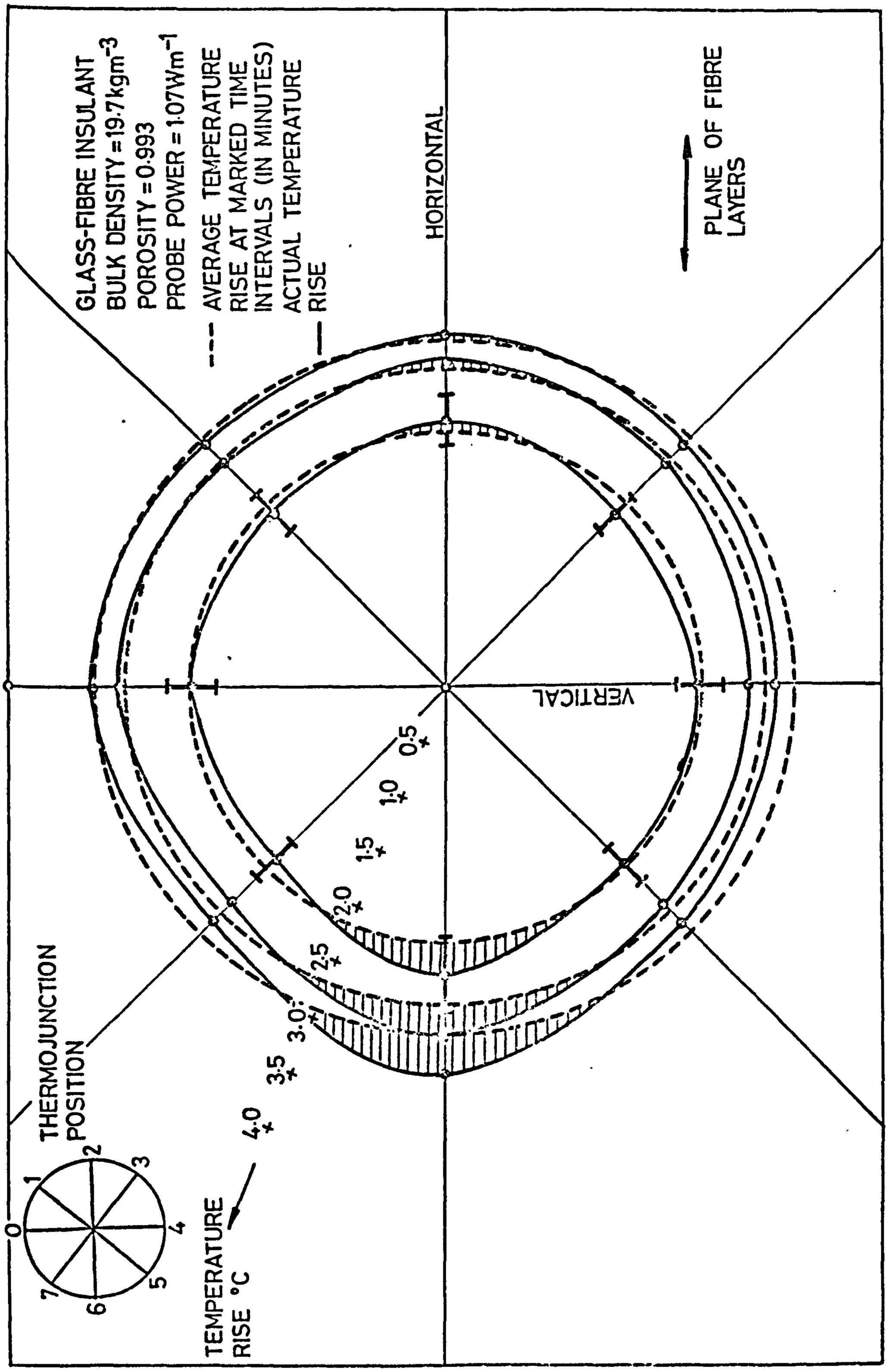

FIG.14. RADIAL TEMPERATURE FIELDS AT A DISTANCE OF 30 mm FROM A CENTRALLY-PLACED PROBE TAKEN AT 15 MINUTE INTERVALS FROM THE START OF HEATING.

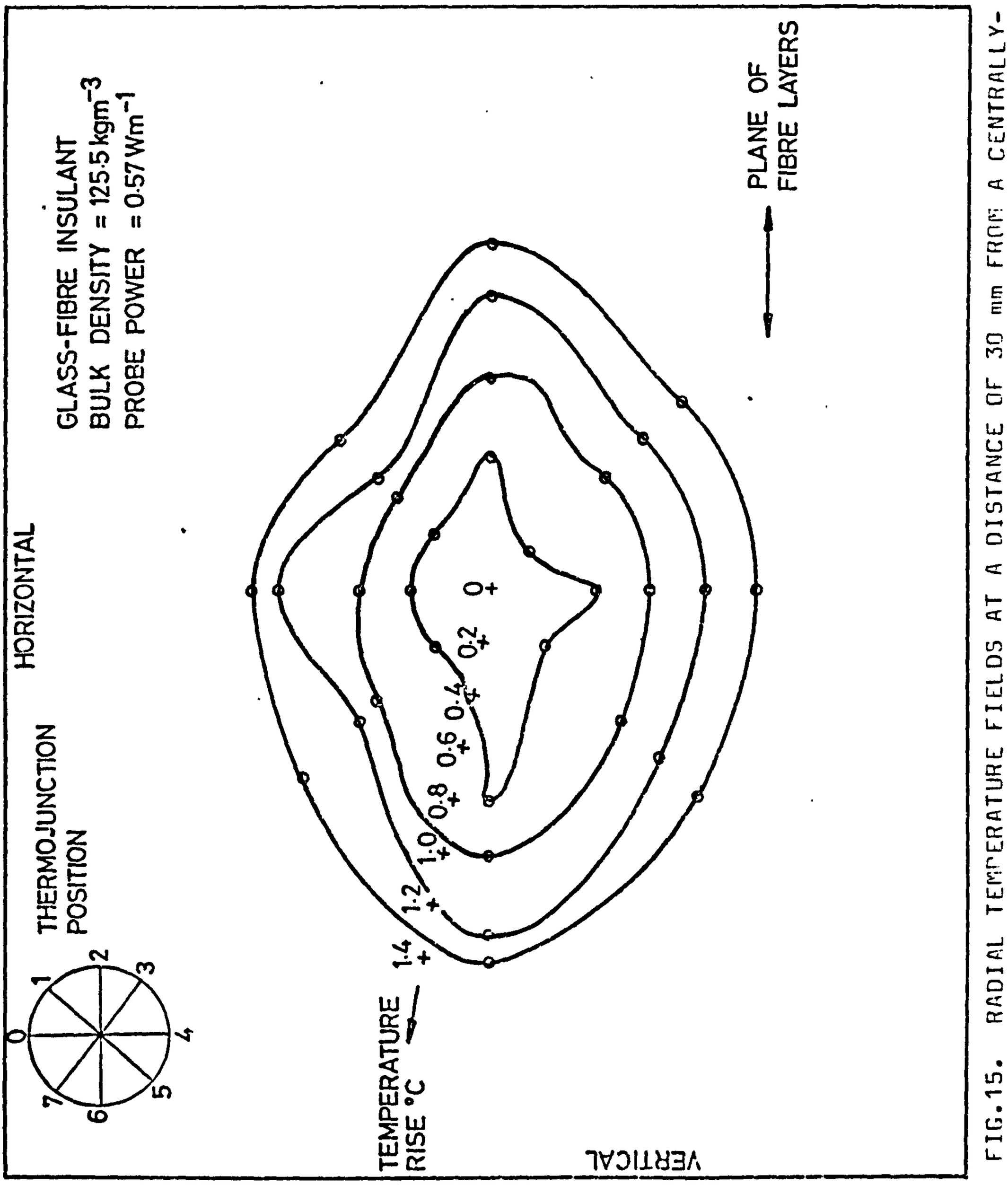

RADIAL TEMPERATURE FIELDS AT A DISTANCE OF 30 mm FROM A CENTRALLY-PLACED PROBE TAKEN AT 15 MINUTE INTERVALS

FIG.15.

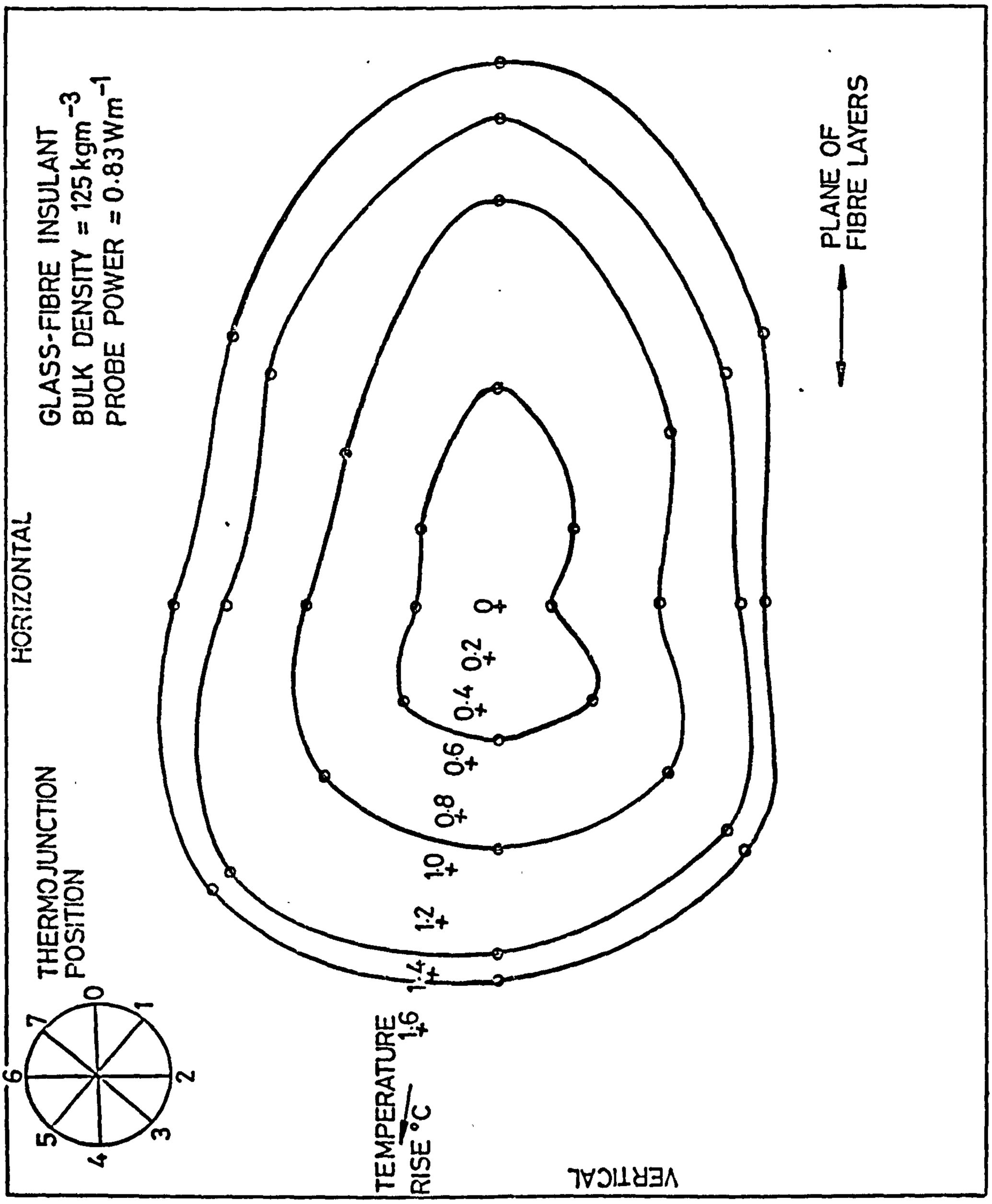

FIG.16. RADIAL TEMPERATURE FIELDS AT A DISTANCE OF 30 mm FROM A CENTRALLY PLACED PROBE MEASURED AT 15 MINUTE INTERVALS FROM THE START OF HEATING.

This was investigated by placing 8 thermojunctions at a 30 mm radius from a thermal probe but still well within the insulant (see fig. 13). The probe was switched on and the thermojunction temperatures measured every 15 minutes using a data logger. The thermocouples had been calibrated previously in melting ice and their responses to changing temperatures investigated utilising a heated and stirred water bath.

Measurements were made for glass-fibre insulants of bulk densities 20 kgm^{-3} and 125 kgm^{-3} having porosities of 0.993 and 0.950 respectively, and the results plotted as radial temperature fields - see figures 14 → 16. Error bars have only been shown on one set of data in order to keep the amount of presented data within reasonable bounds: the same values however correspond to the thermocouples, as enumerated on figure 14, throughout figures 14 → 16.

It can be seen that at a bulk density of 20 kgm^{-3}, the temperature field is effectively radial and thus the thermal conductivity measured would be the same in all directions. However when the bulk density is increased to 125 kgm^{-3}, the temperature rises in the plane parallel to the fibre layers are greater than for those perpendicular to this plane. The orientation of the thermocouples in the samples were rotated through 90^{o} to ensure that this phenomenon was not due to any function of the thermocouple measurements (figure 16) and a similar conclusion was obtained.

The greater heat flow in the fibre layer plane would explain why the thermal probe/hot-wire techniques give higher values of the effective thermal conductivity than the steady-state technique, which measures the rate of heat transfer in the orthogonal direction.

The results obtained with the thermal probe technique correspond closely to the manufacturers' values of the thermal conductivities. The measured thermal conductivity of the brick of density 1660 kgm^{-3} was 0.625 $Wm^{-1}K^{-1}$ at $0^{o}C$. Similarly the value obtained for aerated concrete block (see fig.11) agreed well with manufacturer's data. The probes constructed were of the form shown in fig. 17(b) and 17(c). It was found to be extremely difficult to produce probes of the type shown in figure 17(d), at the probe diameters required without introducing local hot spots along the

lengths of the probes due to variations in 'coil-turns' density.

It is clear that the probe technique may be used to good effect in masonry materials but that further research and development must be undertaken in order that the limitations of the technique for use with low-conductivity porous materials may be understood properly.

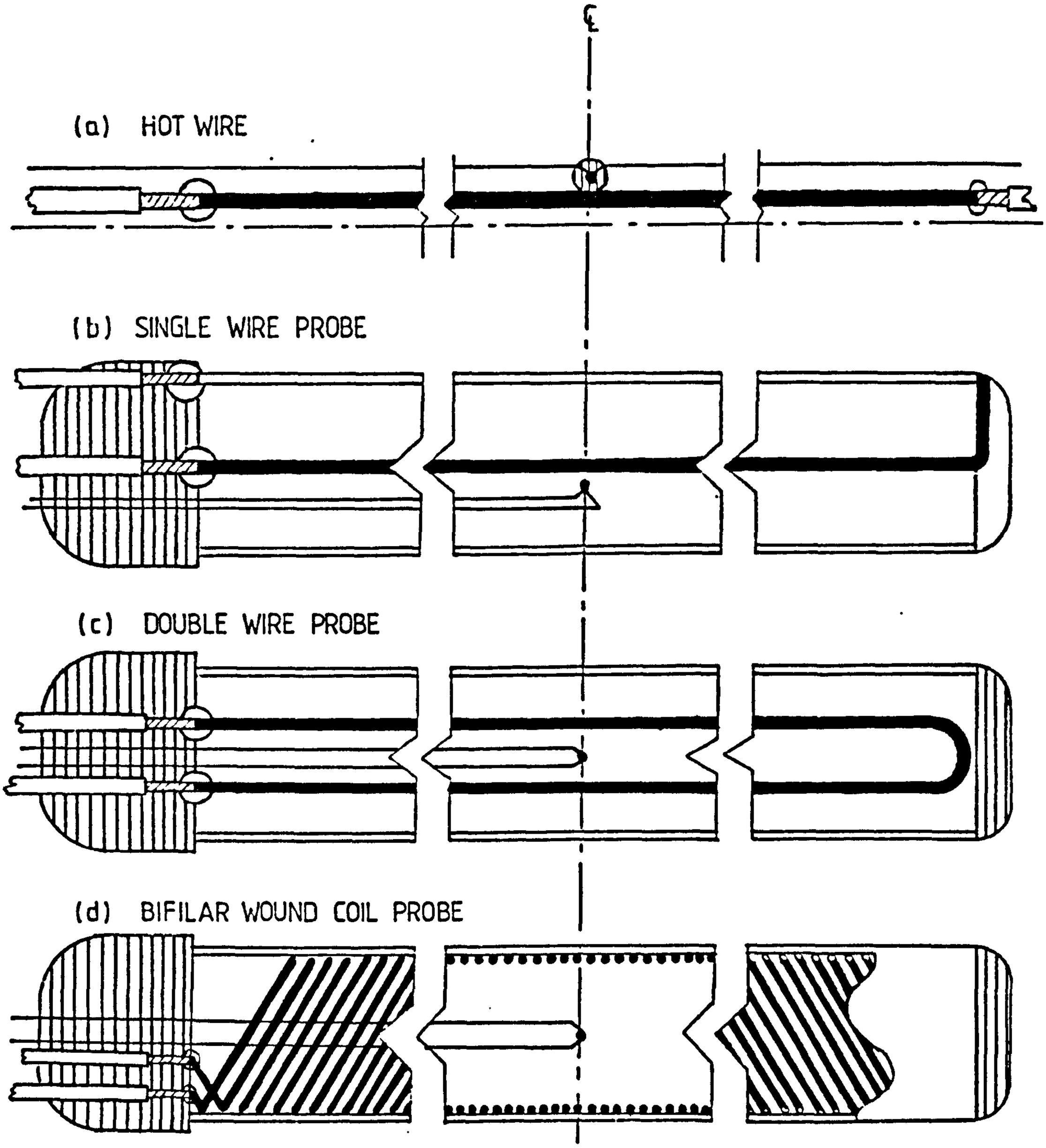

FIG.17. VARIOUS PROBE CONSTRUCTIONS.

R E F E R E N C E S

(1) CARSLAW, H.S., & JAEGER, J.C., "Conduction of heat in solids", Clarendon Press, OXFORD p 345, and p 63, 2nd Edition 1959.

(2) VOS, B.H., "Measurements of thermal conductivity by non-steady-state method". Applied Scientific Research, Section A, Vol. 5, pp 425-438, 1955.

(3) ANDERSSON, P., & BÄCKSTRÖM, G., "Thermal conductivity of solids under pressure by the transient hot-wire method". Review of Scientific Instruments 47, 2, pp 205-209, 1976.

(4) BLACKWELL, J.H., "A transient-flow method for the determination of thermal constants of insulating materials in bulk". Journal of Applied Physics, 25, 2, pp 137-144, 1954.

(5) van der Held, E.F.M., & van DRUNEN, F.G., "A method of measuring the thermal conductivity of liquids". Physica, 15, pp 865-881, 1949.

(6) SANDBERG, O., ANDERSSON, P., & BACKSTROM, G., "Heat capacity and thermal conductivity from pulsed wire probe measurements under pressure". Journal of Physics E: Scientific Instruments Vol. 10, pp 474-477, 1977.

(7) BLACKWELL, J.H., "Radial-axial heat flow in regions bounded internally by circular cylinders". Canadian Journal of Physics, Vol 31, pp 472-9, 1953.

(8) BLACKWELL, J.H., "The axial-flow error in the thermal conductivity probe". Canadian Journal of Physics, Vol 34, pp 412-17, 1956.

(9) OZISIK, M.N., & HUGHES, D., "Thermal contact conductance of smooth-to-rough contact joints". ASME 66-WA/HT-54. Presented at the Winter Annual Meeting and Energy Systems Exposition, New York, December 1966.

(10) HOLMAN, J.P., Heat Transfer, 5th Edition, pp 48-51, McGraw-Hill, New York. 1981.

(11) HAYWARD, A.T.J., "Repeatability and Accuracy". Mechanical Engineering Publication Ltd., London, 1977.

(12) BRITISH STANDARDS INSTITUTE BS 5233 "Glossary of terms used in metrology". B.S.I. London, 1975.

(13) BOOK, S.A., Statistics: basic techniques for solving problems. McGraw Hill, New York, 1977.

(14) ANONYMOUS Insulation Handbook Comprint Ltd., Watford, England, 1961.

(15) MAXWELL, J.C., "A Treatise on Electricity and Magnetism", Clarendon Press, Oxford, Vol. 1, 3rd Edn., pp 435-441, 1904.

(16) RUSSELL, H.W., "Principles of heat flow in porous insulators", J. Amer. Chem. Soc, 18, 1, pp 1-5, 1935.

(17) CHENG, S.C., & VACHON, R.I., "The prediction of the thermal conductivity of two and three-phase solid heterogeneous mixtures". Int. J. Heat Mass Transfer 12, pp 249-264, 1969.

(18) WOODSIDE, W., "Probe for thermal conductivity measurements of dry and moist materials". Heating, Piping and Air Conditioning, 30, pp 163-170, 1958.

(19) Van der HELD, E.F.M., "The contribution of radiation to the conduction of heat", Applied Scientific Research, Section A, Vol 3, pp 237-249, 1952.

(20) Van der HELD, E.F.M., "The contribution of radiation to the conduction of heat: boundary conditions, Applied Scientific Research, Section A, Vol. 4, pp 77-99, 1953.

* * * * * * * * *

CHAPTER 5.

USE OF THE THERMAL-PROBE TECHNIQUE FOR THE MEASUREMENT OF THE APPARENT THERMAL CONDUCTIVITIES OF MOIST MATERIALS

Missing page

THE PROBLEM

There has been a need for many years to be able to measure the thermal conductivity of building materials in-situ. Predictions, mathematical models and heat loss assessments depend upon the accuracies of the data they utilise. Accurate measurement of the thermal conductivities of the nominally dry materials, i.e. in the 'as-received' state with air relative humidities in the range 25 to 65% have been made utilising the plain or guarded hot-plate technique. Measurement of the thermal conductivities of these materials'in-situ' has proven more difficult.

The recommended hot-plate techniques, as prescribed by BS 874, require careful preparation of the test sample, which has to remain under test in the laboratory for a minimum of two days. While the technique is very accurate for dry homogeneous materials, it is inappropriate for porous materials containing moisture. The long testing periods required for the apparatus to achieve steady-state conditions leads to the moisture migrating from the hotter regions of the specimen (1).i.e. the test affects the system being measured.

Because of the natural porosity of building materials, they tend to become moisture laden. The water held in the building's structural components may result from normal construction moisture, exposure to rain, water drawn from the ground or water vapour diffusion from the building interior. This accumulation of water within these porous materials results in apparent thermal conductivities that are often much greater than those obtained using standard tests.

Thus there is a need for a cheap but relatively accurate measuring technique which will allow measurement of the thermal properties of building structural materials in-situ. Any methods used should not intrude upon the building's occupants, and the measuring device should be cheap enough (i) to allow measurements to be made at many points and (ii) to be abandoned in-situ in the structure when tests are completed. It was considered that the thermal-probe technique , which has been fully described in many papers, (2-14), potentially fulfilled these criteria. Such devices could be embedded in the building structure during construction and thus provide a non-destructive

method for the measurement of the thermal conductivities of the structural components.

It was not considered to be the purpose or intention of this study to suggest that the thermal-probe technique could be accepted as a 'standard' method but that it should be assessed to determine whether or not it could be used to give realistic results for the measurement of the thermal conductivity of moist materials under conditions of use.

EFFECT OF MOISTURE ON HEAT FLOWS THROUGH POROUS MEDIA

A dry specimen of a porous material will tend to adsorb water. When water vapour is confined within the porous medium then the relationship between the pressure and volume of the vapour is not the same as if it were confined as a free gas of identical volume to the gas contained in the pores. Peculiar to fluids within porous media, there are certain effects which result from the close proximity of the solid surfaces to the majority of the fluid molecules. When only the vapour phase is present the important physical process is that of adsorption of fluid particles at the surfaces of the pores (15). The influence of the pore surfaces may induce some of the vapour to condense to form a liquid phase which will cover the walls of the pores as a film. If this film merges to form menisci then 'capillary condensation' has occurred (15).

Moisture movement may be initiated by various potential differences, e.g. due to : gravity, osmosis, vapour pressure gradients or temperature gradients. The transport of water may take place in the vapour phase, the liquid phase or both simultaneously. It is possible for these flows to occur in parallel or in series, and in the same or opposite directions.

It is desirable when measuring the thermal conductivities of moist materials to disturb the existing temperature and moisture concentration fields as little as possible. It follows that heat inputs necessary for the measurement to be taken should be small and of short duration.

THE THERMAL-PROBE TECHNIQUE

This technique utilises the theory of a linear heat source of infinite length and negligible thickness which is a perfect thermal conductor generating heat at a constant rate over its entire length. This source is considered to be in perfect thermal contact with its surrounding medium, which is assumed to be homogeneous and infinite in extent. Variations from these ideal conditions and their effects on probe design have been considered previously (7, 8, 14).

Heat transfer per unit length of probe, immersed in a medium of apparent thermal conductivity, k, is described by the equation (2-14)

$$T_2 - T_1 = \frac{Q}{\ell\, 4\pi k} \ell n\left(\frac{t_2}{t_1}\right) \qquad \ldots(1)$$

A plot of the temperature history of the probe after activation contains a section where the temperature-natural logarithm of elapsed time plot is linear, see fig. 1. If the power input per unit length is measured accurately and the slope of the temperature vs. ℓn time curve assessed utilising regression analysis, then the apparent thermal conductivity may be calculated from equation (1).

Many researchers have attempted to construct probes with very small diameters (< 1 mm) to satisfy the theoretical condition of negligible thickness. However, the work of Blackwell (6,7,8) indicates that this criterion is not nearly so important as many suggest. Woodside (11) even concluded that, to avoid moisture migrations while using the thermal probe technique in moist materials, probe diameters should be as large as the test material dimensions allow. He asserted that the greater surface areas of larger diameter probes result in lower temperature gradients at the probe surface for the same rate of heat output. Thus moisture migration would be reduced.

It was considered essential that the effect of probe diameter on the measured value of the apparent thermal conductivity of moist materials be assessed in order that the viability of the thermal-probe technique could be ascertained.

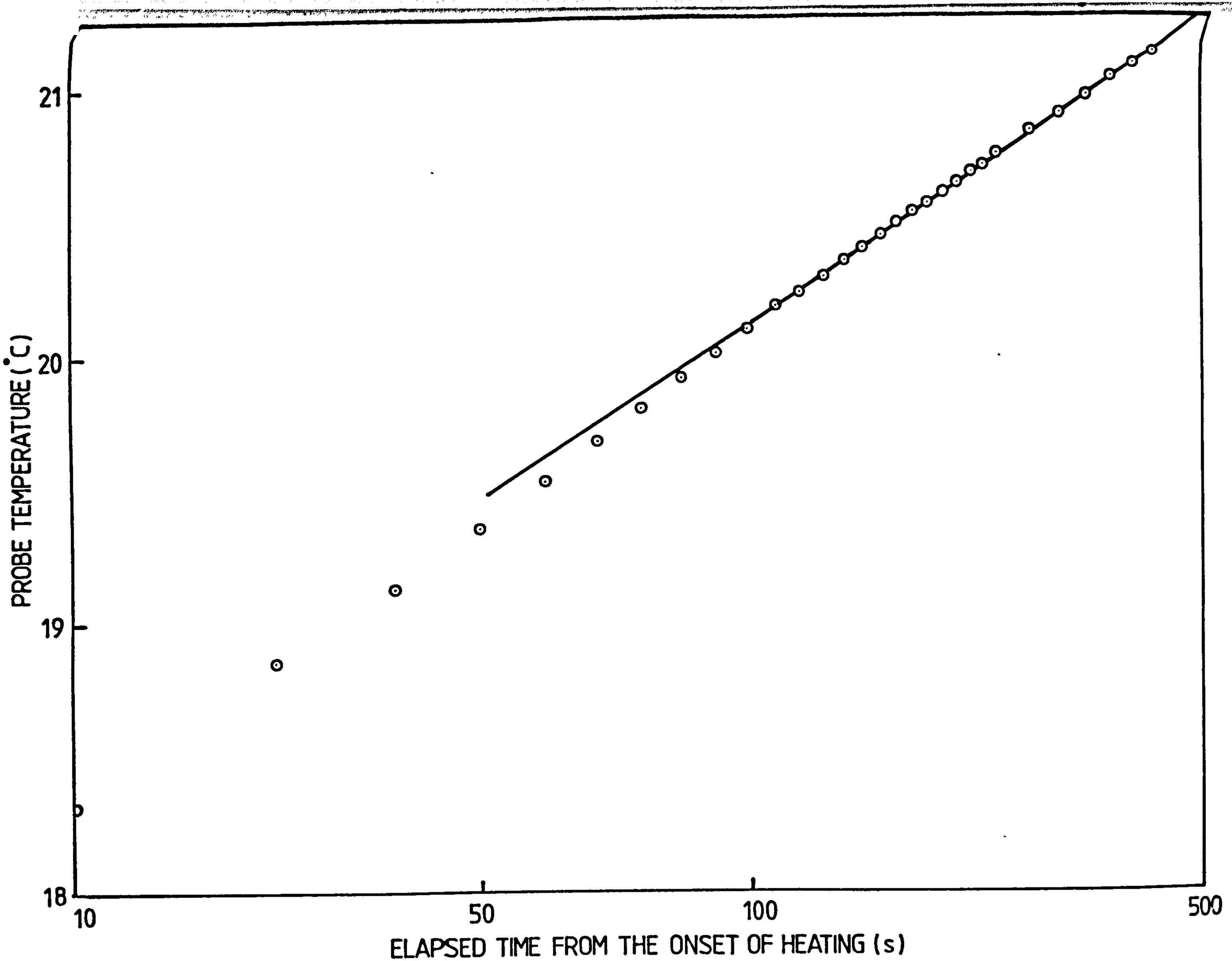

FIG. 1 TEMPERATURE RESPONSE OF A THERMAL PROBE INSERTED IN AERATED CONCRETE

PROBE MANUFACTURE

The probes were designed utilising Blackwell's criteria (8) to reduce errors due to axial heat flows to less than 0.5%. Two types of probe were designed as can be seen from fig. 2.

The copper-sheathed probes were of a similar design to those previously used to measure the thermal conductivities of dry materials (14) and were heated by a double wire of constantan. Separate leads were attached to this heater wire for the delivery of the electrical power and to measure the voltage drop across the heating element. A chromel-constantan thermojunction was attached to the sheath at the heater wire midlength. This was achieved using a cyano-acrylate fast setting adhesive which ensured good thermal contact, whilst acting as an electrical insulator.

Probes were also constructed using constantan tubes which acted as the heating element. Power connections were made at each end of the constantan tubes using copper wires of low electrical resistance.

Both types of probes were constructed with tubes of various external diameters as shown in table 1. The largest diameter probes, 4.85 mm and 5.00 mm for the copper and constantan respectively, were made with two length-to-diameter ratios.

CALIBRATION TESTS

The probes were tested for accuracy using paraffin wax (melting point $49^{0}C$) as the test medium. The thermal conductivity of the wax had been measured previously, using the plain hot-plate technique and found to have a value of 0.25 $Wm^{-1}\ K^{-1}$.

Each probe was placed in melted wax held in metal containers,which were allowed to cool slowly so that good thermal contact resulted between the probe and the solidified wax. The containers were well insulated with expanded polystyrene and placed in an environmental chamber maintained at a temperature of $15(\pm 0.5)^{o}C$. Temperature fluctuations in the chamber, caused by temperature control limitations, were reduced to an undetectable level (for an instrumentation resolution of 1μV) by the surrounding insulation.

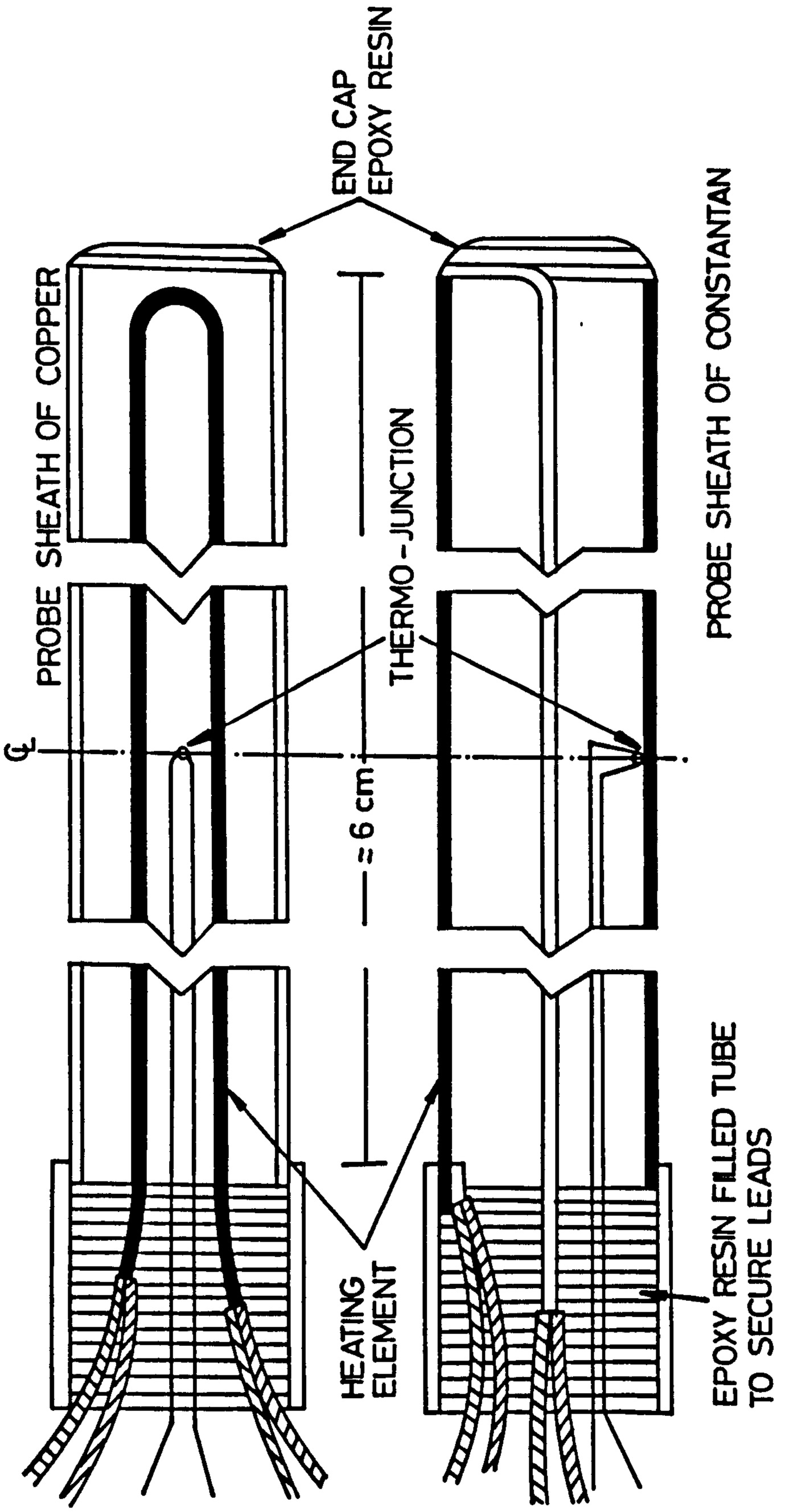

FIG.2 TESTED THERMAL-PROBE DESIGNS

PROBE NUMBER	PROBE MATERIAL	DIAMETER (mm)	LENGTH (cm)	$\frac{\ell}{r_o}$
1	COPPER	2.40	5.75	47.9
2		2.40	6.10	50.8
3		3.30	5.80	35.2
4		3.30	6.45	39.1
5		4.05	6.03	29.8
6		4.85	6.03	24.9
7		4.85	9.63	39.7
8	CONSTANTAN	2.00	5.85	58.5
9		3.00	5.80	38.7
10		4.00	5.95	29.8
11		5.00	6.10	24.4
12		5.00	9.50	38.0

Table 1. Probe Specifications.

To ensure steady-state conditions at the start of each test, the samples were allowed to settle for twenty-four hours before any measurements were undertaken. The temperature sensing and power circuits were set up as shown in figures 3 and 4.

Each probe was switched on, in turn, and its temperature recorded after prescribed time intervals. The electrical current was set for each test and the potential difference across the heater wire measured using a digital voltmeter having a 0.1 mV resolution. This procedure was repeated 10 times for each probe and its prepatability and accuracy assessed for a 95% confidence limit as recommended (14) by

$$\text{Accuracy} = \sqrt{(\text{repeatability})^2 + (\text{half-range systematic uncertainty})^2}$$

It can be seen from figure 5 that the copper sheathed probes gave fair results with accuracies ranging from 8% to 18%. The constantan-sheath probes did not perform as well in these tests exhibiting very poor repeatabilities of 20 and 24% in two cases as well as displaying poor accuracies ranging from 13 to 56% (see table 2).

It was decided that the constantan-sheathed probes did not perform well enough to warrant their use in further tests with wet clay. A probe factor was assessed for each of the copper-sheathed probes to take account of their systematic uncertainties, viz

$$f = \frac{k_s}{k} \qquad (2)$$

Further values as measured with each probe were multiplied with this calibration factor thus

$$k_c = fk$$

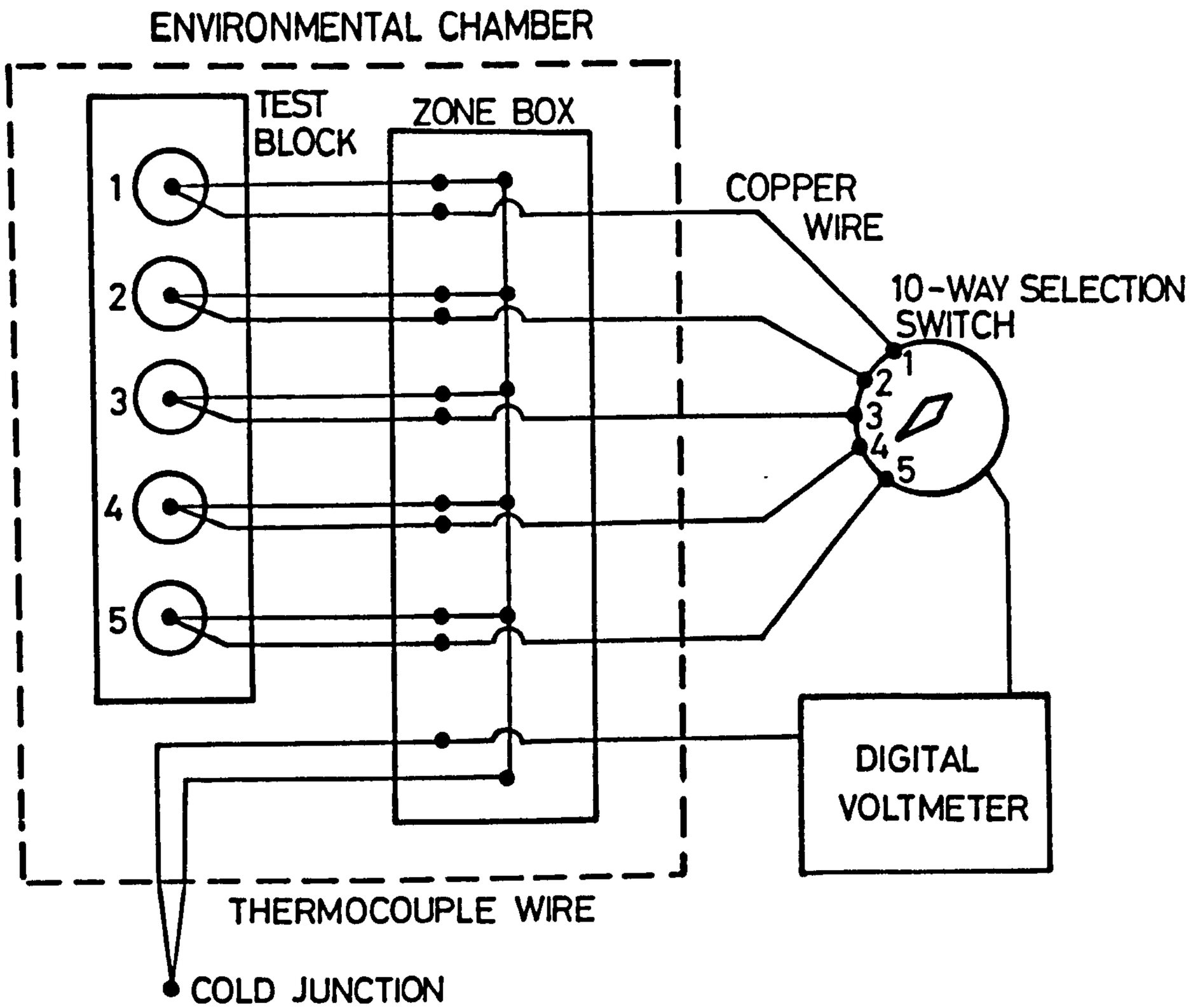

FIG. 3 TEMPERATURE MEASUREMENT - CIRCUIT DIAGRAM

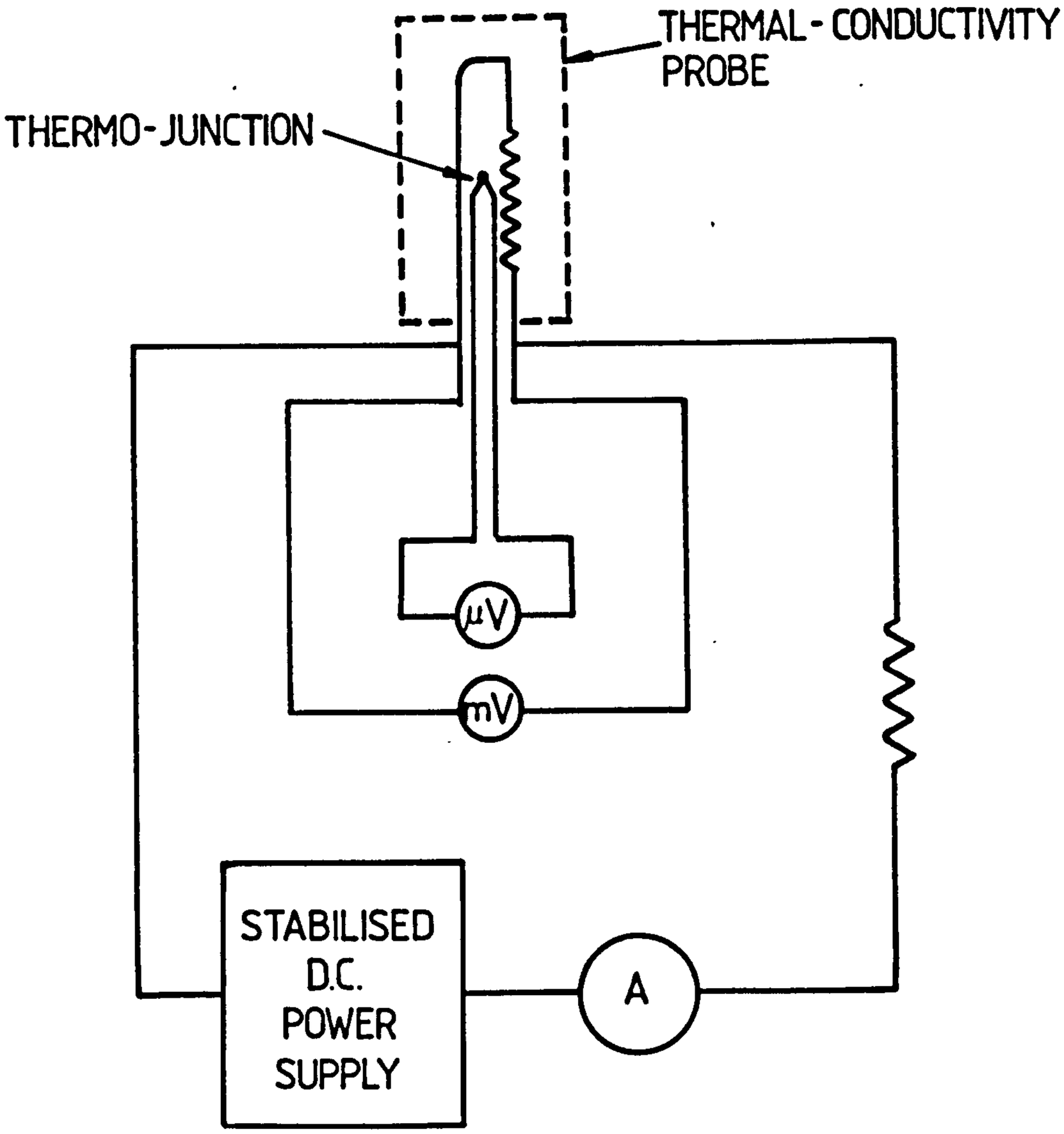

FIG. 4 PROBE'S POWER CIRCUIT

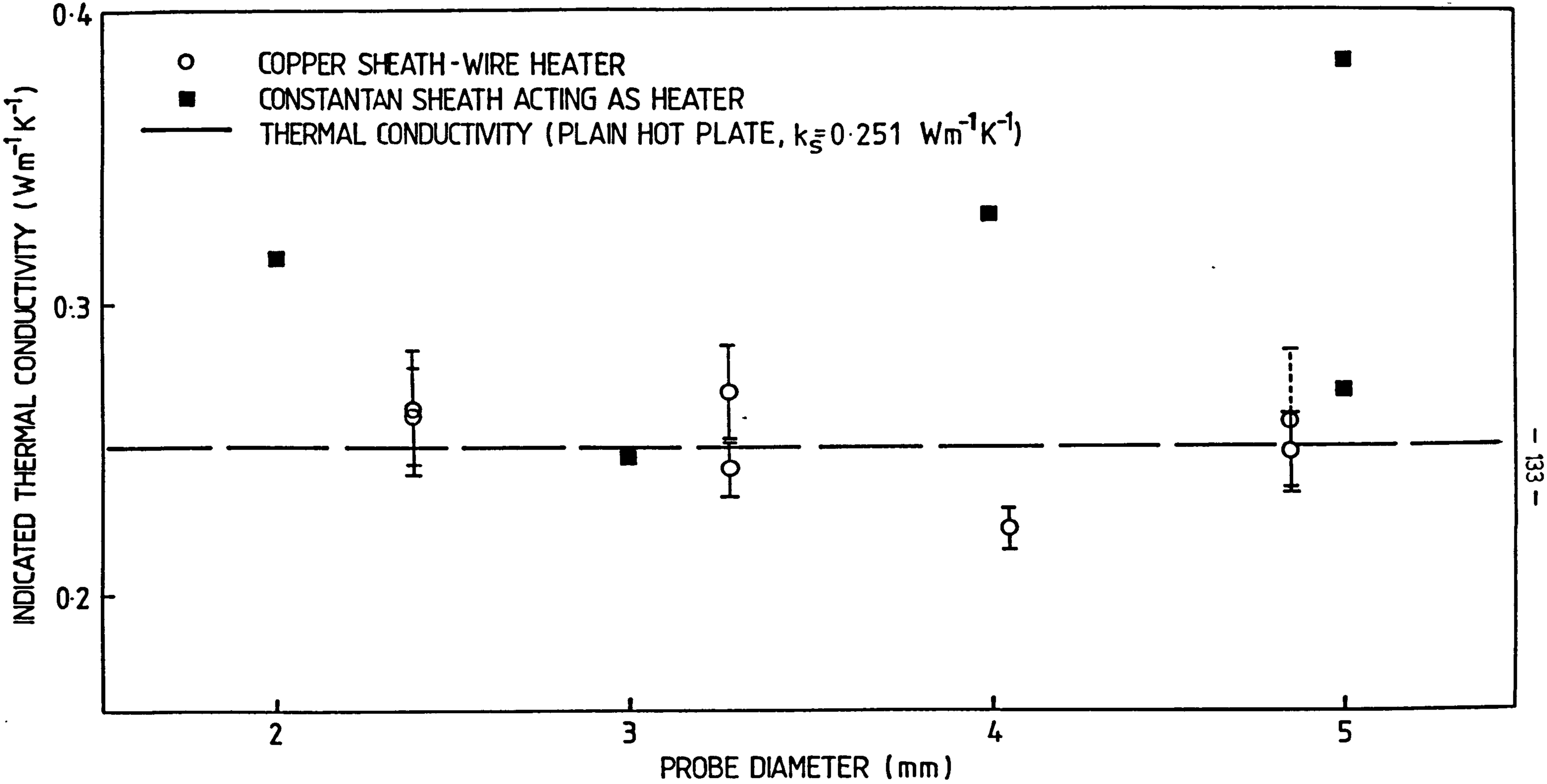

FIG. 5 THERMAL CONDUCTVITY Vs. PROBE DIAMETER FOR COPPER AND CONSTANTAN SHEATHED PROBES, WITH PARAFFIN WAX AS THE THERMALLY CONDUCTING MEDIUM

PROBE NUMBER	PROBE DIAMETER (mm)	MEAN VALUE OF OBSERVED CONDUCTIVITY ($Wm^{-1}\ K^{-1}$)	REPEATABILITY %	ACCURACY %
1	2.40	0.2616	6.4	12.4
2	2.40	0.2629	8.0	14.8
3	3.30	0.2698	6.0	15.1
4	3.30	0.2429	4.2	9.1
5	4.05	0.2224	3.6	17.4
6	4.85	0.2497	5.1	7.8
7	4.85	0.2599	9.7	18.1
8	2.00	0.3160	5.6	25.6
9	3.00	0.2474	8.2	13.1
10	4.00	0.3318	19.1	43.8
11	5.00	0.2717	8.4	17.8
12	5.00	0.3827	24.6	55.9

Table 2. Repeatability and accuracy of the probes when measuring the thermal conductivity of paraffin wax (of melting point $49^{o}C$).

WET-CLAY TESTS

The aim of this series of tests was to measure the thermal conductivity of the wet-clay samples and to assess the probe performance in a moist medium which was in good thermal contact with the probe. 'Reduction' stoneware clay with an oven-dry (i.e. dried at 120°C) density of 1845 kg m^{-3} was used throughout the tests. This material had the advantage of being very homogeneous and easy to handle.

The clay samples tested were to be contained in metal cans. Each can was marked with the number of the probe it was to contain and then weighed. It was then filled with clay to approximately one centimeter below the can's lip and weighed again. Each probe was then fitted with a paper disc which was a little larger than the diameter of the cans and the probes pushed into their respective samples. Melted wax was poured on top of the paper discs up to the lip of the can (see fig. 6).

The purpose of the paper was to help prevent moisture loss and allow easy separation of the wax and clay at the end of the tests. The wax sealed each can and provided support for the probe to ensure that it would not be disturbed during handling. Moisture loss was inhibited by setting the environmental chamber to a relative humidity of 100%.

The two banks of probes were then wired into the 'zone' box and left in the environmental chamber for three days to attain steady-state conditions.

Initially a long test was completed on one sample to discover the heating characteristics at a high level of power. More tests established the power necessary for each probe to maintain a reasonable temperature rise over the test period. These levels were maintained in all subsequent tests. The test procedure was the same as for the calibration tests.

When the tests with the wet clay were completed, i.e. ten tests had been carried out, the probes were removed and the cans re-weighed to ensure that no moisture loss had occurred during testing. The test samples were then dried in an oven for three days. After cooling in a chamber containing a desiccant, they were weighed again to find their dry mass. A further cycle of heating, cooling and weighing ensured that the samples had achieved

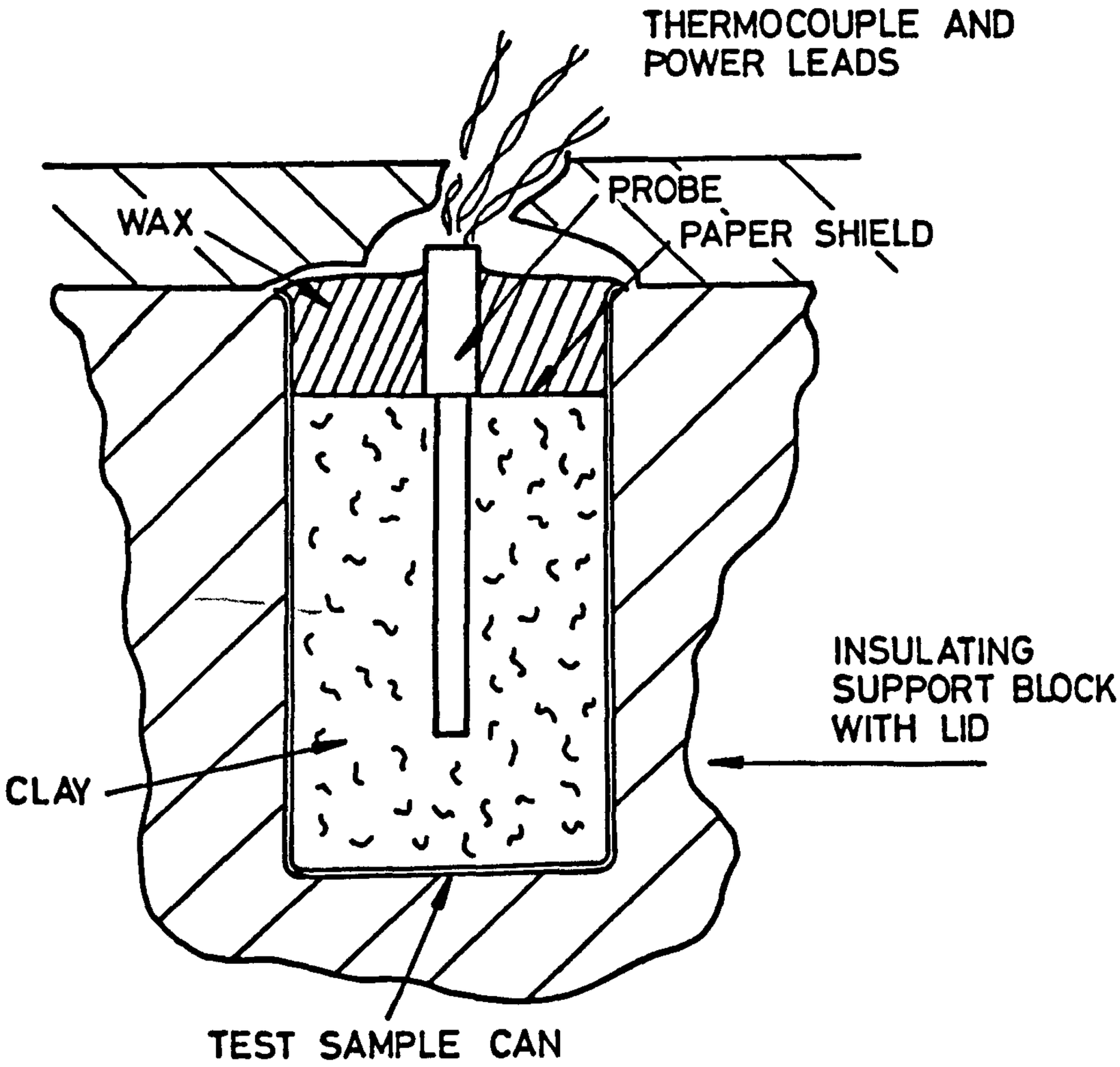

FIG. 6 CROSS SECTION THROUGH A PROBE IN A WET CLAY TEST CAN

constant mass, i.e. they were completely dry. The moisture content per unit mass and per unit volume were calculated as a percentage. The results are summarised in table 3 and figure 7.

PROBE NUMBER	MEAN THERMAL CONDUCTIVITY k, ($Wm^{-1}K^{-1}$)	CORRECTED THERMAL CONDUCTIVITY kf ($Wm^{-1}K^{-1}$)	REPEATABILITY %	MOISTURE CONTENT % BY VOLUME ($\pm$ 0.5)
1	1.80	1.72	4.4	42
3	1.88	1.75	7.9	42
4	1.89	1.95	6.0	42
5	1.72	1.95	10.4	42
6	1.99	2.01	7.4	42

Table 3. Results for the wet-clay tests.

Attempts to use the constantan-sheathed probes, where the sheath was also the heating element, were abandoned due to their extremely poor performance. The temperature versus natural logarithm of the elapsed time graphs did not contain a recognisable linear asymptote when these probes were immersed in the wet clay.

DRY-CLAY TESTS

A further set of tests were undertaken to measure the thermal conductivity of the dry clay. These tests gave an average value of the thermal conductivity for the oven dry clay of density 1845 kg m^{-3}, of 0.86 $Wm^{-1}K^{-1}$ at 15^{o}C.

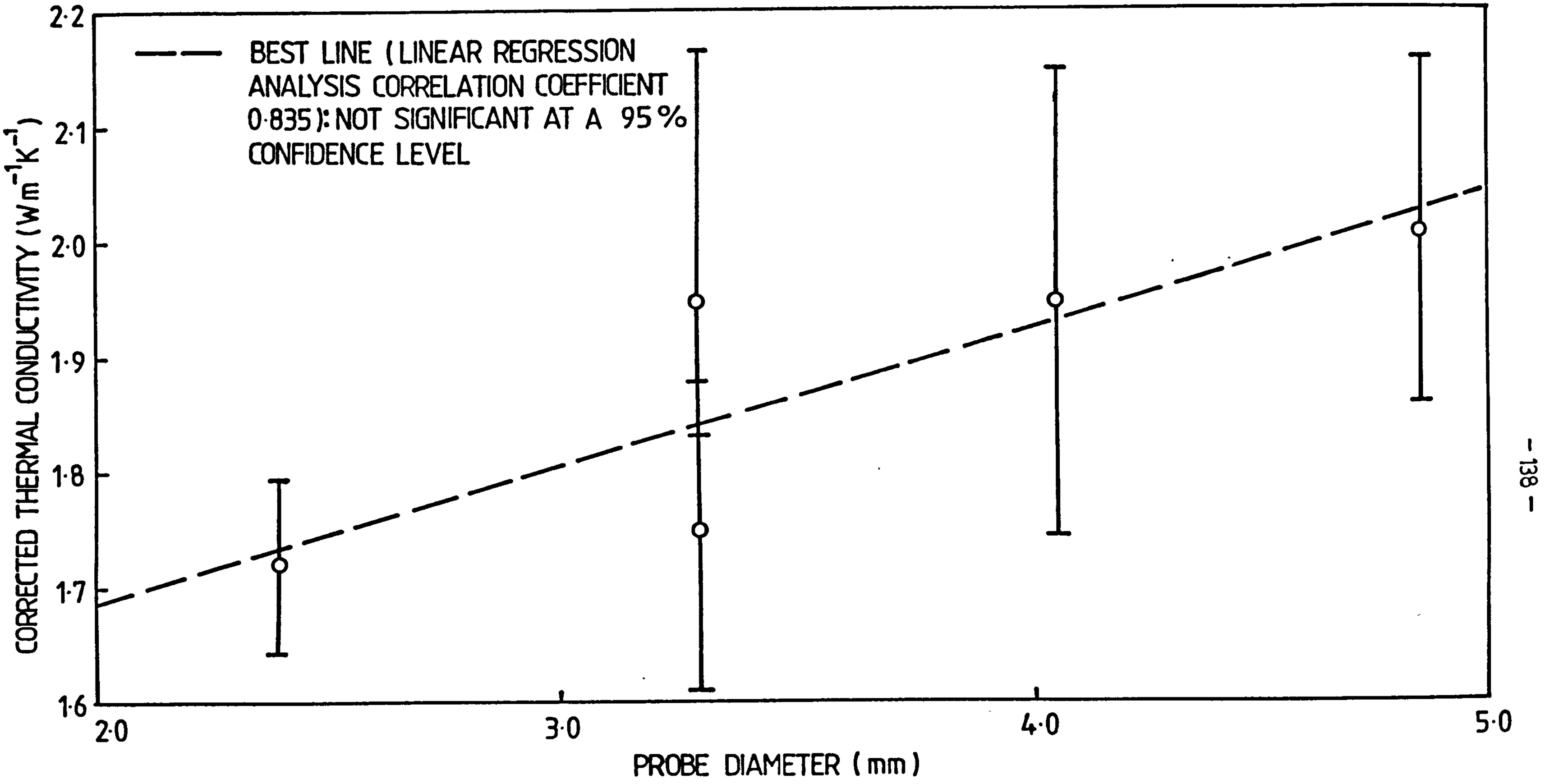

FIG. 7 EFFECT OF PROBE DIAMETER ON THE CORRECTED THERMAL CONDUCTIVITIES OF WETCLAY SAMPLES MEASURED AT 15 °C.

EFFECT OF THE PROBE DIAMETER ON THE VALUE OF THE MEASURED THERMAL CONDUCTIVITY OF WET CLAY

When the graph of fig. 7 showing the relationship between the probe diameter and the measured thermal conductivity is examined, it would appear initially that the measured thermal conductivity increases with probe diameter. However, a linear regression analysis of the data gives a very poor correlation coefficient of 0.835 and this correlation is not statistically significant at a 95% confidence level. The significance of the data was assessed utilising the relation

$$t = \frac{c\sqrt{n-2}}{\sqrt{1-c^2}} \qquad \ldots (3)$$

where t is the probability density function and n is the number of measurements in the sample. The experimental data result in a value of t of 2.6 for 3 degrees of freedom, i.e. $(n-2)$. Tables of the probability-density function t for various levels of confidence give $t = 3.2$ for 3 degrees of freedom at a confidence level of 95%. It is possible that with more data this result could be shown to be significant.

The possible increase of the measured thermal conductivity with probe diameter would not be due to the reduction of temperature gradient at the probe surface. It would be expected that heat transfers due either to water movement resulting from density changes in the liquid or evaporation and vapour transfers would decrease with probe diameter and thus lower measured values of the thermal conductivities would result. If the relationship suggested in fig. 7 exists, the observed behaviour must have another explanation.

If the probe length-to-diameter ratio used for the large probe were too small, then axial heat losses along the probe length would be expected to give rise to higher measured values of the thermal conductivity. However, Table 4 shows that the expected percentage error using Blackwell's equations (8) decreases for the larger probes as constructed.

	PROBE NUMBER				
	1	3	4	5	6
r_o (mm)	1.20	1.65	1.65	2.03	2.43
ℓ/r_o	47.92	35.16	39.10	29.80	24.90
E(%)	0.25	0.26	0.16	0.17	0.04

Table 4. Theoretical errors due to axial flows for copper-sheathed probes set in wet clay.

Therefore it must be assumed that the probe diameter has no effect on the measured value of the thermal conductivity of wet clay for the probe dimensions and the number of samples used in this investigation.

MEASUREMENT OF THE EFFECT OF MOISTURE CONTENT ON THE THERMAL CONDUCTIVITIES OF AERATED CONCRETE BLOCKS USING THE THERMAL-PROBE TECHNIQUE

The linear dimensions of five aerated concrete block samples were measured at 20°C. Each block was then oven dried at a temperature of 120°C and weighed after cooling in a desiccator. This process was repeated until a constant mass was achieved for two successive weighings. A copper-sheathed thermal probe, of 2.4 mm diameter, was inserted into pre-drilled holes in each of the blocks which were slightly smaller than the probe diameter.

After weighing, each block was placed in a double skin polythene bag manufactured from 0.09 mm thick polythene sheeting welded together at two edges. The open end was tightly clamped around a plastic plug which allowed access to the probe leads and contained a valve as shown in fig. 8.

When the tests on the oven-dry materials had been completed, the samples were evacuated to a pressure of 5×10^2 Nm^{-2} ($\simeq$ 0.4 torr). A measured quantity of water from a graduated syringe was then introduced into the evacuated sample through the valve. After 24 hours, the sample was opened to the atmosphere and allowed to attain atmospheric pressure. Further measurements of the thermal conductivity of the blocks were undertaken at this new moisture content.

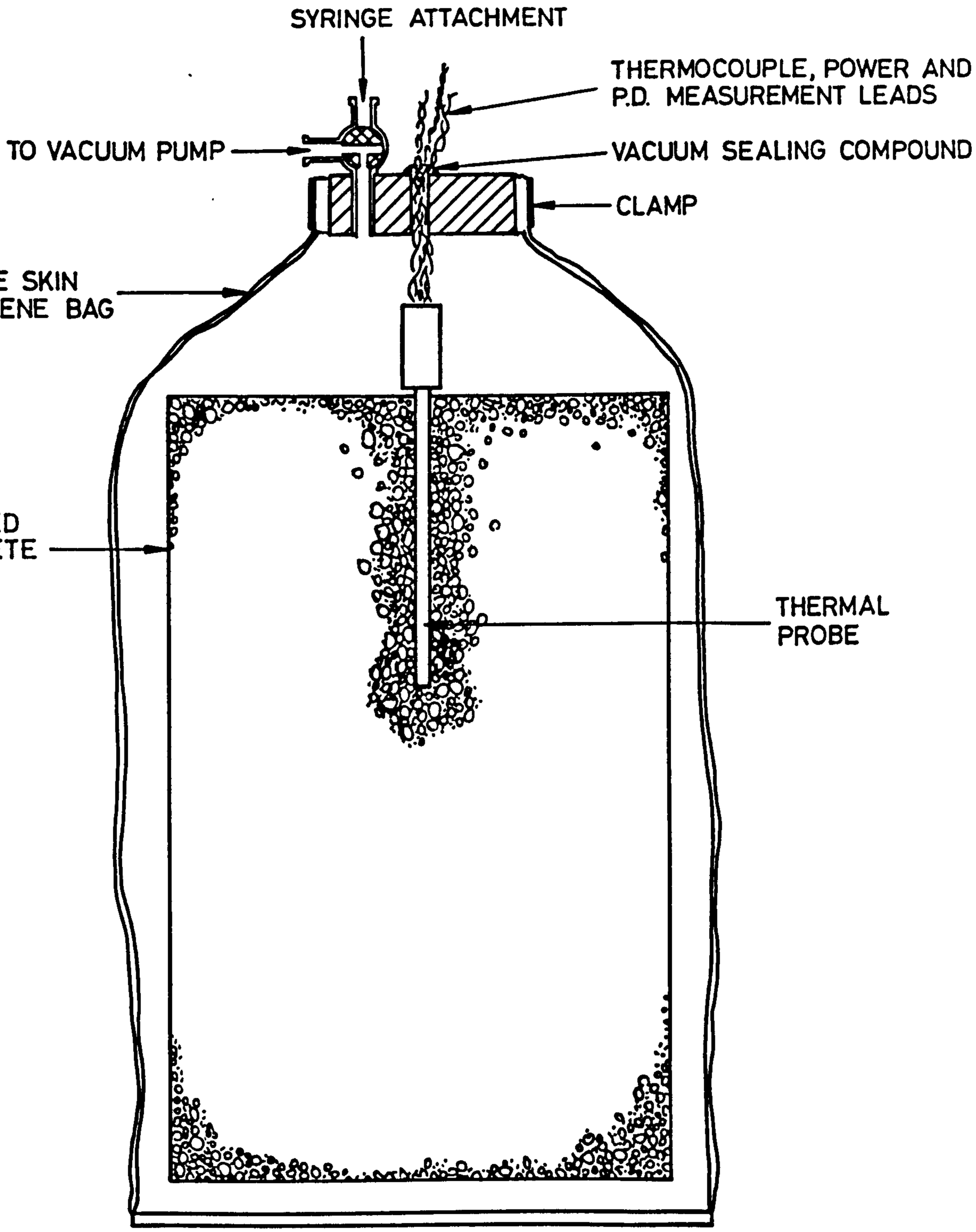

FIG. 8 AERATED CONCRETE BLOCK SAMPLE

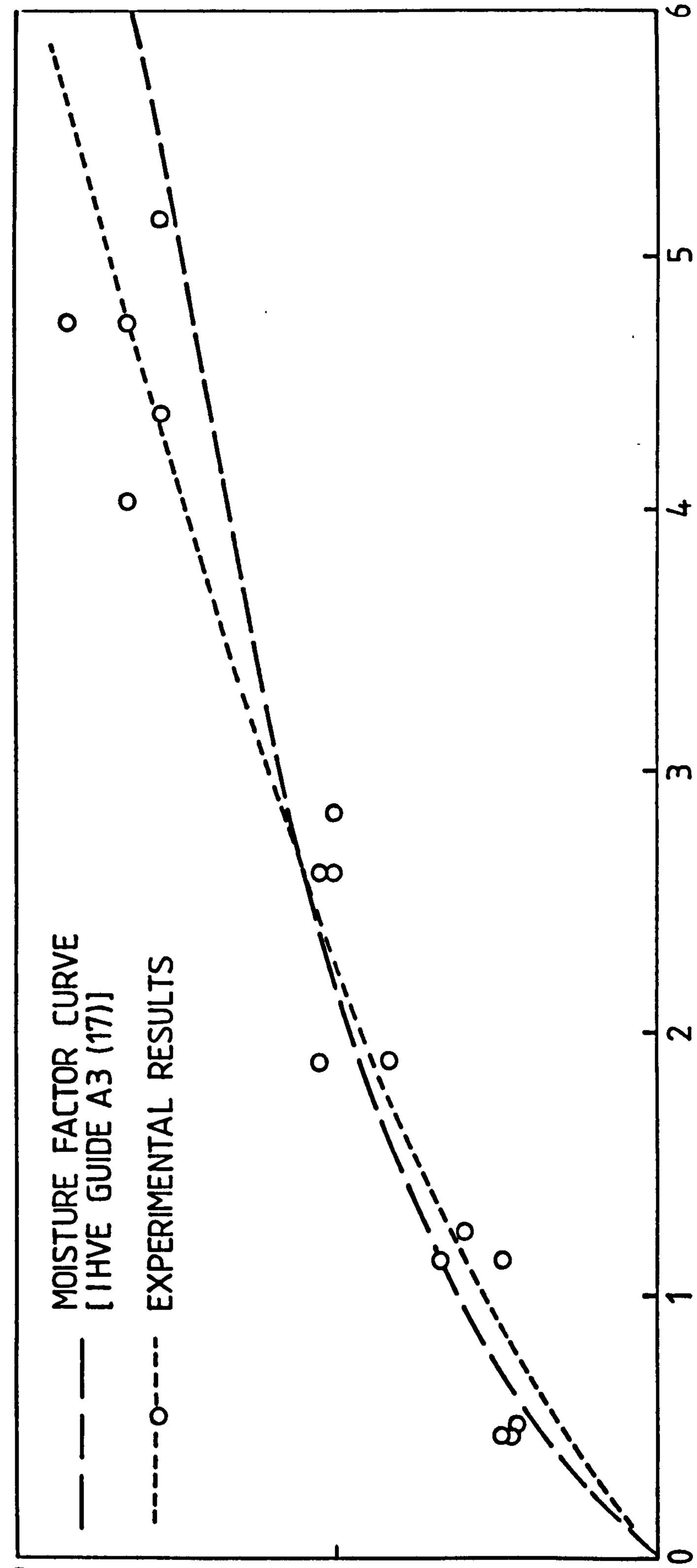

FIG. 9 EFFECT OF MOISTURE CONTENT ON THE APPARENT THERMAL CONDUCTIVITY OF AN AERATED CONCRETE BLOCK

On completion of these tests the sample was evacuated to remove the added water. This evaporation caused the temperature of the block to decrease, as measured by the thermo-junction in the thermal probe. When the temperature of the block once more attained the controlled environment temperature of 20 (±1)^{0}C, then it was assumed that all the water in the block has been removed.

This process was repeated for various water additions. It was found for moisture contents greater than 2% by volume that the indicated apparent thermal conductivities took up to three weeks to stabilise to give three similar consecutive values. The results of this investigation are shown in figure 9.

DISCUSSION

The measured thermal conductivities of wet materials showed that, for the diameters considered, any effects of varying the thermal probe diameters were insignificant. The copper-sheathed probes with an internal heater gave an average thermal conductivity of 1.88 Wm^{-1} K^{-1} for wet clay, with a bulk density of 2068 kg m^{-3} and a moisture content of 42% by volume. This compares well with published data (16) which gives a value of 1.68 Wm^{-1} K^{-1} for clay with a bulk density of 1495 kg m^{-3} and a moisture content of 44.7% by volume. The measured value for the dry clay of 0.86 Wm^{-1} K^{-1} also compares well with the value of 0.93 Wm^{-1} K^{-1} from the published data.

The tests with aerated concrete block samples gave results which agreed well with the moisture factors published in IHVE guide, section A.3 (17), shown as the broken line in figure 9.

This investigation suggests that the thermal-probe technique is both an accurate and a rapid technique for the measurement of thermal conductivities of moist masonry materials.

REFERENCES

1) N.B. HUTCHEON and J.A. PAXTON — "Moisture migration in a closed guarded hot-plate". Trans. A.S.H.V.E., 52, pp 301-320, 1952.

2) E.M.F. van der HELD and F.G. van DRUNNEN — "A Method to Measure the Heat Conductivity in Liquids' Physica, Vol. 15, pp 865-881, 1949.

3) F.C. HOOPER and F.R. LEPPER. — "Transient Heat Flow Apparatus for the Determination of Thermal Conductivities". Trans. A.S.H.V.E., 56, pp 309-324, 1950.

4) D. D'EUSTACHIO and R.E. SCHREINER — "A Study of a Transient Heat Method for Measuring Thermal Conductivity". Trans. A.S.H.V.E., 58, pp 311-342, 1952.

5) F.C. HOOPER and S.C. CHANG — "Development of the Thermal Conductivity Probe", Trans. A.S.H.V.E., Vol. 59, pp 463-472, 1953.

6) J.H. BLACKWELL — "Radial-Axial Heat Flow in Regions Bounded Internally by Circular Cylinders". Canadian Journal of Physics, 31, pp 472-9, 1953.

7) J.H. BLACKWELL — "A Transient-flow Method for the Determination of Thermal Constants of Insulating Materials in Bulk". Journal of Applied Physics, 25, 2, pp 137-144, 1954.

8) J.H. BLACKWELL — "The Axial-Flow Error in the Thermal Conductivity Probe". Canadian Journal of Physics, 34, pp 472-9, 1956.

9) B.H. VOS — "Measurements of Thermal Conductivity by Non-Steady-State Method". Applied Scientific Research Section A, Vol. 5, pp 425-438, 1955.

10) F.A. JOY — "Thermal Conductivity of Insulation Containing Moisture". ASTM, STP No. 217, pp 65-80, 1957

11) W. WOODSIDE — "Probe for Thermal Conductivity Measurement of Dry and Moist Materials", Heating Piping and Air Conditioning, 30, pp 163-170, 1958

12) H.S. CARSLAW and J.C. JAEGER — "Conduction of Heat in Solids", Clarendon Press, Oxford, p 345, 1959.

13) H.J. ERKELENS — "Development of a Probe for Measuring the Coefficient of Thermal Conductivity in Building Materials", J.I.H.V.E., pp 281-296 Jan. 1960.

14) W.J. BATTY, P.W. O'CALLAGHAN, and S.D. PROBERT — "Assessment of the Thermal-Probe Technique for Rapid, Accurate Measurement of Effective Thermal Conductivities", Applied Energy, 16, pp 83-113, 1984.

15) A.E. SCHEIDEGGER — "The Physics of Flow through Porous Media", Oxford University Press, Revised Edition, 1963.

16) K. RAZNJEVIC — 'Handbook of Thermodynamic Tables and Charts', Hemisphere Publishing Corporation, Washington, USA, 1976

17) ANONYMOUS — Section A3, Thermal and Other Properties of Building Structures, I.H.V.E., Guide A, 1970.

APPENDIX

ASSUMED PROPERTIES USED FOR THE ASSESSMENT OF THE AXIAL FLOW ERRORS ASSOCIATED WITH THE THERMAL PROBES IN WET CLAY

	Thermal Conductivity $Wm^{-1}\ K^{-1}$	Specific heat Capacity $J\ kg^{-1}\ K^{-1}$	Density $kg\ m^{-3}$
Wet Clay	1.88	2275	2068
Copper	386	389	8960

The test duration for all measurements in wet clay was 250 seconds.

Probe sheath wall thickness = 0.5 mm

CHAPTER 6.

CONVECTION AND RADIATION IN LAYERS OF LOW DENSITY FIBROUS INSULANTS.

N O M E N C L A T U R E

c_p	specific heat capacity at constant pressure	$Jkg^{-1}\ K^{-1}$
g	local acceleration due to gravity	ms^{-2}
h_c	convective heat transfer coefficient	$Wm^{-2}\ K^{-1}$
k	apparent thermal conductivity	$Wm^{-1}\ K^{-1}$
$\dot{q}$	heat flux rate, i.e. heat flow per unit area perpendicular to the direction of the net heat transfer.	Wm^{-2}
A	area	m^2
B_o	permeability coefficient	m^2
Gr	Grashof number	
L	length	m
$\overline{Nu}_L$	Nusselt number	
Pr	Prandtl number	
$\dot{Q}$	total heat flow rate	W
Ra	Rayleigh number	
T	temperature	^oK
α	thermal diffusivity ($\equiv k\ \rho^{-1}\ C_p^{-1}$)	$m^2\ s^{-1}$
β	coefficient of volumetric expansion	K^{-1}
β	radiation extinction coefficient as used in equation (11)	
δ	thickness	m
ε	emissivity	
ρ	density	$kg\ m^{-3}$
σ	Stefan Boltzmann constant ($= 5.67 \times 10^{-8}\ Wm^{-2}\ K^{-4}$)	
ν	kinematic viscosity	$m^2\ s^{-1}$

Suffices

b	of the base
c	due to conduction
c_v	due to convection
g	gas conduction
h	height
i	interaction between gas and other modes of heat transfer
m	arithmetic mean
r	due to transmission, scattering and absorption of radiation
R	due to radiation
T	Total

- - - - o 0 o - - - -

RECOMMENDED INSULANT THICKNESSES

During the 1960's, the recommended thickness of loft insulation in the U.K. was 1 inch (= 25.4 mm) of mineral/glass fibre or other low-density thermal insulant. Pressure from the trade associations of the insulation industry and a realisation of the value of the insulation in the building stock as an energy conserving measure have since led to an obligatory thickness of 100 mm (4") of domestic loft insulant in order that statutory 'U'-values are achieved (1,2).

If the cost of energy relative to other commodities has remained the same, then the economic insulant thickness for the U.K. would in mid 1981 be ≃ 110 mm (4.3"). However, between 1977 and 1981 the unit cost of energy rose by 5% in relation to other commodities indicating an economic thickness of 190 mm (7.5").

In other countries insulation standards required for dwellings are often stricter than in the U.K. (2,3). The thermal transmittance U-values, allowed for roofs in various countries, are shown in Table 1.

Country	Year	U-value ($Wm^{-2}\ K^{-1}$)
Sweden (north)	1980	0.12
Sweden (south)	1980	0.17
Denmark	1979	0.2
Switzerland	1980	0.5
U.K. (a)	1978/81	0.6 - 0.35
Netherlands	1978	0.78
Italy (b)	1976	0.87 - 0.48
U.S.A. (c)	1980	0.4 - 0.28
Canada (d)	1977	0.62 - 0.29

(a) 0.6 for industrial buildings, offices, etc, 0.35 for domestic dwellings.
(b) depends on surface/volume ratio, number of degree days and building type.
(c) depends on number of heating degree-days.
(d) depends on type of heating and number of heating degree-days (for which there are five designated zones).

Table 1. Comparison of maximum allowable roof thermal transmittances for various nations.

The thickness of insulation required by statute, in buildings has increased markedly since the oil crisis of 1973. Reduction of the rate of energy loss has obviously been the prime motivation for this increase, and has to some extent been achieved, but often it has been assumed that the thermal conductivity of insulating materials used has been a constant for all thicknesses.

Measurements of thermal conductivity for materials specification purposes have generally been undertaken utilising a 300 mm x 300 mm guarded hot-plate rig which limits the thickness of the sample to a maximum of 50 mm, if accurate measurements are to be obtained. However the now widely accepted "thickness effect" acts to increase the thermal conductivity of low density insulants with increasing thickness (6). A critical thickness appears to be reached at which no further increase in thermal conductivity occurs for increasing insulant thickness (6).

This suggests that there is an urgent need to study, in more detail, the thermal transmission behaviour of these materials so that the actual behaviours at installed thicknesses may be more accurately assessed.

Heat transfer in thermal insulants

It has been shown by workers such as Pelanne (4) and Bankvall (5) that heat transfers in low-density porous insulants occur through a combination of several modes acting simultaneously. These would include conductions through the solid and gaseous phases, heat transmission by natural or forced convections in open pore systems, such as fibres, and heat transmissions by radiation.

Convection arises when temperature-induced density changes in a fluid give rise to buoyancy forces which are sufficient to overcome the viscous forces within the medium. The ability of the buoyancy forces to produce air movements will be lessened by the increased resistance to air flows introduced by the solid matrix of the porous material. Generally pore sizes are sufficiently small to suppress convection within individual pore spaces.

The 'thickness effect' is claimed to be due to radiation (6,11). A layer of still air enclosed between two infinite parallel planes 1 and 2 composed of materials of emissivity ε_1 and ε_2 at absolute temperatures of T_1 and T_2 would have a radiant heat flux described by

$$\dot{q}_R = \frac{\sigma \varepsilon_1 \varepsilon_2}{(\varepsilon_1 + \varepsilon_2) - \varepsilon_1 \varepsilon_2} (T_1^4 - T_2^4) \qquad \ldots (1)$$

i.e. the radiation heat flux does not depend upon the distance between plates.

Conduction through the gas between the two plates is described by the expression:-

$$\dot{q}_c = \frac{k_m (T_1 - T_2)}{\delta} \qquad \ldots (2)$$

where k_m is the true thermal conductivity of the gas enclosed by the two plates and δ is the separation between the plates.

The total steady-state heat flux $\dot{q}_T$ due to both radiation and conduction would therefore be

$$\dot{q}_T = \dot{q}_R + \dot{q}_c$$

$$= \frac{\sigma \varepsilon_1 \varepsilon_2}{(\varepsilon_1 + \varepsilon_2) - \varepsilon_1 \varepsilon_2} (T_1^4 - T_2^4) + \frac{k_m}{\delta} (T_1 - T_2) \qquad \ldots (3)$$

The apparent thermal conductivity of the air layer k is thus described by

$$k = \frac{\dot{q}_T \delta}{(T_1 - T_2)}$$

Therefore from this and equation (3)

$$k = k_m + \sigma \frac{(T_1 + T_2)(T_1^2 + T_2^2)}{\left(\frac{1}{\varepsilon_1} + \frac{1}{\varepsilon_2}\right) - 1} \delta \qquad \ldots (4)$$

As ε_1 and ε_2 are both less than unity, the second term on the right-hand side of equation (4) is essentially positive. Therefore under the stated conditions, $k > k_m$.

It can be seen from equation (4) that the apparent thermal conductivity of the air layer due to the combined modes of conduction and radiation is a function of both the temperature difference across the considered space as well as its thickness, and increases with the thickness. The effect of thickness for air layers between surfaces of differing emissivity and foamed insulants were shown in the investigation of Jones (5), as can be seen in Figs. 1 and 2. Figure 1 illustrates clearly the effect of the emissivity of the bounding surfaces, The extremely low emissivity of the aluminium foil ($\varepsilon \simeq 0.05$) results in little change of apparent thermal conductivity with air layer thickness. However, for polystyrene films ($\varepsilon \simeq 0.4$) there is a marked thickness effect. Thus the steeper the slope of the apparent thermal conductivity versus thickness curve the greater is the radiation contribution. It is clear from Fig.2 that the radiation component for sample A exceeds that for sample B, which in turn is greater than that for sample C. Although sample B has a lower density than sample A, it had a much smaller cell structure ($\simeq 10^{-1}$ linear dimension) and would thus cause more scattering of the incident radiation. Sample C had cell sizes almost identical to those of Sample B..
That a thickness effect exists, and is at least partly due to radiation transfers, therefore is not in doubt.

Although it has been stated that natural convection within the pore spaces or cells of a thermal insulant is generally suppressed, the onset of convection of a fluid through a permeable medium as a result of a vertical temperature gradient needs further consideration. Horton and Rogers (7) solved the problem for the onset of convection in an infinite flat layer of a permeable medium bounded by perfectly conducting media. The minimum temperature gradient for which convection could occur was given as

$$\frac{\Delta T}{\delta} > \frac{4\pi^2 \alpha \nu}{B_o g \beta \delta^2} \qquad \ldots (5)$$

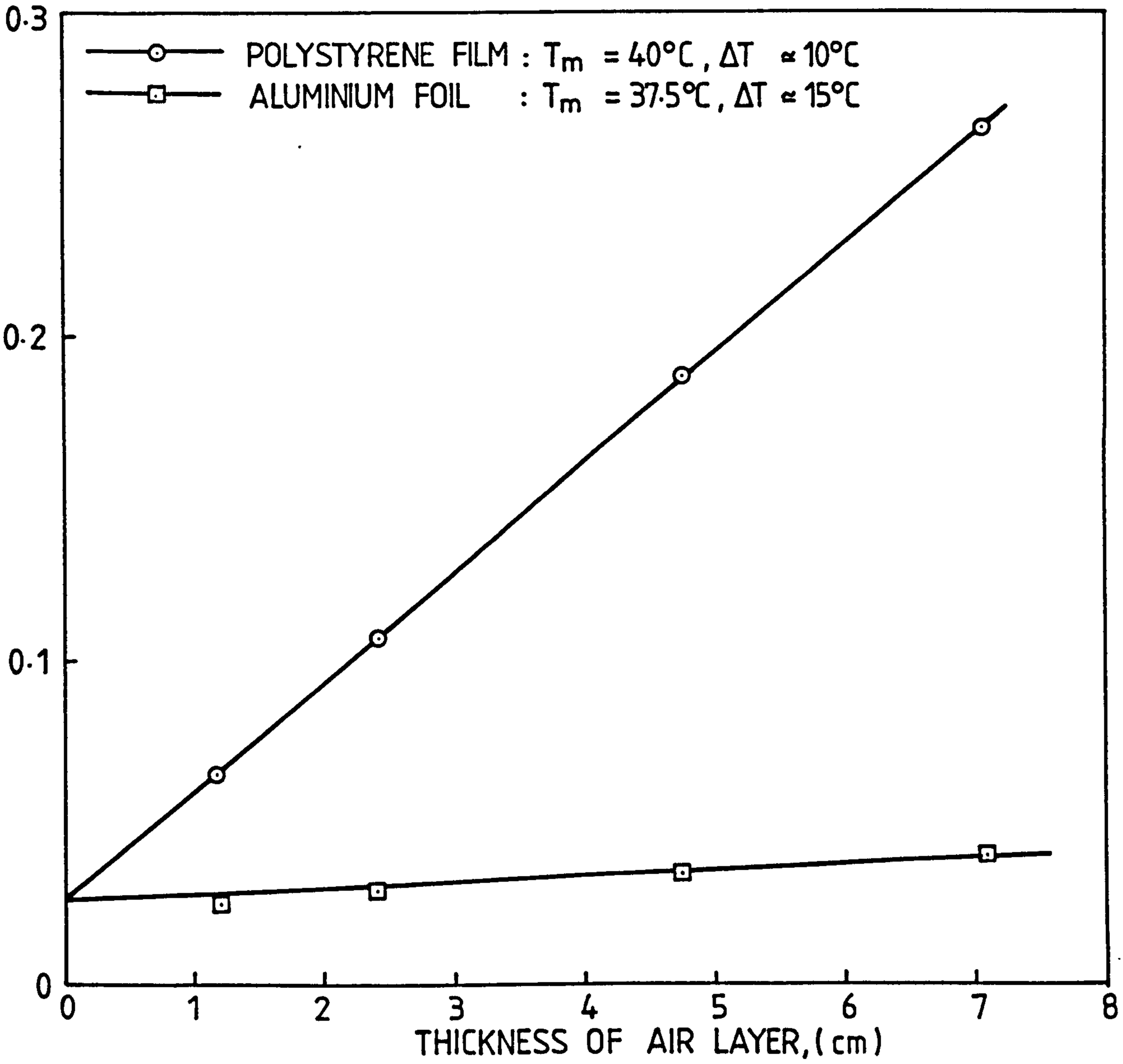

FIG.1. EFFECT OF THICKNESS ON THE APPARENT THERMAL CONDUCTIVITY OF STILL AIR LAYERS BOUNDED BY SURFACES OF DIFFERING EMISSIVITIES (JONES(5)).

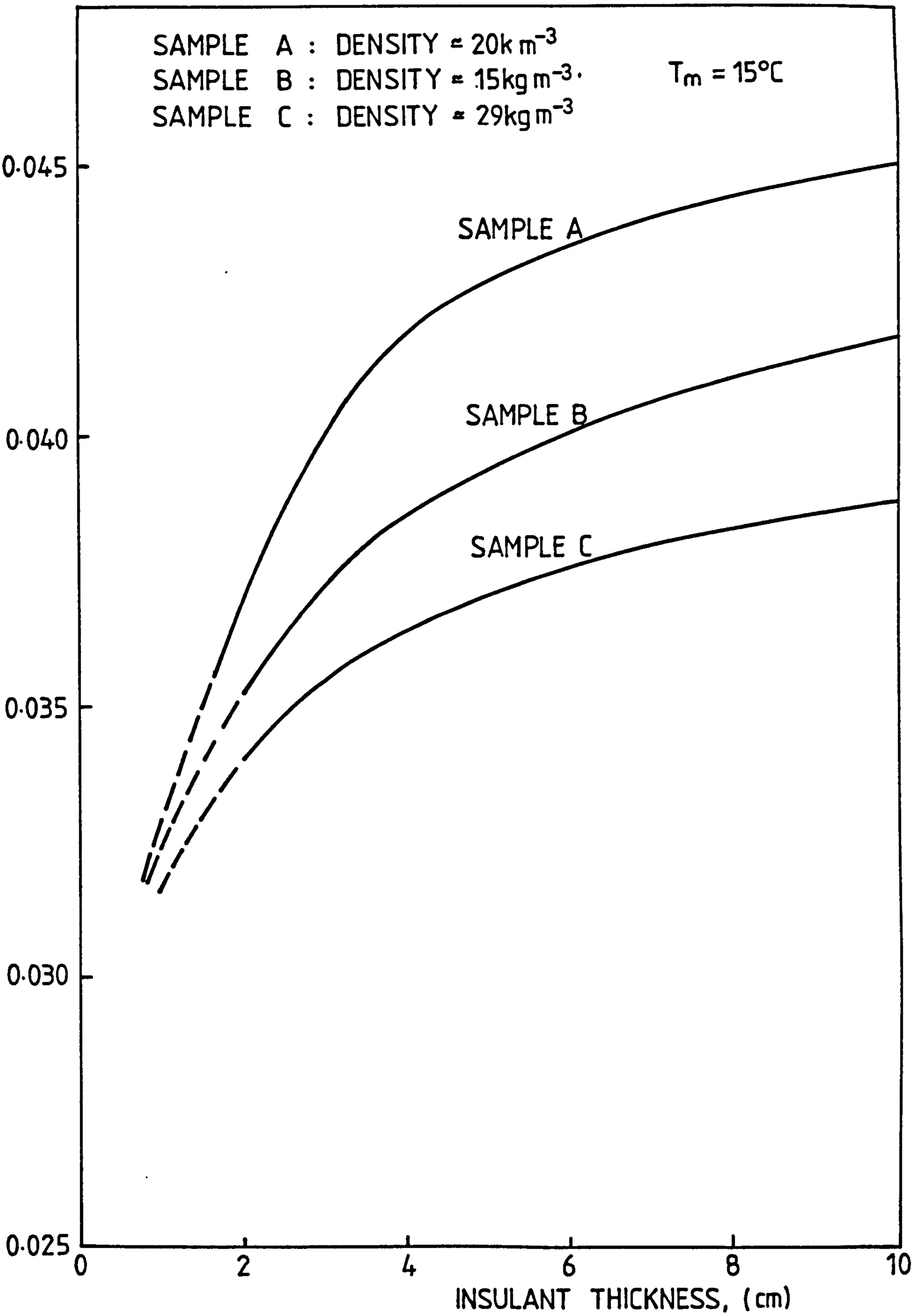

FIG.2. EFFECT OF THICKNESS ON THE APPARENT THERMAL CONDUCTIVITY OF THREE SAMPLES OF FOAMED INSULANT (JONES (5)).

This statement is expressed in the form of the modified Rayleigh number Ra*. Thus

$$Ra^* = \frac{\beta\, c_p\, \rho_g}{\nu}\, \delta\, B_o\, \frac{\Delta T}{k} \qquad \ldots (6)$$

for specimens traversed by a vertical temperature gradient, the onset of convection occurs when $Ra^* > 4\pi^2$ ($\simeq 40$).

This expression was utilised by Horton and Rogers (7) to predict the existence of convection currents in geological formations. The geological evidence of salt distributions in the formations studied (7) required the existence of convection currents but the utilisation of equation (5) failed to predict convection. Thus it was considered that this expression predicted temperature gradients had to be larger than was necessary in practice for convection to ensue.

Lapwood (8) independently followed a similar approach to that of Horton and Rogers, and arrived at the expression

$$\frac{\Delta T}{\delta} = \frac{4\pi^2\, \alpha}{K\, \beta\, \delta^2} \qquad \ldots (7)$$

for the critical condition marking the onset of convection between two impervious conducting boundaries separated by a porous material. In this equation K represents the coefficient of permeability (which incorporates the viscosity terms found in equation (5)). Other boundary conditions were explored by Lapwood (8) who arrived at the expression

$$\frac{\Delta T}{\delta} = \frac{27.1\, \alpha}{K\, \beta\, \delta^2} \qquad \ldots (8)$$

for conducting boundaries which were impervious below and had fluid above. The numerical solution for conducting boundaries which were impervious below and had a free surface above was considered to lie between the solutions described by equations (7) and (8). However the theory was inadequate near the boundaries and it was thus difficult to relate conductive and convective heat transfers (8).

Bankvall (9) and Fournier and Klarsfeld (10) measured the specific permeability coefficient for fibrous insulants of various densities. Their results were in close agreement as can be seen from Figure 3. Utilising these results for glass-fibre insulation of bulk density

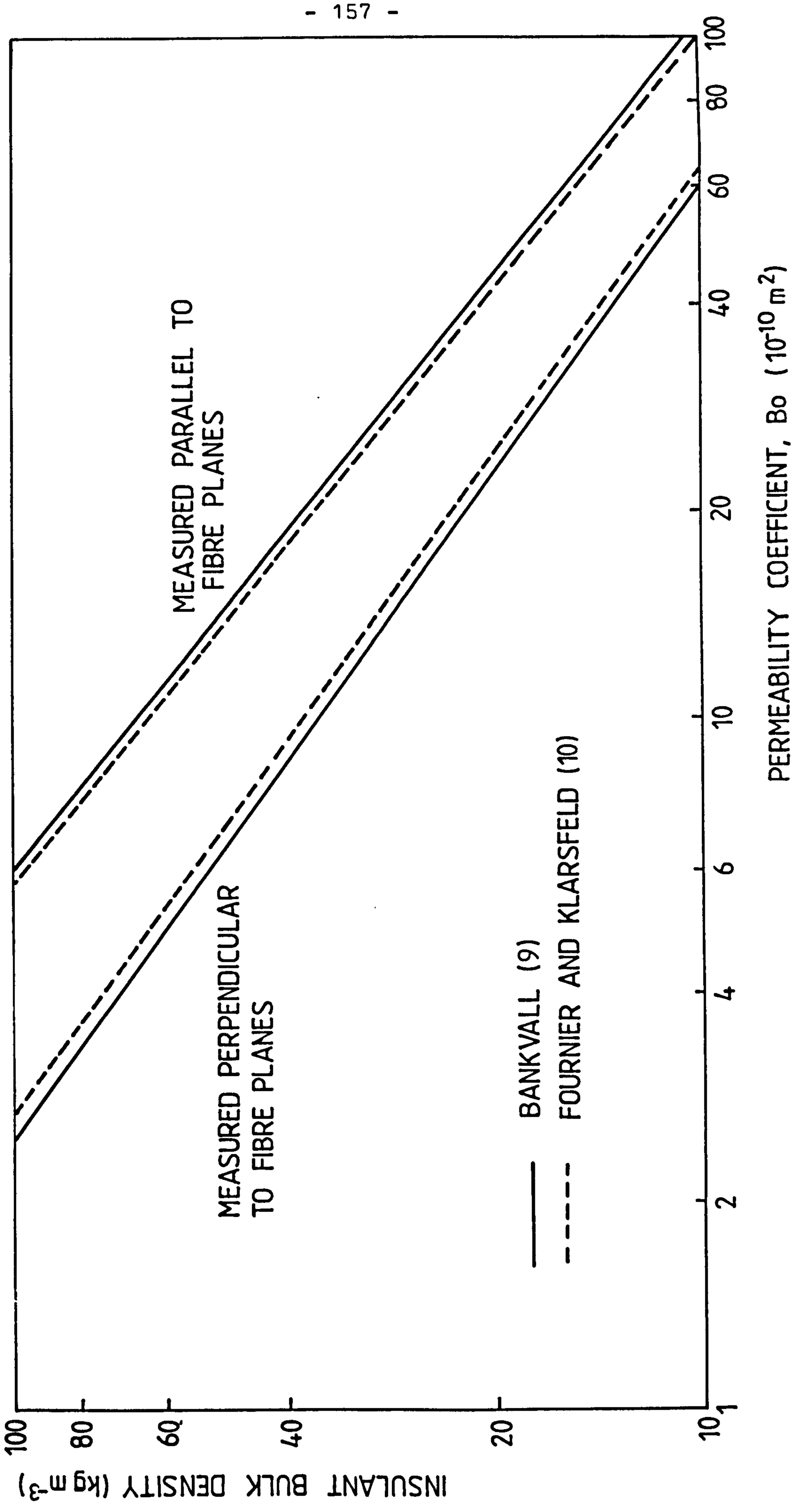

FIG.3. PERMEABILITY COEFFICIENT FOR GLASS FIBRE INSULANT.

12 kgm^{-3} and thickness 100 mm, typically used in loft insulation, with a temperature difference of 25°C across its horizontal faces, then the modified Rayleigh number, from equation (6), is ≃ 0.8 and thus convection through the bulk of the material should be suppressed.

The condition stated in equation (8) for a fluid boundary above the insulant also predicts the suppression of bulk convective effects.

Temperature distribution and thermal conductivity measurements for a loose-fill mineral fibre insulant of various thicknesses

The temperature distribution through the depth of a loose-fill mineral fibre insulation open to undisturbed air at its upper surface was measured utilising suspended thermojunctions as shown in Fig. 4. Heat was provided using the horizontal hot-plate shown which had below it (and thermally insulated from it) a horizontal guard heater to eliminate downward heat losses from the main heater. To prevent lateral heat losses throughout the depth of the insulant a series of individual strip heaters were constructed to surround the box containing the insulant. Thermojunctions at the midpoint of each strip were connected to form a differential thermometer with another thermojunction at the same height and lateral position placed along the centre line of the contained insulant (see Fig. 5).

The temperature distribution and main heater power input were measured for various depths of insulant. At each depth the base guard-heater and side strip guard-heaters were adjusted so that no heat flow occurred downwards through the base or through the sides of the apparatus under steady-state conditions. The main heater powers for the various depths of insulation studied are shown in Table 2 and the temperature distributions in Fig. 6. The temperature distribution for a depth of 125 mm does not lie between that for 100 mm and 150 mm, as might be expected, because of the higher power used in this particular instance giving rise to higher temperatures. In order that the temperature distributions could be located at the same origin the difference between the base temperature at the main heater surface

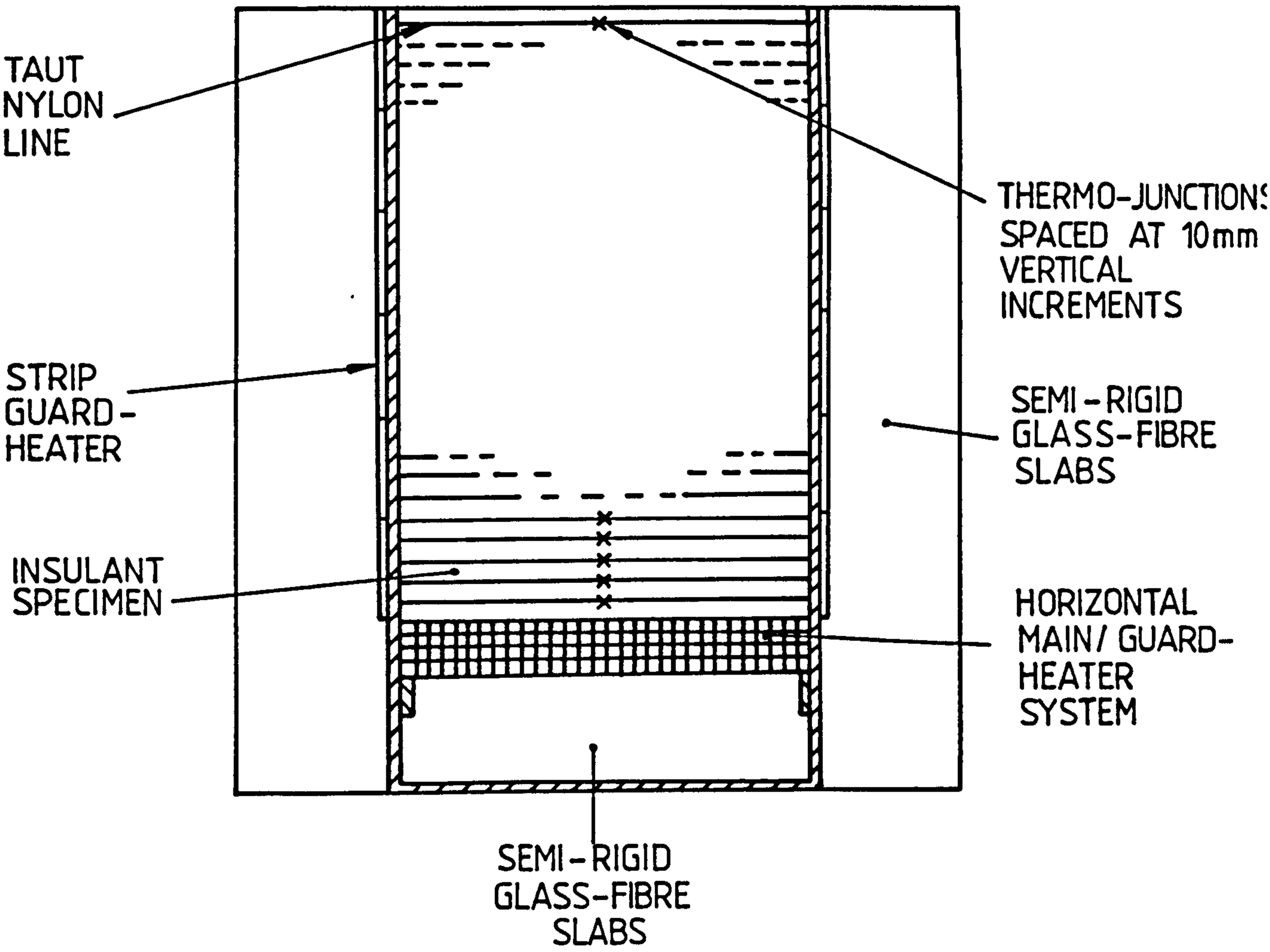

FIG.4. VERTICAL SECTION THROUGH THE APPARATUS TO MEASURE THE THERMAL CONDUCTIVITY OF LARGE THICKNESSES OF INSULANT.

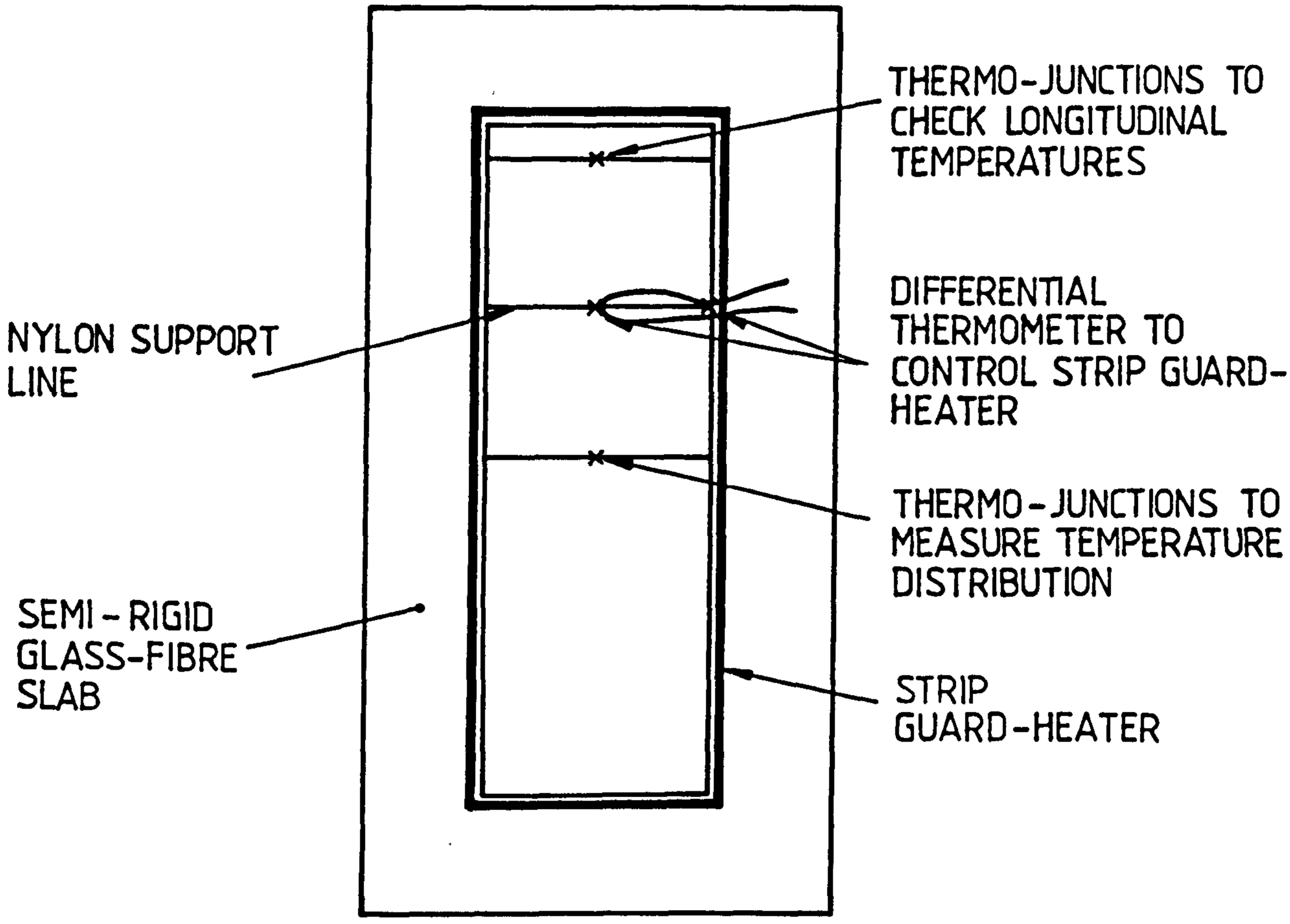

FIG.5. PLAN VIEW OF APPARATUS.

FIGURE 6.

TEMPERATURE DISTRIBUTION THROUGH MINERAL FIBRE LOOSE-FILL INSULANT OF VARIOUS THICKNESSES.

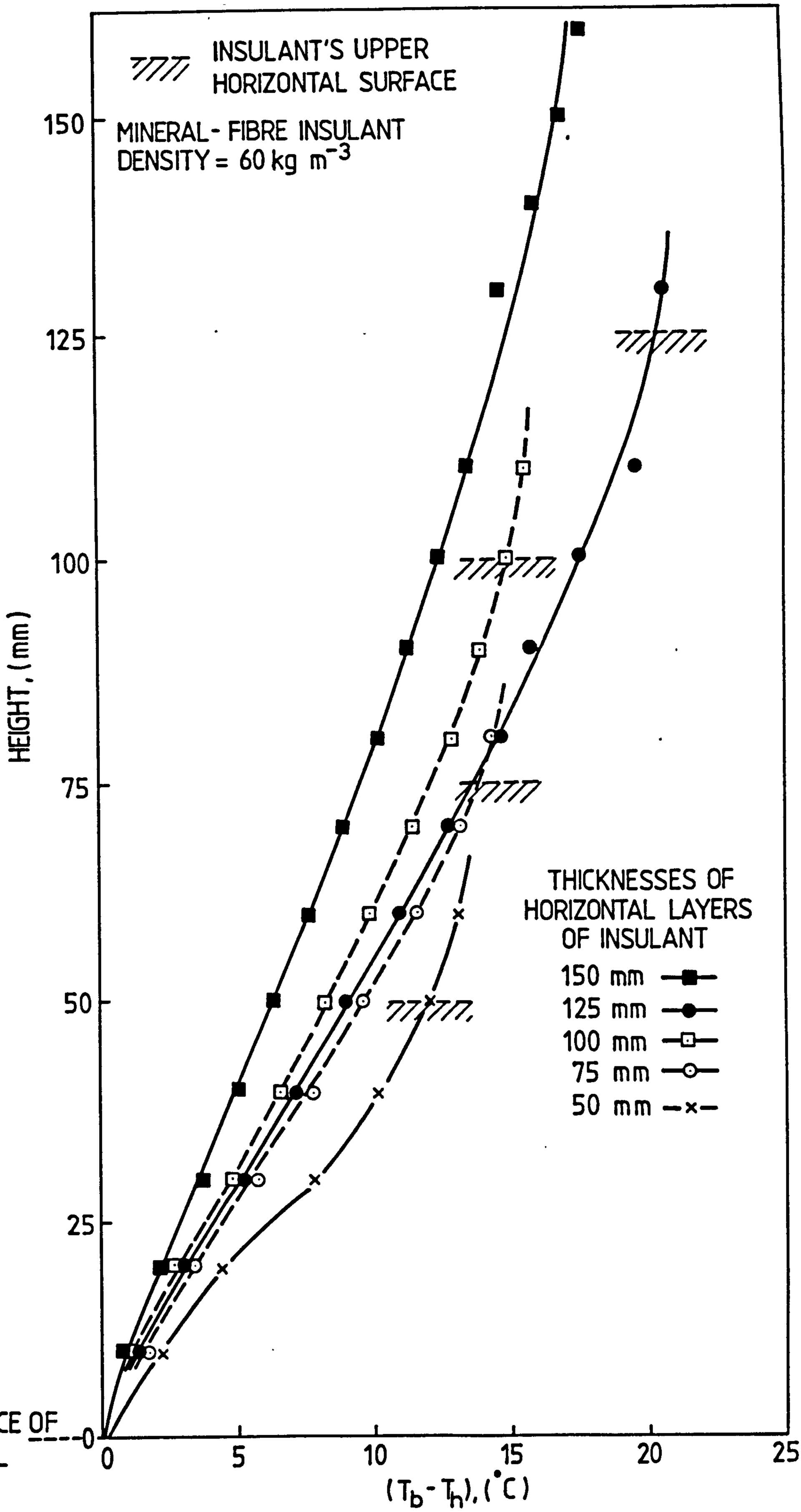
INSULANT'S UPPER HORIZONTAL SURFACE
MINERAL-FIBRE INSULANT
DENSITY = 60 kg m^{-3}
HEIGHT, (mm)
150
125
100
75
50
25
0
THICKNESSES OF HORIZONTAL LAYERS OF INSULANT
150 mm
125 mm
100 mm
75 mm
50 mm
TOP SURFACE OF HORIZONTAL HEATER
0
5
10
15
20
25
$(T_b - T_h)$, (°C)

INSULANT THICKNESS (mm)	MAIN HEATER POWER (W)	APPARENT THERMAL CONDUCTIVITY ($Wm^{-1}\ K^{-1}$)
50	3.27	0.049
75	3.84	0.074
100	3.64	0.087
125	4.65	0.101
150	3.62	0.113

Table 2. Main Heater powers and measured apparent thermal conductivities for various thicknesses of mineral fibre insulation.

(T_b) and the temperatures at 10 mm height intervals (T_h) was plotted against height.

The thermal conductivity for each thickness was calculated utilising the expression

$$k = \frac{\dot{Q}\,\delta}{A\,\Delta T}$$

where ΔT was the temperature difference between the heater surface and the top surface of the insulant. When the insulant's upper surface occurred midway between two thermojunctions, the surface temperature was read from the temperature distribution graph in Fig. 6.

The variation of the apparent thermal conductivity with thickness was plotted in Fig. 7.

FIGURE 7.

APPARENT THERMAL CONDUCTIVITY VS THICKNESS

FOR LOOSE-FILL MINERAL FIBRE INSULANT

WITH ITS TOP SURFACES EXPOSED TO AIR.

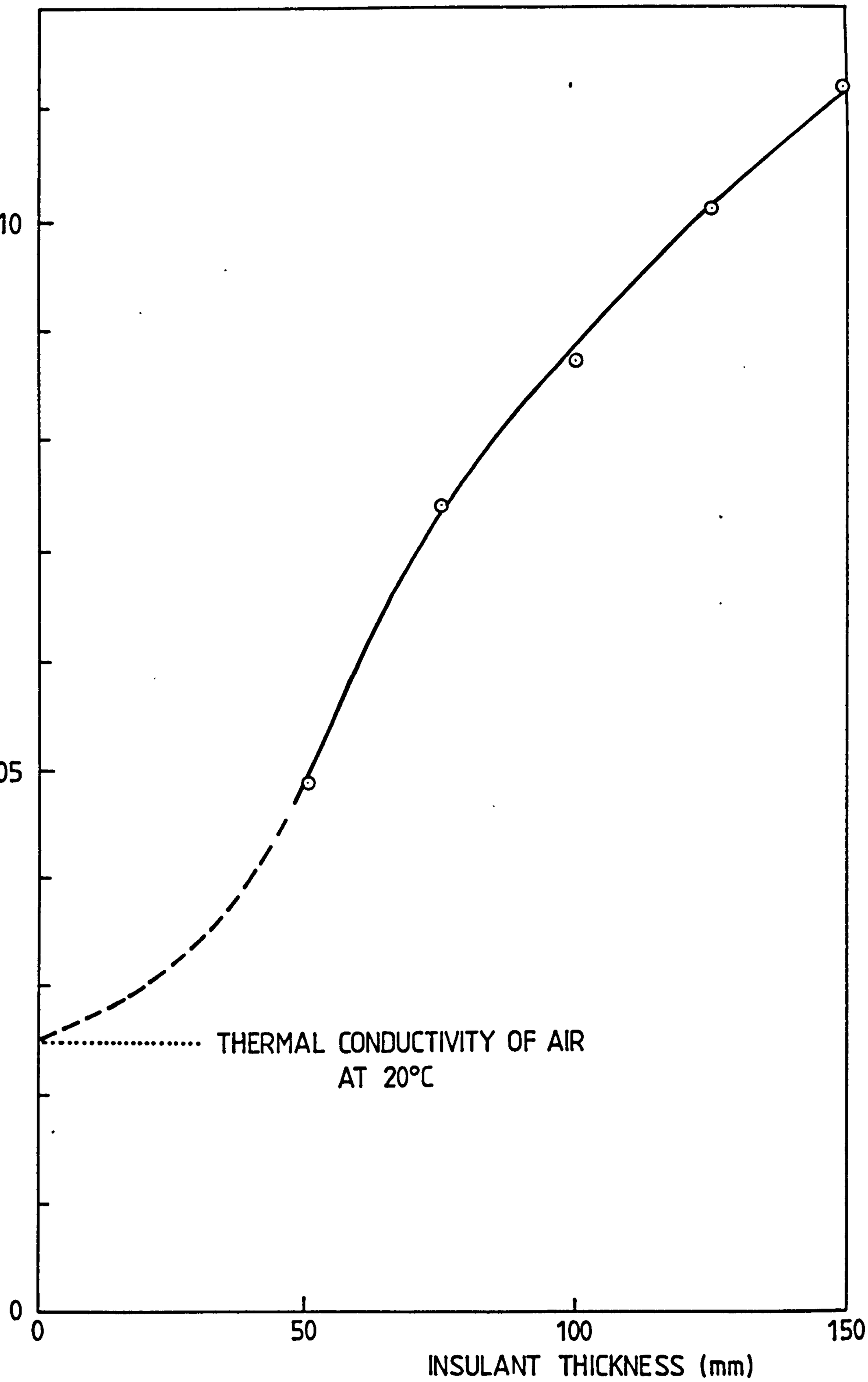
APPARENT THERMAL CONDUCTIVITY, ($Wm^{-1} K^{-1}$)
0·10
0·05
0
THERMAL CONDUCTIVITY OF AIR AT 20°C
0
50
100
150
INSULANT THICKNESS (mm)

INFERENCES

It can be seen from Fig.6 that the temperature distribution curves contain three distinct regions which have been exaggerated in Fig.8. There is a marked decrease in temperature gradient in region I, close to the heater and in region III, close to the insulant-air interface, whereas in region II the temperature difference increases linearly with height. The thermal conductivities measured over the linear regions of the curves in Fig.6 are compared with the apparent thermal conductivity of the total insulant thickness in Table 3. The ratio k_{II}/k is constant within expected experimental error. The apparent thermal conductivity is considerably larger than suggested in the commercial literature, and increases with the thickness of the specimen. Nevertheless an additional thickness of insulant always led to a reduction of the rate of heat loss.

INSULANT THICKNESS (mm)	APPARENT THERMAL CONDUCTIVITY, k ($Wm^{-} K^{-}$)	THERMAL CONDUCTIVITY REGION II, k_{II} $Wm^{-} K^{-}$	$\frac{k_{II}}{k}$
50	0.049	0.043	0.88
75	0.074	0.066	0.90
100	0.087	0.079	0.91
125	0.101	0.089	0.88
150	0.113	0.103	0.91

Table 3. Comparison of the apparent average thermal conductivity for the whole specimen with that for region II.

In order to explain the shape of the temperature distribution curve (fig.8) the heat transfer behaviour of each region will need to be considered in more detail.

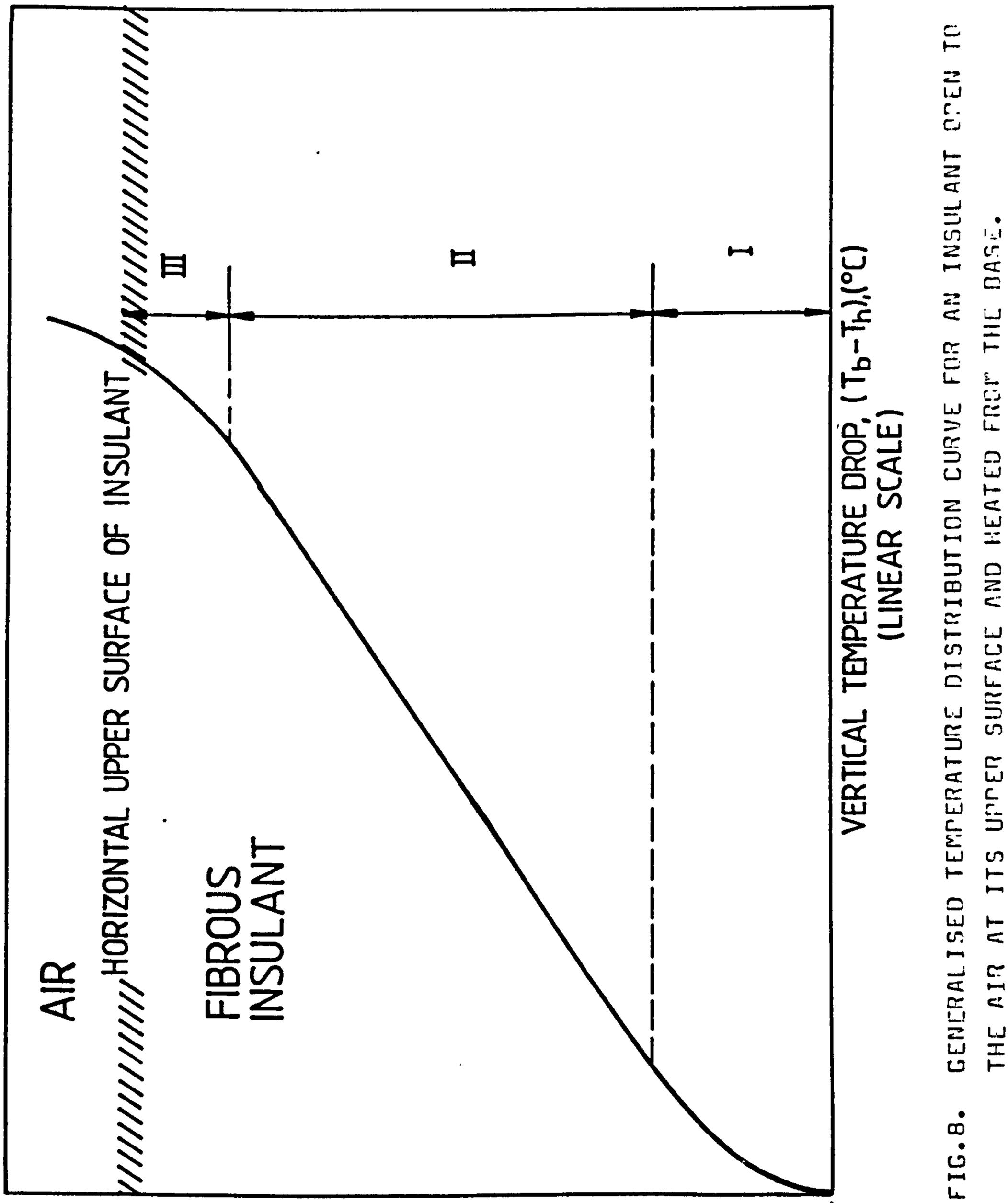
AIR
HORIZONTAL UPPER SURFACE OF INSULANT
FIBROUS INSULANT
III
II
I
HEIGHT ABOVE TOP SURFACE OF HEATER (LINEAR SCALE)
VERTICAL TEMPERATURE DROP, (T_b–T_h),(°C) (LINEAR SCALE)
HORIZONTAL TOP SURFACE OF HEATER
GENERALISED TEMPERATURE DISTRIBUTION CURVE FOR AN INSULANT OPEN TO THE AIR AT ITS UPPER SURFACE AND HEATED FROM THE BASE.

FIG.8.

Region I

It was considered by Pelanne (4) that the apparent thermal conductivity of a fibrous insulant could be described by the expression

$$k = k_g + k_{cv} + k_s + k_r + k_i \qquad \ldots (9)$$

where k_s and k_g are the components due to conduction through the solid and trapped air respectively, k_{cv} is due to convection, k_r to radiation and k_i is described as being due to the interaction between air and the other modes. If the insulant is evacuated, the effective thermal conductivity becomes,

$$k = k_s + k_r \qquad \ldots (10)$$

Thus if k_g is known at the mean temperature for the air filled and evacuated tests, then $(k_i + k_{cv})$ can be derived from these results. This is clearly shown for hot-plate surface emissivities of 0.08 and 0.95 in Fig. 9. These results suggest that there is significant absorption of thermal radiation within the sample. (Radiation scattering would not be expected to distort the temperature distribution because the radiant energy is not transformed in the scattering process).

The results of Fig. 10, also due to Pelanne (4), show that the surface emissivity of the hot-plate has more effect in the evacuated (rather than the air-filled) insulant which would suggest that the air rather that the fibre matrix is causing the absorption of radiation which leads to the temperature distribution distortions from linearity seen in region I. But only water vapour and CO_2 contribute to the radiation absorption.

Rennex (11) considered this situation by applying the expression

$$\dot{q}_t = \dot{q}_c + \frac{\text{constant}}{3/4\ \beta\delta + 2/\varepsilon - 1} \qquad \ldots (11)$$

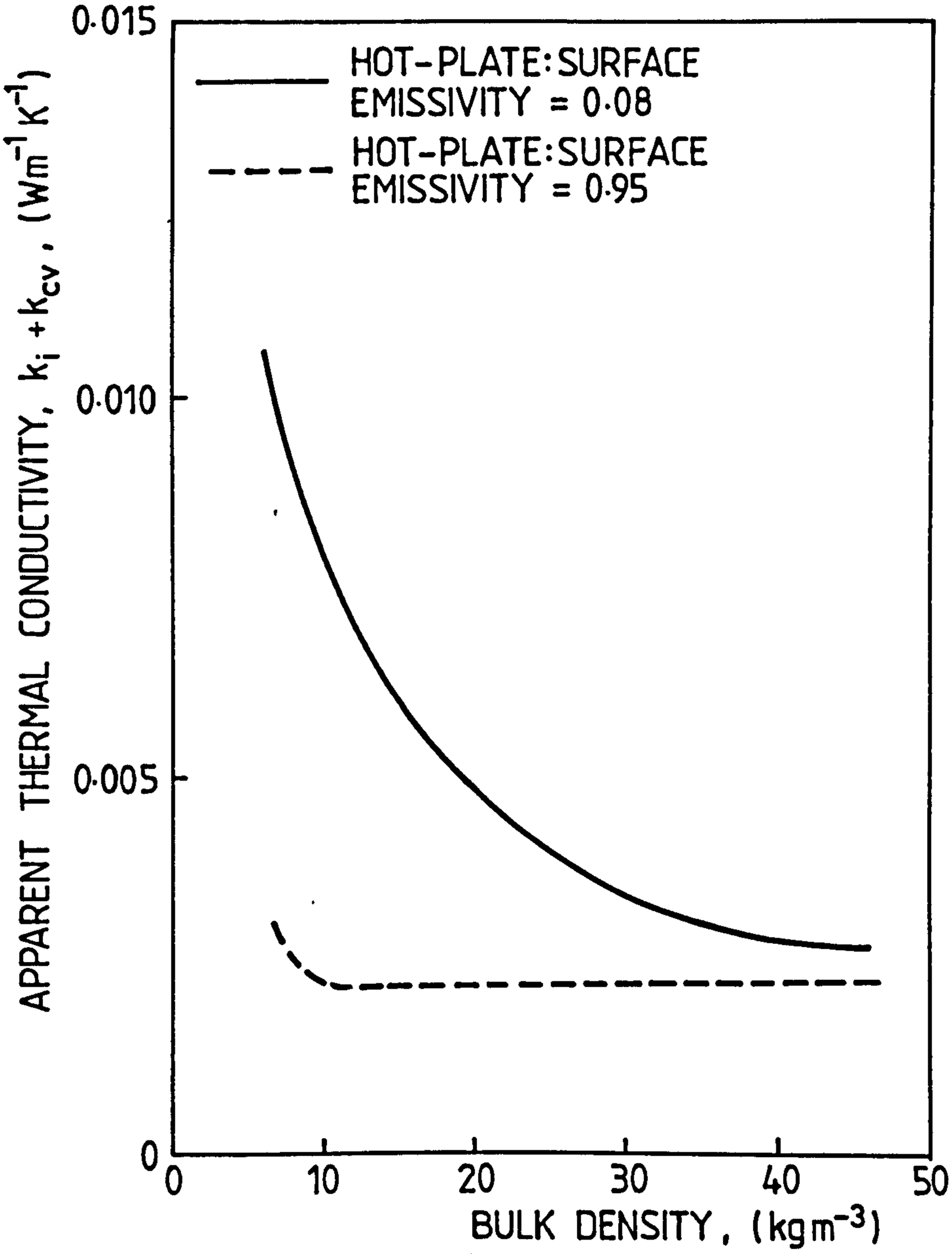

FIG.9. EFFECT OF A HOT PLATES SURFACE EMISSIVITY AND INSULANT DENSITY ON THE CONVECTIVE AND INTERACTIVE COMPONENTS(EQUATION 9) OF THE APPARENT THERMAL CONDUCTIVITY : (PELANNE (4)).

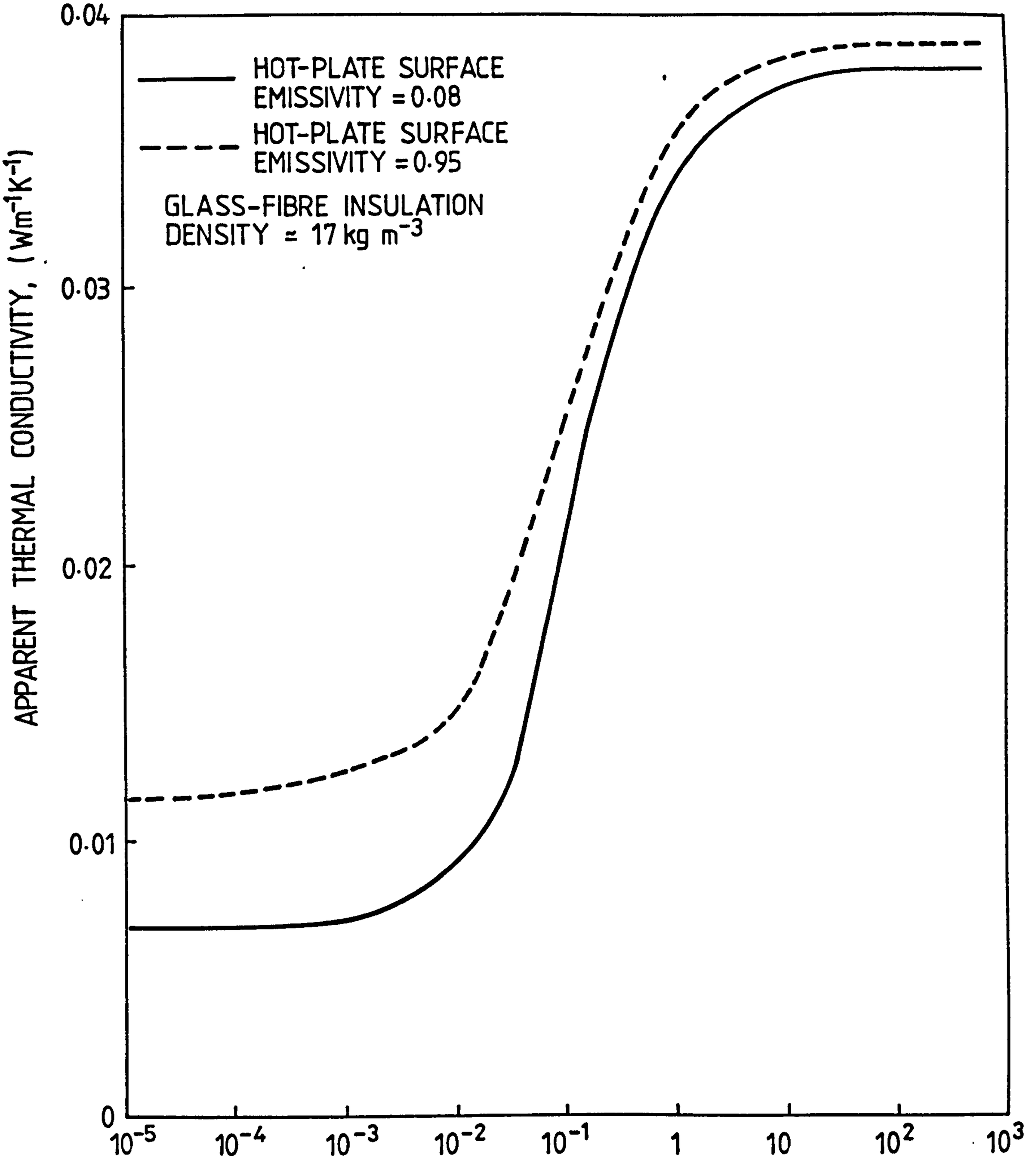

FIG.10. EFFECTS OF AIR PRESSURE AND HOT PLATE SURFACE EMISSIVITY ON THE APPARENT THERMAL CONDUCTIVITY OF GLASS FIBRE INSULATION (PELANNE (4)).

The radiation extinction term β, which is the sum of the scattering and absorption coefficients, would be smaller in the vacuum case than at atmospheric pressure if absorption in the air actually occurred. Utilising equation (11) Rennex concluded that differences between, $\dot{q}_t$, for the high emissivity surface and the low emissivity surface would be larger under evacuated than under atmospheric pressure conditions.

Region II

It is clear from Fig. 6 that in region II the temperature gradient is approximately linear within experimental error. This suggests that absorption of thermal radiation does not occur in this layer although the increase in the apparent thermal conductivity in this layer with thickness (see Table 3), suggests that radiation scattering is still an important mode of heat transfer.

Region III

The departure from linearity displayed in region III cannot be due to radiative effects but must be due to interactions between the free air above and the air in the surface layers of the insulant. The average temperature difference between the insulant surface and the bulk atmosphere above it was 2.5°C. If the insulant surface were considered as a flat horizontal plate, then the convective heat transfer coefficient would be deduced from the correlation

$$\overline{Nu}_L = 0.54(G_r\ P_r)^{0.25} \qquad \ldots (12)$$

where

$$\overline{Nu}_L = \frac{h_c\ L}{k_g} \qquad \ldots (13)$$

This gives a convective heat transfer coefficient of 2.7 $Wm^{-1}\ K^{-1}$ at the insulant surface. Therefore it is possible that air is entrained from the surface layers of the insulant by pressure differences created by the convecting air layer at the insulant surface. The insulant surface was consequently investigated qualitatively to detect the presence

of air circulation. Investigations of air movements over the insulant surface were undertaken using commercial smoke tubes to create smoke trails. Smoke was observed to enter the surface of the insulant and reappear at a location well away from the point of entry. The distance between the points of entry and reappearance was measured at several locations over the insulant/air interface for heater powers of 1W and 5W for an insulant thickness of 50 mm. It was found that the average circulation cross-section dimensions (i.e. separations between entry and exit of the smoke) were approximately 15 mm and 23 mm for heater powers of 1 watt and 5 watts respectively.

DISCUSSION

Measurements of the thermal conductivity of porous insulants are usually undertaken using the guarded hot-plate technique, where both the hot and cold surfaces of the insulant are bounded by the solid surface of the hot or cold plate. Often however, and particularly in attic spaces, the top surface of the insulant is left open to the air in the loft. Convection currents set up by the difference in temperature between the insulant surface and the air or air movements within the space above the insulant such as draughts will cause air to be entrained from the surface layers of the insulant, thus enhancing the rate of heat transfer.

The thickness effect illustrated by these results and the convective enhancements of insulant surface heat transfers result in apparent thermal conductivity values higher than those generally quoted by data sources. It is important that these effects should be further investigated and measurement techniques improved in order that their economic implications may be confidently assessed.

The presented results for the particular sample considered suggest that doubling and trebling the insulant thickness from 50 mm results in increases of thermal resistance of only 1.12 and 1.3 respectively.

R E F E R E N C E S

(1) British Standards Institution — "The Building (First Amendment) Regulations, Part FF, No. 723". British Standards Institution, London, 1978.

(2) British Standards Institution — "The Building (Second Amendment) Regulations, Part F, No. 1338". British Standards Institution, London, 1981.

(3) Eurosol 1981 — Eurosol U.K., 'Insulation Fact Sheet No. 9., British and European Standards of Insulation', October 1981.

(4) Pelanne, C.M. — 'Experiments in the separation of heat transfer mechanisms in low-density fibrous insulation', Proc. Eighth Conference on Thermal Conductivity, Purdue University, Indianna, pp 897-911. 1968.

(5) Bankvall, C.G. — 'Heat transfers in fibrous materials', Document D4: 1972, National Swedish Building Research, Lund Institute of Technology, Sweden, 1972.

(6) Jones, T.T. — "The effects of thickness and temperature on heat transfers through foamed polymers". Proc. 7th Conf. on Thermal Conductivity, NBS Special Publication 302, pp 737-748, 1968.

(7) Horton, C.W. and Rogers, F.T. — 'Convection currents in a porous medium', J. Appl. Phys. 16, pp 367-370, 1945.

(8) Lapwood, E.R. — 'Convection of a fluid in a porous medium', Proceedings of the Cambridge Philosophical Society, Vol. 44, pp 508-521, 1948.

(9) Bankvall, C.G. — 'Natural convective heat tranfer in permeable insulation', Thermal Transmission measurements of Insulation, ASTM, STP 660, R.P. Tye, Ed., ASTM pp 73-81, 1978.

(10) Fournier, D. and Klarsfold, S. — 'Some recent experimental data on glass-fibre insulating materials and their use for reliable design of insulations at low temperatures'. Heat Transmission and Measurements in Thermal Insulation, ASTM STP 554, ASTM pp 223-242, 1974.

(11) Rennex, B.G. — 'Thermal parameters as a function of thickness for combined radiation and conduction heat transfer in low-density insulation, J. of Thermal Insulation, Vol. 3, pp 37-61, 1979.

CHAPTER 7.

APPARENT THERMAL CONDUCTIVITIES OF HIGH-POROSITY CELLULAR INSULANTS.

NOMENCLATURE

a	constant as defined by fig.5	
B	constant as defined by equation 3	
C	constant as defined by equation 3	
C_1	universal constant (3.74×10^{-16})	$J\ m^2\ s^{-1}$
C_2	universal constant (1.43×10^{-2})	$m\ K$
e	volume fraction of cell voids, i.e. the porosity	
e_1	1-dimensional porosity as in fig.1	
e_2	2-dimensional porosity as in fig.1	
e_s	volume fraction of the solid phase	
f	volume fraction of fluorocarbon as in equation (24)	
k_C	conductive component of the apparent thermal conductivity due to the continuous phase	$Wm^{-1}\ K^{-1}$
k_D	conductive component of the apparent thermal conductivity due to the dispersed phase	$Wm^{-1}\ K^{-1}$
k_s	thermal conductivity of the solid phase	$Wm^{-1}\ K^{-1}$
k_g	thermal conductivity of the gaseous phase	$Wm^{-1}\ K^{-1}$
n	suffix indicating the number of the radiation surface considered	
p_a	partial pressure of air	Nm^{-2}
p_f	partial pressure of fluorocarbon gas	Nm^{-2}
$\dot{q}$	heat flux rate	Wm^{-2}
R_g	thermal resistivity due to the gaseous phase (Fig.6)	$m^2K\ W^{-1}$
R_{s_I}	thermal resistivity due to the solid phase which is in series with the gaseous phase in the heat flow direction (Fig.6)	$m^2K\ W^{-1}$
$R_{s_{II}}$	thermal resistivity due to the solid phase in parallel with the gaseous phase in the heat flow direction (Fig.6)	$m^2K\ W^{-1}$
R_T	total thermal resistivity as defined by equation (10)	$m^2K\ W^{-1}$
s	separation between cell walls in the heat flow direction (Fig.8)	m

T	temperature	K
T_m	mean temperature	K
T_n	temperature at the nth. component	K
T_o	temperature at the emitting surface	K
δ	thickness of the sample	m
ε	emissivity of the surfaces bounding the insulant sample	
ε_1	emissivity of surface 1	
ε_2	emissivity of surface 2	
ε_c	emissivity of cell wall of the cellular insulant	
λ	wavelength of electromagnetic radiation	m
ρ_b	bulk density	kg m^{-3}
ρ_g	density of gas contained in cells of the insulant	kg m^{-3}
ρ_s	density of the solid matrix of the insulant	kg m^{-3}
μ	arithmetic mean value of a sample	
σ	standard deviation	

INTRODUCTION

Devising an accurate and comprehensive model of heat transfers through multi-phase materials has been attempted for many years. Initially, an analogy with the model proposed by Maxwell (1) for predicting the electrical resistance of a heterogeneous systems, consisting of spheres of one medium distributed randomly in another was used. Subsequently, in order to solve the thermal resistance problem, several theoretical structural parameters, or empirical coefficients (whose physical meanings with respect to the structures of the materials often have not been identified) were introduced (2-14). These parameters, chosen to permit the development of theoretical models of the process of thermal conduction through a heterogeneous system are often extremely difficult to measure experimentally.

It was considered by Tsao (15) that there was a need to develop a general model to describe the heat transfer behaviours of two-phase materials. A probabilistic approach was used to derive an expression for the effective thermal conductivity of the two-phase material in terms of the mean and standard deviations of the one-dimensional porosity, in the direction of the heat flow.

The two-phase material, shown in figure 1(a), was sectioned as in figure 1(b), into layers perpendicular to the direction of heat flow. Each layer was chosen to be sufficiently thin so that the two-dimensional porosity in the yz plane could be assumed to be invariant throughout the thickness of a specific layer. The

PAGE NUMBERING AS ORIGINAL

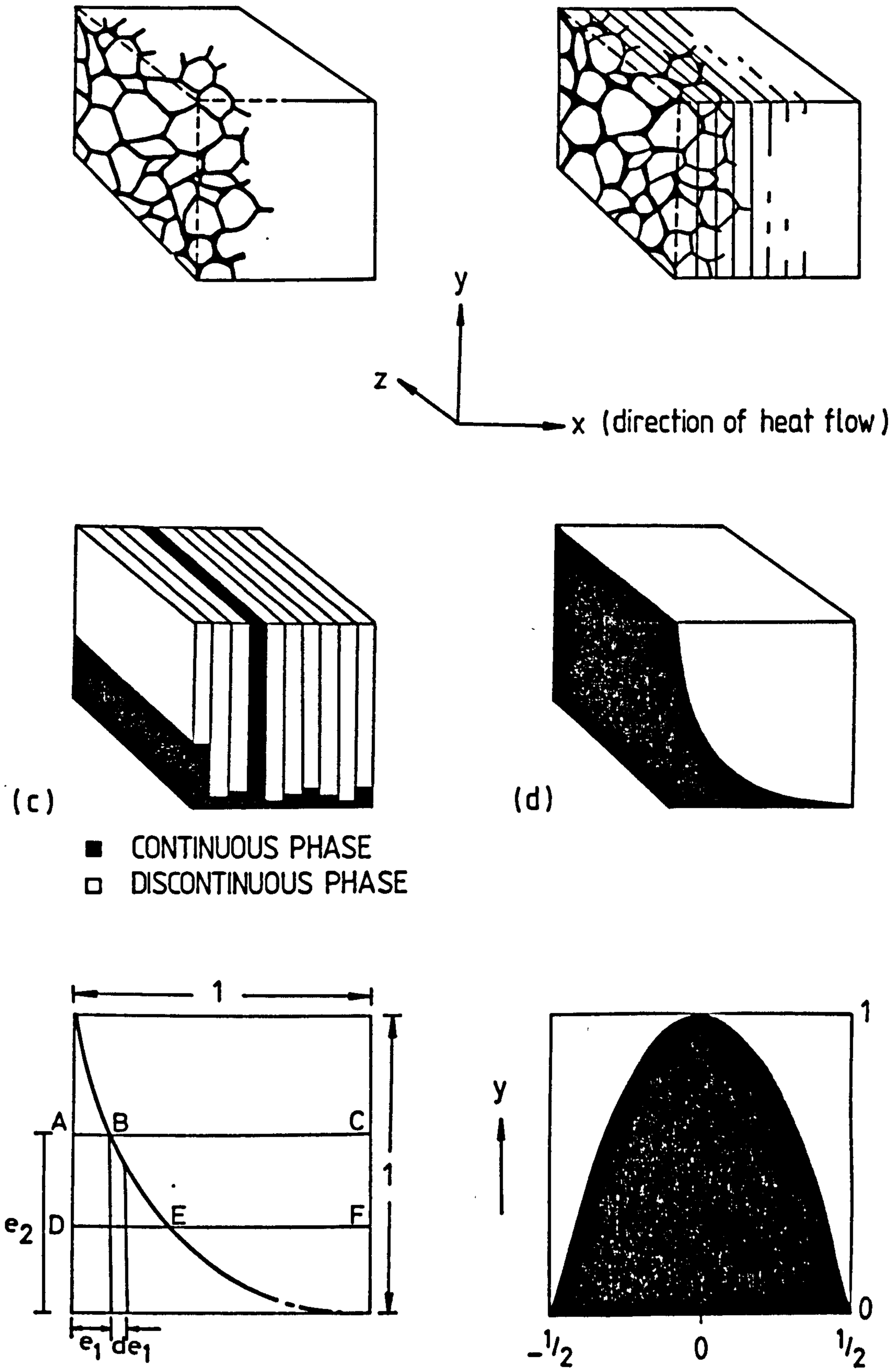

FIG.1. THE CONSIDERED SPECIMEN .

conductances of the continuous and discontinuous phases were considered as being permitted to be added in parallel and it was assumed that, the material could be re-arranged as in figure 1(c) without changing the effective thermal conductivity of each layer. The thin layers were then re-arranged as in figure 1(d) with the two-dimensional porosity e_2 decreasing in the direction of the heat flow.

If the cube(of fig.1) is considered to have each linear dimension of unity, then it can be seen from figure 1(e) that the probability of the one-dimensional porosity of any horizontal line drawn below ABC, such as DEF, being greater than e_1 is e_2. When an infinite number of horizontal lines are considered in the unit area and each line is divided into n-segments such that every segment is made up of either continuous or discontinuous phases, then the probability of any segment being occupied by discontinuous phase is e, i.e. the porosity or volume voidage. Tsao (15) considered that the probability of having $e_1 n$ out of n segments occupied by the discontinuous phase followed a binomial distribution which for large values of n approaches a normal (Gaussian) distribution. Utilising these assumptions he derived the expression for the effective thermal conductivity as

$$\frac{1}{k} = \int \frac{de_1}{k_C + (k_D - k_C) \int_{e_1}^{1} \frac{1}{\sigma\sqrt{2\pi}} \exp\left[-\frac{1}{2\sigma^2}(e_1 - \mu)^2\right] de_1} \quad .. (1)$$

where the mean μ was considered to be equal to the volume fractions of the dispersed phase e.

Image analyses of thinly-sliced samples of porous materials such as fired clay-bricks or polyurethane foams (see figs. 2 and 3) may be undertaken using image analysis computers, such as the 'Quantimet'. Generally such analysers divide the picture up into picture points: in the case of the Quantimet 720 instrument, a maximum of 500,000 picture points are available for each image. The detector selects features for measurement according to their grey levels and defines feature boundaries. It is possible using this technique, with suitably prepared specimens, to measure the area, the total perimeter and the size distribution of the features detected. To charactrise fully any given material would require a large number of such readings. A brick for example, initially cut into 5 representative cubes which are sliced in orthogonal directions, one of which would be parallel to the direction of heat flow, could generate 4000 measurement frames. Each of these frames would require an area assessment and numerous size distribution counts to characterise one brick, which itself may not be a good representative of the batch of bricks it is taken from.

Although Tsao's model would at first appear to be very attractive, the acquisition of data to be used in the generalised equation (1)

- is time consuming and expensive, because of the need to produce thinly-sliced samples and the large quantity of data required to characterise any given sample.

Cheng and Vachon (16,17) modified and extended this model so that only a knowledge of the individual thermal conductivities of the materials forming the dispersed and continuous phases, and the

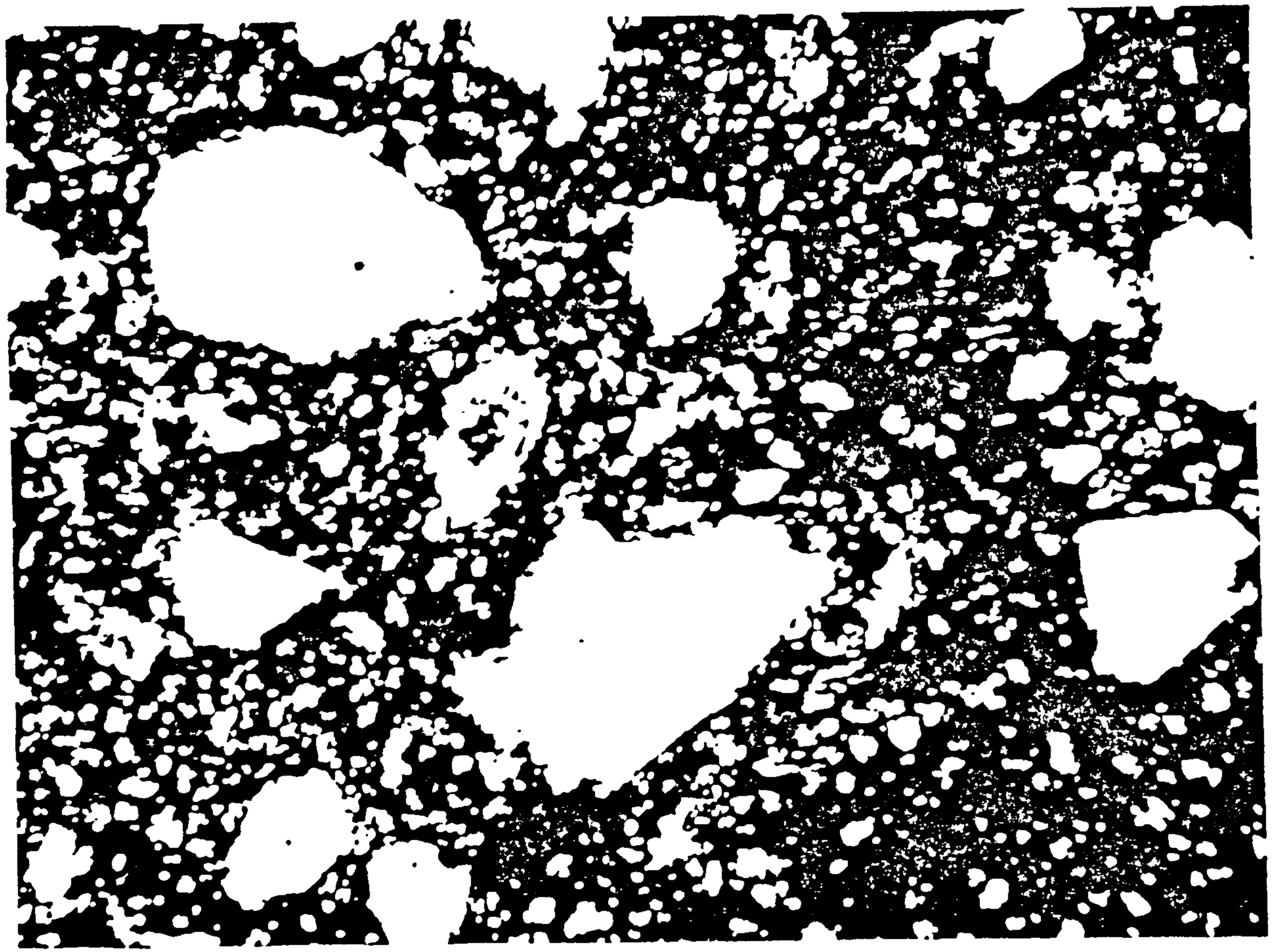

FIG.2. SECTION THROUGH A FIRED CLAY-BRICK SPECIMEN.

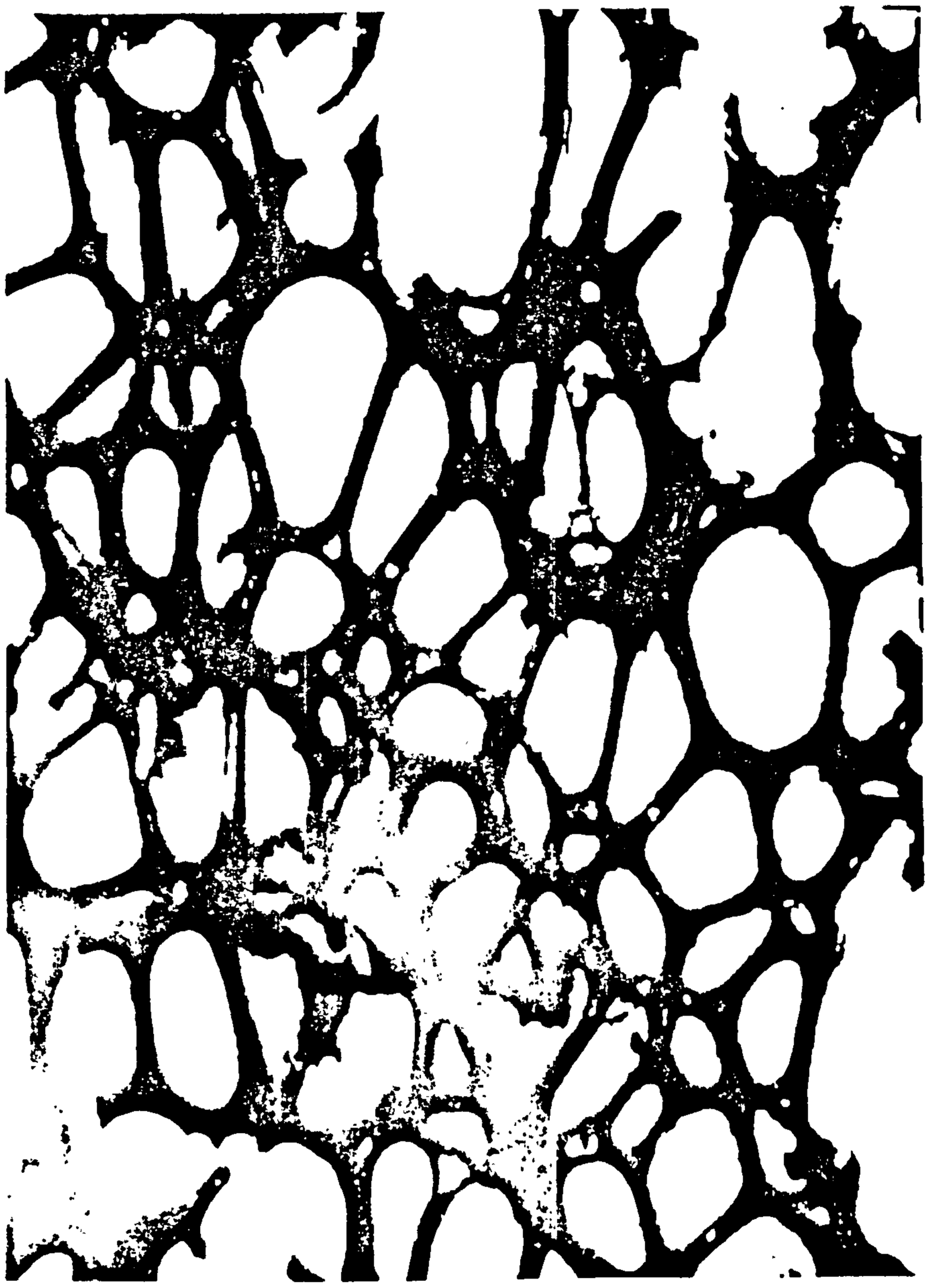

FIG.3. SECTION THROUGH A POLYURETHANE FOAM SPECIMEN.

porosity/volume voidage of the composite was required. Instead of arranging the thin layers as Tsao (15) did in fig.1(e), Cheng and Vachon (16) used the arrangement shown in fig.1(f) in order that the thermal conductivity could be expressed in terms of $y(x)$, i.e. $e_2(e_1)$. The determination of $y(x)$ for various fractions of the materials involved in the heterogeneous media could then be undertaken.

The rearrangement of the laminae, as in fig.1(f) gives a normal distribution of the continuous phase, which can be described by

$$f(x) = \frac{1}{\sqrt{2\pi\ \sigma^2}} \exp\left[-\frac{1}{2\sigma^2}(x - \mu)^2\right] \qquad \ldots (2)$$

With this arrangement, the mean value of the normally-distributed phase, μ, is zero so that the relationship in equation (2) may be simplified to give

$$y = B \exp(-Cx^2) \qquad \ldots (3)$$

In order to determine B and C, Cheng and Vachon (16) expanded the exponential component of equation (3) as a series, i.e.,

$$y = B\left(1 - Cx^2 + \frac{C^2x^4}{2!} - \ldots\right) \qquad \ldots (4)$$

The values of x range from $-\frac{1}{2}$ to $+\frac{1}{2}$ and the series rapidly converges to the expression

$$y \simeq B - Cx^2 \qquad \ldots (5)$$

This approach resulted in two equations :- <u>for $k_C > k_D$</u>

$$\frac{1}{k} = \frac{2}{\sqrt{\{\, C(k_D-k_C)\,\left[k_C+B(k_D-k_C)\right]\}}} \tan^{-} \frac{B}{2}\sqrt{\left[\frac{C(k_D-k_C)}{k_C+B(k_D-k_C)}\right]} + \frac{1-B}{k_C} \qquad \ldots (6)$$

and <u>for $k_D > k_C$</u>

$$\frac{1}{k} = \frac{1}{\sqrt{\{\, C(k_D-k_C)\,\left[k_C+B(k_D-k_C)\right]\,\}}} \frac{\ell n\sqrt{\left[k_C+B(k_D-k_C)\right]}+\frac{B}{2}\sqrt{C(k_D-k_C)}}{\sqrt{\left[k_C+B(k_D-k_C)\right]}-\frac{B}{2}\sqrt{C(k_D-k_C)}} + \frac{1-B}{k_C} \qquad \ldots (7)$$

where $B = \sqrt{\frac{3e}{2}}$

and $C = -4\sqrt{\frac{2}{3e}}$

When this model was applied to glass-fibre insulation, the predictions were in fair agreement with measurements, as can be seen from fig.4. However this approach is limited in its application by the condition that the dispersed phase (i.e. the discontinuous medium) may have a maximum volume fraction of only $^2/3$. Many low density, closed-cell insulants such as isocyanurate foams have discontinuous-phase volume fractions larger than this. These models, therefore, need to be further extended in order that predictions may be made for closed-cell media.

Foams with high voidages, i.e. with greater than 90% by volume for the gas phase, are formed by expanding gas bubbles in the viscous fluid which will set to form the solid matrix. The initially-spherical gas bubbles must deform into polyhedral cells with thin walls for the foam to attain voidages greater than approximately 70% of the volume of the medium. A perfectly closed packed

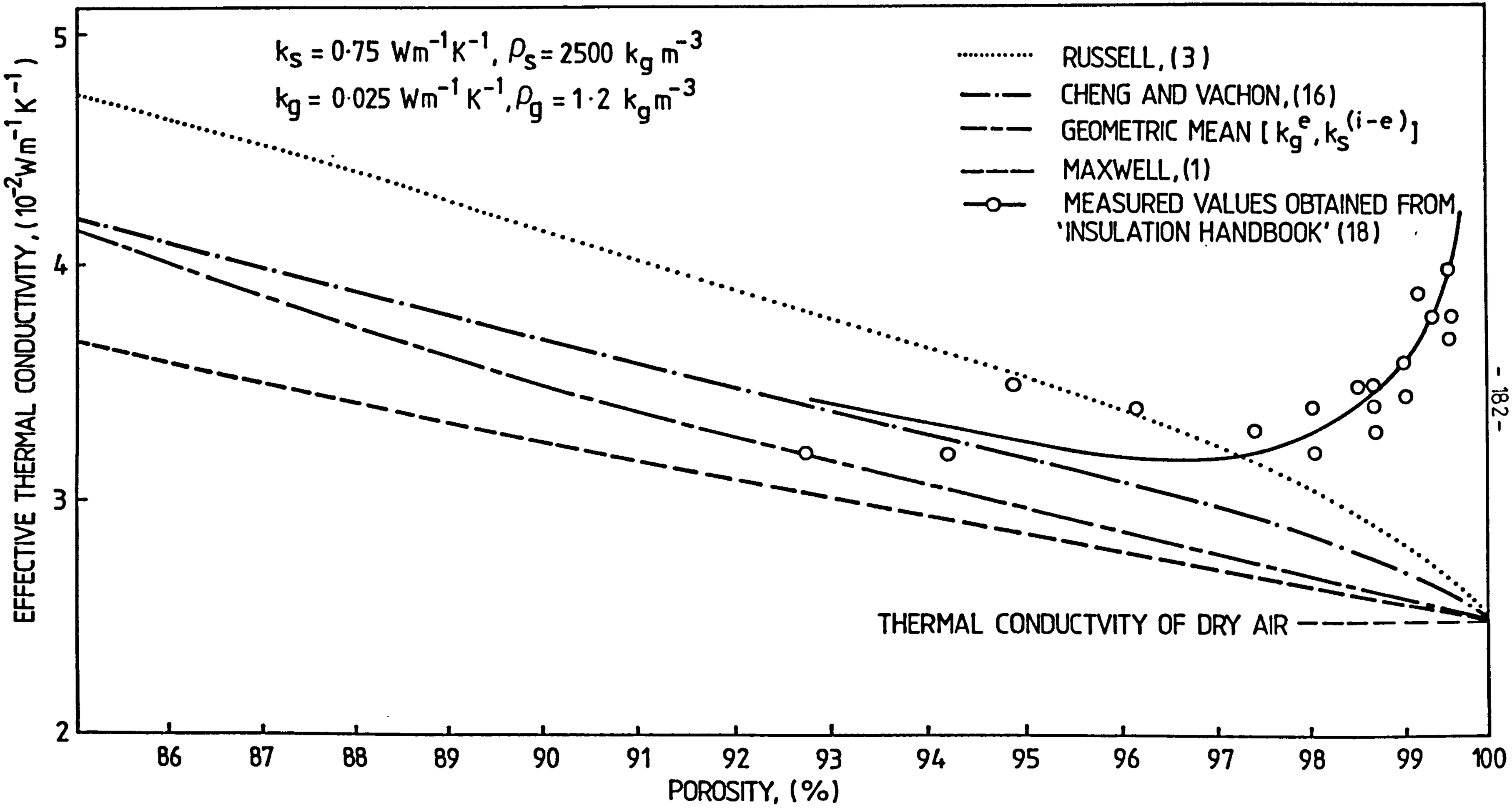

FIG. 4 . THERMAL CONDUCTIVITY OF GLASS FIBRE INSULANTS AT 20°C .

array of uniform spheres would deform into a dodecahedron (i.e. 12-sided structure) with regular pentagonal faces. The structure of real foams however is much more irregular than this and cells may not have exactly 12 faces. It can be seen from fig. 3 that the cells vary in size and orientation and the cell faces are mostly irregular pentagons or hexagons. The cell walls are very thin and join onto thickened'pillars'.

It would be useful if a model similar to that of Cheng and Vachon (16), utilising only the volume fraction of the gaseous phase and the thermal conductivities of those phases present could be developed. It has been assumed for this purpose that the curve enclosing the solid phase is described by a hyperbolic function namely y = a csch x (hyperbolic cosecant) as seen in fig. 5. The function described was utilised because it enabled high porisities to be modelled and was considered to give a good approximation of the expected structure of a unit cell of such a material at these porosities.

The simplifying assumptions made for this analysis are similar to those adopted by Cheng and Vachon (16) and are as follows:-

- The heat flow is one-dimensional, i.e. in the x-direction of fig.1.
- The pores are so small that the convection within them is suppressed, and the relative magnitude of the radiation contribution to the heat flux is negligible.
- Contact resistances between the continuous and discontinuous media are negligible.

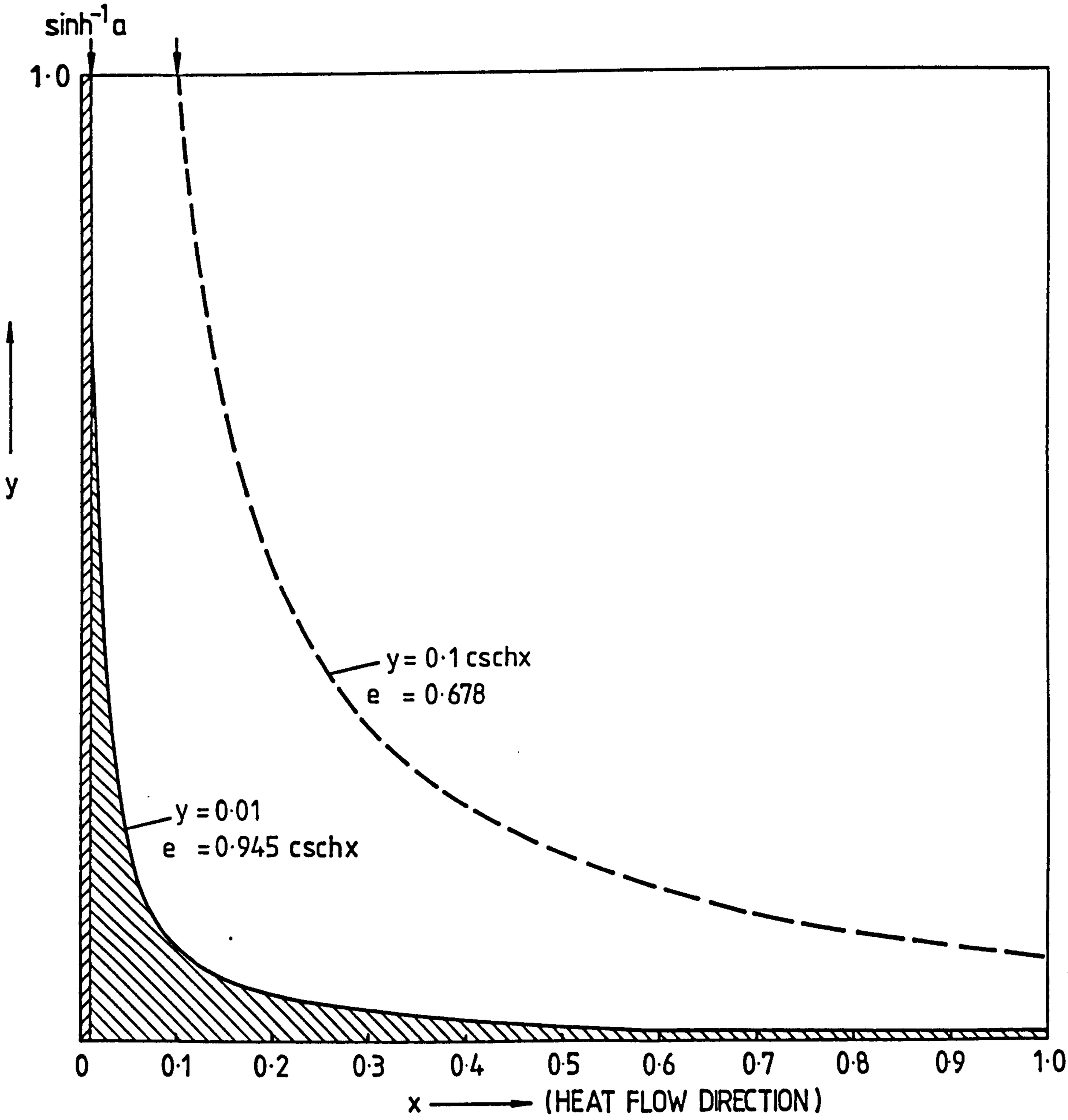

FIG.5. EFFECT OF CHANGING THE CHARACTERISTIC PARAMETER a, i.e. CHANGING THE AMOUNT OF SOLID MATRIX PRESENT.

- The discontinuous material is uniformly distributed throughout the considered specimen, which is therefore thermally isotropic.

The volume fraction of the solid phase can be described (see fig.5) by:-

$$e_s = a \int_{\sinh^{-1}a}^{1} \operatorname{csch} x \, dx + \sinh^{-1} a \qquad \ldots (8)$$

which results in

$$e_s = a \left[\ell n \tanh\left(\frac{1}{2}\right) - \ell n \tanh\left(\frac{\sinh^{-9}}{2}\right) \right] + \sinh^{-1} a \; .. \; (9)$$

The solid phase diminishes as shown in fig.5 and allows the thermal resistance model to be constructed as shown in fig.6.

The resistance network shown in fig.6 will give a total resistivity of:-

$$R_T = R_{S_I} + \frac{1}{1/R_{S_{II}} + 1/R_g} \qquad \ldots (10)$$

where $R_{S_I} = \dfrac{\sinh^{-1}a}{k_s}$

$$R_{S_{II}} = \int_{\sinh^{-1}a}^{1} \frac{dx}{k_s \, a \operatorname{csch} x}$$

and $$R_g = \int_{\sinh^{-1}a}^{1} \frac{dx}{k_g \, (1 - a \operatorname{csch} x}$$

Hence by Solving the integrals

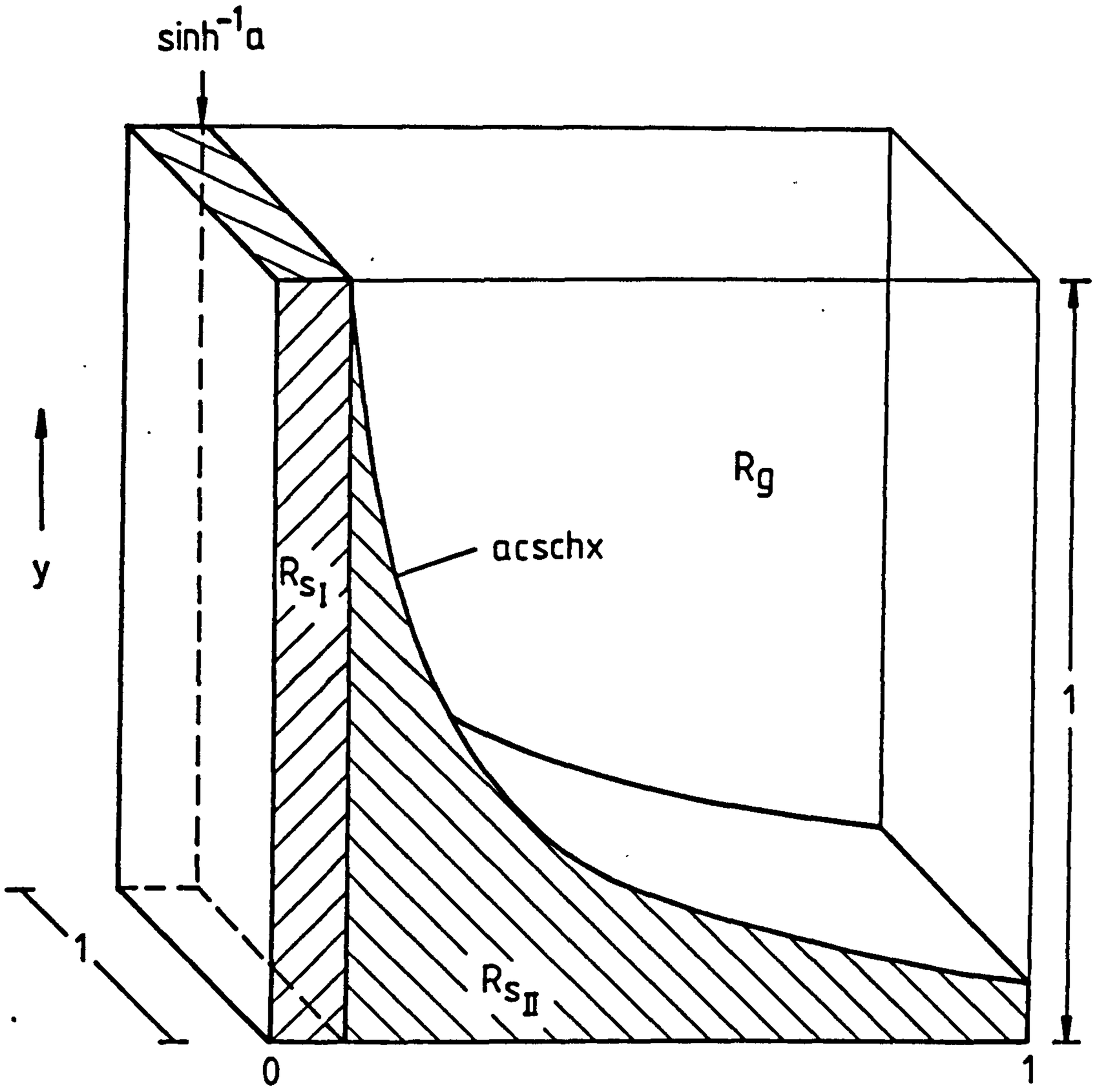

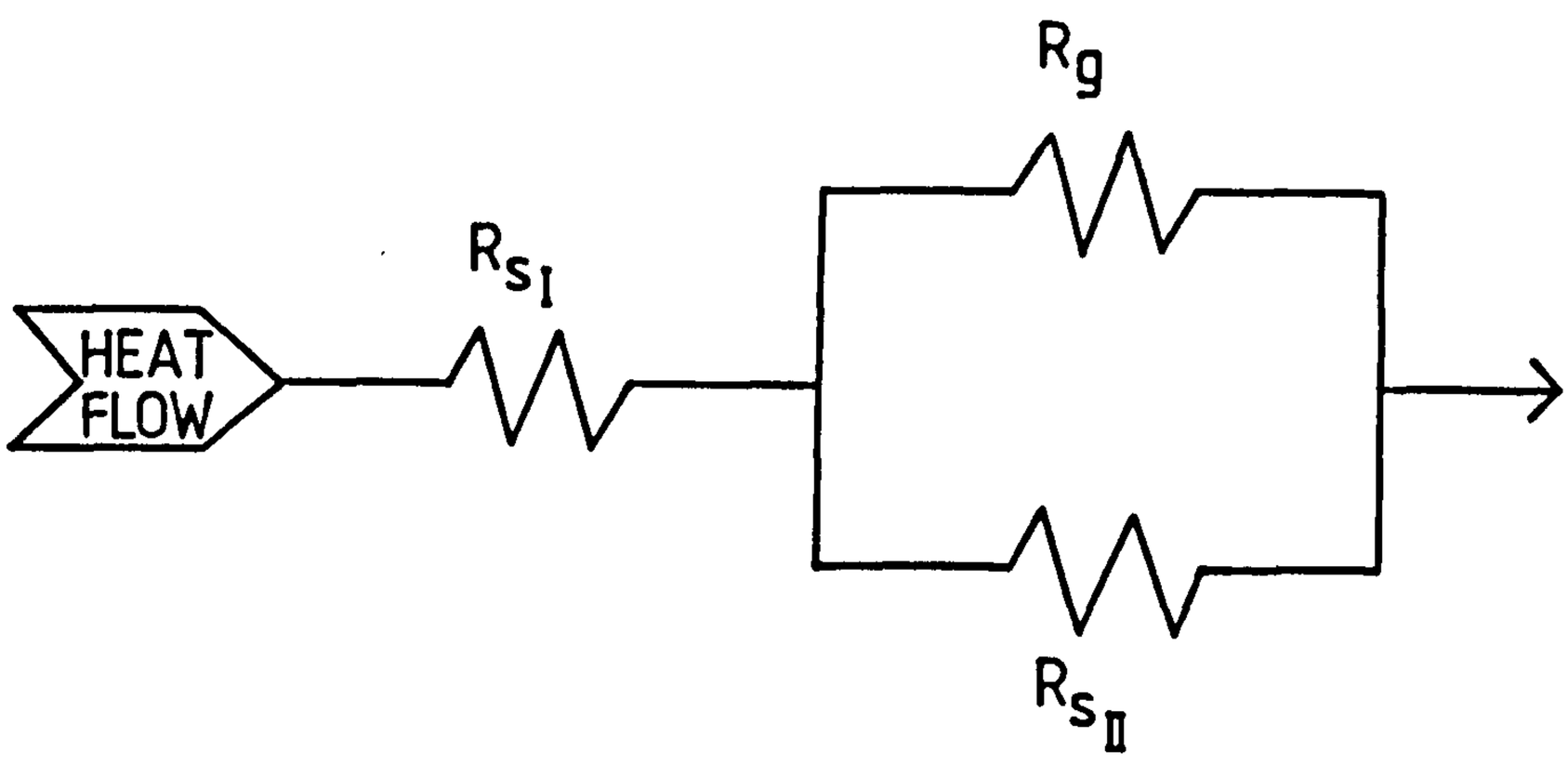

FIG.6. THERMAL RESISTANCE COMPONENTS FOR THE CONSIDERED SPECIMEN.

$$R_T = \frac{\sinh^{-1}a}{k_s} + \frac{1}{\frac{a^{k_s}}{[\cosh 1-\cosh(\sinh^{-1}a)]} + \frac{k_g}{1-\sinh^{-1}a + \frac{a}{\sqrt{1+a^2}} \ell n\left[\frac{(e-e^{\sinh^{-1}a})-a-\sqrt{1+a^2}}{(e-e^{\sinh^{-1}a})-a+\sqrt{1+a^2}}\right]}} \quad \ldots (11)$$

Predictions using this equation are compared with experimental data for high-voidage foams in figs.9 and 10. Generally agreement between the predictions and the experimental measurements is good for specimens with voidages of less than 0.95 provided there are no significant radiation contributions.

Thermal radiation component of heat transfer

Radiant heat transfers through a porous medium may occur by direct transmission through the voids, by scattering, direct transmission through the solid and by absorption and re-radiation. In high porosity insulants, the effect of the radiative component on the overall thermal conductivity will depend on the physical disposition of the solid material, the optical properties and the thickness of the solid component.

The rate of energy emission at a given wavelength is described by Planck's law;

$$q_\lambda = \frac{C_1 \lambda^{-5}}{\exp(C_2/\lambda T) - 1} \quad \ldots (12)$$

where C_1 and C_2 are universal constants;

$C_1 = 3.741 \times 10^{-16}$ $Jm^2 s^{-1}$

and $C_2 = 1.43 \times 10^{-2}$ mK.

The area under the curve of $\dot{q}_\lambda$ versus the wavelength λ is the total rate of emission per unit area of emitter surface as shown in

fig.7. The curve shows a distinct peak of emissive power at a given wavelength which is strongly temperature dependent. For a perfect emitter, i.e. a thermally-black-body, the total rate of emitted radiation is proportional to the fourth power of its absolute surface temeprature, the constant of proportionality being the Stefan-Boltzmann constant, σ. Thus:-

$$\dot{q} = \sigma T^4 \qquad \ldots (13)$$

where $= 5.67 \times 10^{-8}\ Wm^{-2}\ K^{-4}$

A perfect emitter will by definition absorb all the radiation incident upon its surface. In practice surfaces do not behave in this ideal way and the emittance at a given wavelength is generally less than that predicted for a black body. If the surface does not show a strong tendency to high or low emittances at selected wavelengths, it can be assumed to be a grey surface and the absorptivity, α, for incident radiation at a different temperature from the emitting temperature can be considered to be equal to an average emissivity ε. The emissive power per unit surface of a grey body at a temperature T K can be described by the expression

$$\dot{q} = \varepsilon \sigma T^4 \qquad \ldots (14)$$

The radiation process in a cellular material is very complicated; radiant energy being possibly absorbed and re-radiated, transmitted, reflected and scattered during its journey through the material. It can be seen from fig.7 that glass and polystyrene are opaque to the dominent wavelength at ambient temperatures so that transmission through the material will not occur at these temperatures.

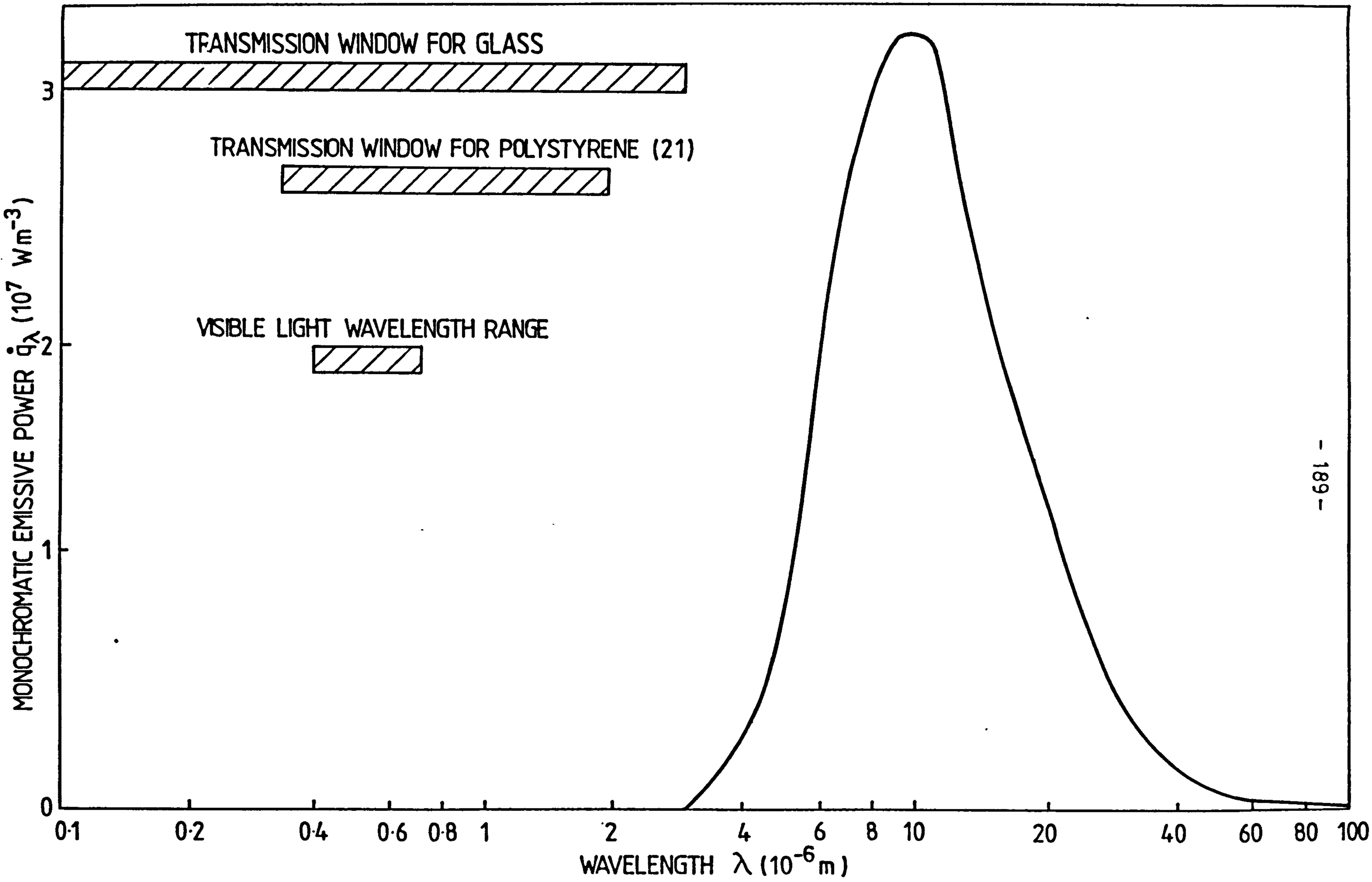

FIG.7. CHARACTERISTIC RADIATION FROM A THERMALLY-BLACK BODY AT 20°C.

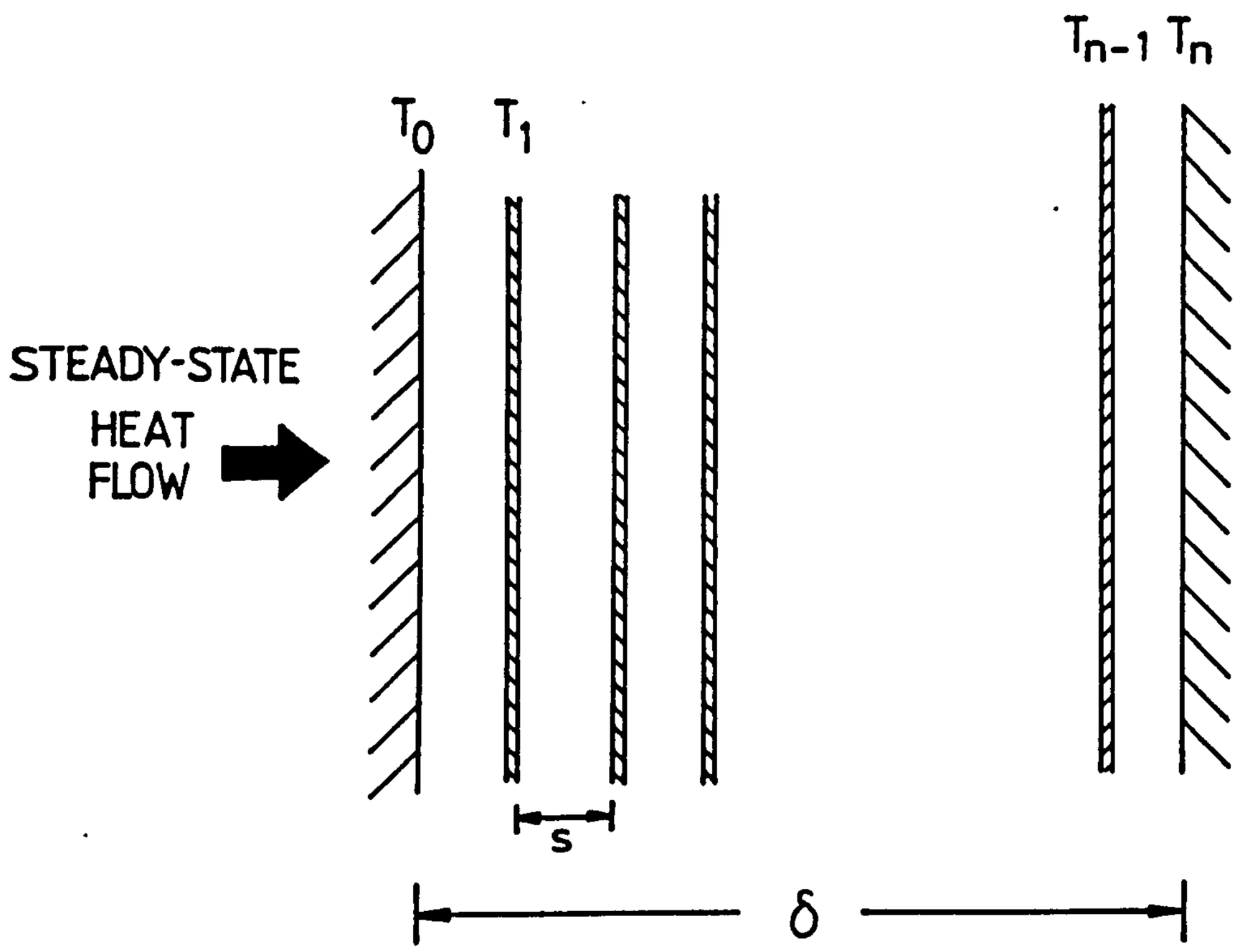

FIG.8. ASSEMBLY OF (n-1) PARALLEL THIN THERMALLY-FLOATING RADIATION SHIELDS.

The cellular, foam materials will be considered as an array of cubes to facilitate the modelling of radiation effects, as shown in Fig.8. It is assumed that the cell walls interacting with the thermal radiation are in layers orthogonal to the direction of heat flow. The boundaries at temperatures T_o and T_n of emissivity ε_c will be considered to behave as grey, non-transparent bodies. All reflected radiation from the parallel surfaces will be assumed to be returned to the emitter. It is shown in standard texts that the steady-state net rate of radiation interchange, $\dot{q}_R$, between two such parallel grey surfaces can be described by

$$\dot{q}_R = \frac{1}{(1/\varepsilon_1) + (1/\varepsilon_2) - 1} \sigma (T_1^4 - T_2^4) \qquad \ldots (15)$$

Consequently the steady-state heat flow through unit area of cellular material, as described by fig.8, would be:-

$$\dot{q}_R = \frac{\sigma(T_o^4-T_1^4)}{(1/\varepsilon)+(1/\varepsilon_c)- 1} = \frac{\sigma(T_1^4-T_2^4)}{(2/\varepsilon_c) - 1} = \ldots = \frac{\sigma T_{n-1}^4-T_n^4}{(1/\varepsilon_c)+(1/\varepsilon) - 1} \qquad \ldots (16)$$

where (n-1) cell walls lie between the boundaries. In order that the heat flux may be described by the boundary temperatures and the surface emissivities alone, the expressions describing the heat transfer between the boundaries and the adjacent walls were added to give the equation,

$$2\dot{q}_R = \frac{\sigma}{\left(\frac{1}{\varepsilon} + \frac{1}{\varepsilon_c}\right) - 1} (T_o^4 - T_1^4 + T_{n-1}^4 - T_n^4) \qquad \ldots (17)$$

while the expressions for the remaining(n-2) cavities were added to give the equation

$$(n - 2)\,\dot{q}_R = \frac{\sigma}{\left(\frac{2}{\varepsilon_C} - 1\right)} \left(T_1^4 - T_{n-1}^4\right) \qquad \ldots (18)$$

These simultaneous equations were added to obtain the expression

$$\dot{q}_R = \frac{\sigma \left(T_o^4 - T_n^4\right)}{\left\{2 \left[\left(\frac{1}{\varepsilon} + \frac{1}{\varepsilon_C}\right) - 1\right] + (n-2)\left(\frac{2}{\varepsilon_C} - 1\right)\right\}} \qquad \ldots (19)$$

which can be re-written in the form

$$\dot{q}_R = \frac{\sigma \quad T_o^4 - T_n^4}{(n-1)\left[\left(\frac{2}{\varepsilon} - 1\right) \frac{1}{n-1} + \left(\frac{2}{\varepsilon_C} - 1\right)\right]} \qquad \ldots (20)$$

where n is the number of voids in the heat flow direction and equals δ/s, see fig.8. If it is assumed that the difference between the absolute temperatures T_o and T_n is small compared with their values, then the radiative component of the apparent thermal conductivity may be written in terms of the mean temperature T_m, i.e.

$$k_R = \frac{4\sigma\,\delta\,T_m^3}{\left[\left(\frac{2}{\varepsilon} - n\right) + \left(2\frac{(n-1)}{\varepsilon_C}\right)\right]} \qquad \ldots (21)$$

The apparent thermal conductivity will be the sum of the conductive and radiative components. i.e.,

$$k = \frac{1}{\frac{\sinh^{-1}a}{k_s} + \frac{1}{\frac{a\,k_s}{\cosh 1-\cosh(\sinh^{-1}a)} + \frac{k_g}{1-\sinh^{-1}a + \frac{a}{\sqrt{1+a^2}}\,\ell n\left[\frac{(e-e^{\sinh^{-1}a})-a-\sqrt{1+a^2}}{(e-e^{\sinh^{-1}a})-a+\sqrt{1+a^2}}\right]}}}$$

$$+ \frac{4\,\sigma\,\delta\,T_m^{\,3}}{\left[\left(\frac{2-n}{\varepsilon}\right) + 2\left(\frac{n-1}{\varepsilon_c}\right)\right]} \qquad \ldots (22)$$

Predictions utilising equation (23) are compared with experimetnal data from various sources in fig.9 for air-filled polystyrene foam, and in figure 10 for polyurethane foam filled with an assumed gas mixture of fluorocarbon and air. The thermal conductivity of this gas mixture was calculated using the data of Norton (21) for mixtures of trichlorofluoromethane (C $C\ell_3F$) and air. That study showed that a linear relationship exists between the reciprocol of the thermal conductivity and the volume fraction of fluorocarbon (C $C\ell_3F$), viz

$$k_g = \frac{1}{40 + 79f} \qquad \ldots (23)$$

where f is the volume fraction of the fluorocarbon gas in the mixture, which is at an average temperature of $20^{o}C$. The thermal conductivity of the air and fluorocarbon (C $C\ell_3F$) are 0.025 $Wm^{-1}K^{-1}$ (19) and 0.0084 $Wm^{-1}K^{-1}$ (22) respectively.

Gas compositions within the cells of polyurethane foams change with time. The low initial apparent thermal conductivities occur when the cells are completely filled with fluorocarbon. Oxygen and

nitrogen very rapidly diffuse into the cells of unprotected foams, i.e. into foam slabs not covered with membranes, thereby increasing their apparent thermal conductivities. Further reductions in the apparent thermal conductivity occur as the fluorocarbon dissolves in the solid cellular material. It was considered by Brandreth (24) that the initial pressure of the fluorocarbon in the cells is 0.6 atmospheres. In an earlier publication (23) figures were given for the percentage of fluorocarbon dissolved in the polymer matrix for eleven samples of foam. From this data, an average fluorocarbon cell gas percentage has been assessed to be 0.66 of the total fluorocarbon. The volume fraction of fluorocarbon, f, utilised in equation (24) was thus taken as 0.396 (i.e. 0.6 x 0.66) for the calculation of the cell gas thermal conductivity. The remaining cell gas was, for simplicity, considered to be air. This procedure resulted in a cell gas thermal conductivity of 0.014 $Wm^{-1}K^{-1}$, which was utilised to obtain the theoretical curve of fig.10.

The radiative components of the theoretical curves were calculated utilising the cell size as denoted in fig.9 and as shown in table 1 for fig.10.

Porosity	Assumed cell size mm.
0.985	1.5
0.970	1.0
0.960	0.5
0.945	0.5

Table 1.

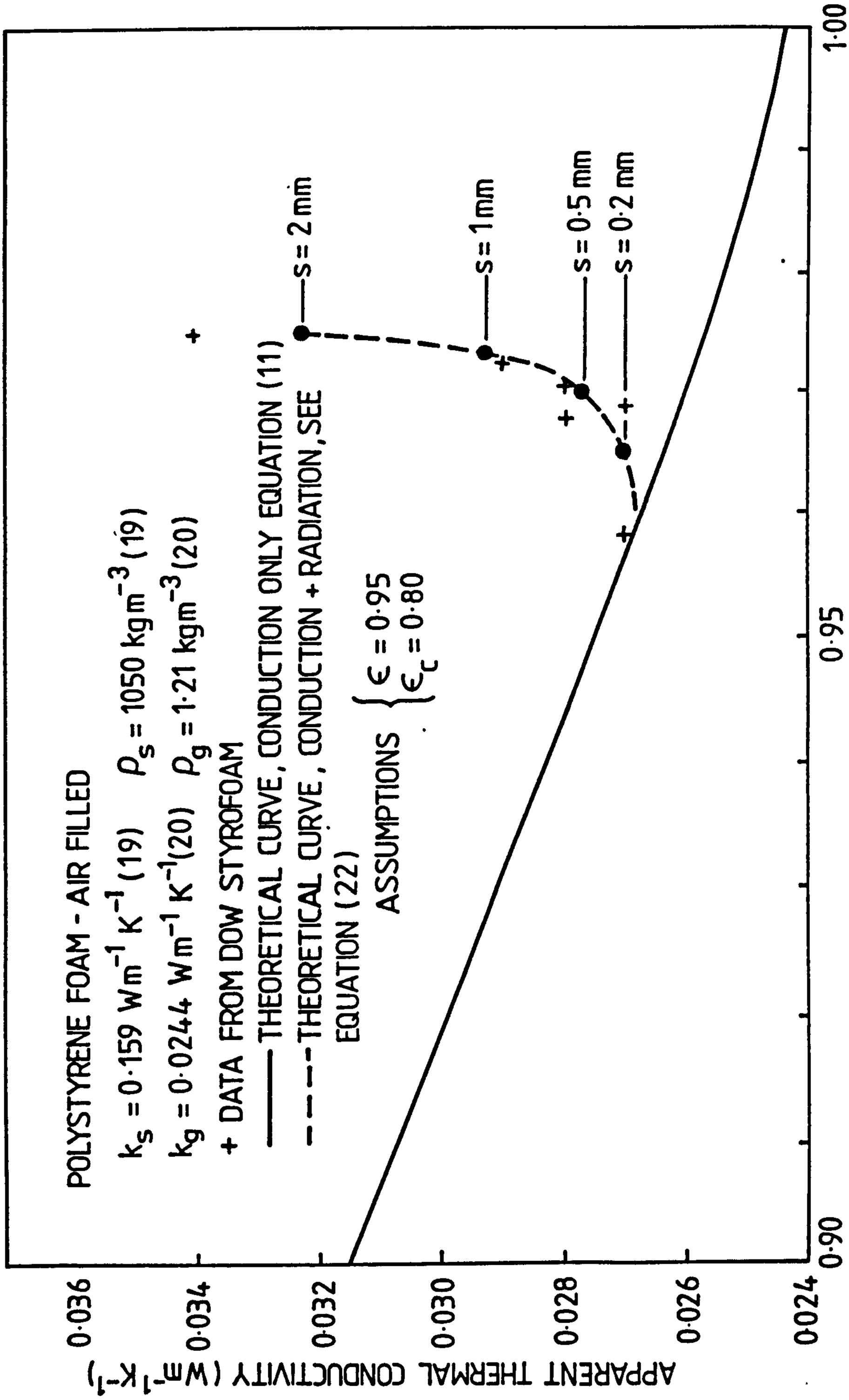

FIG.9. THERMAL CONDUCTIVITY OF AIR-FILLED POLYSTYRENE FOAM AT 10°C.

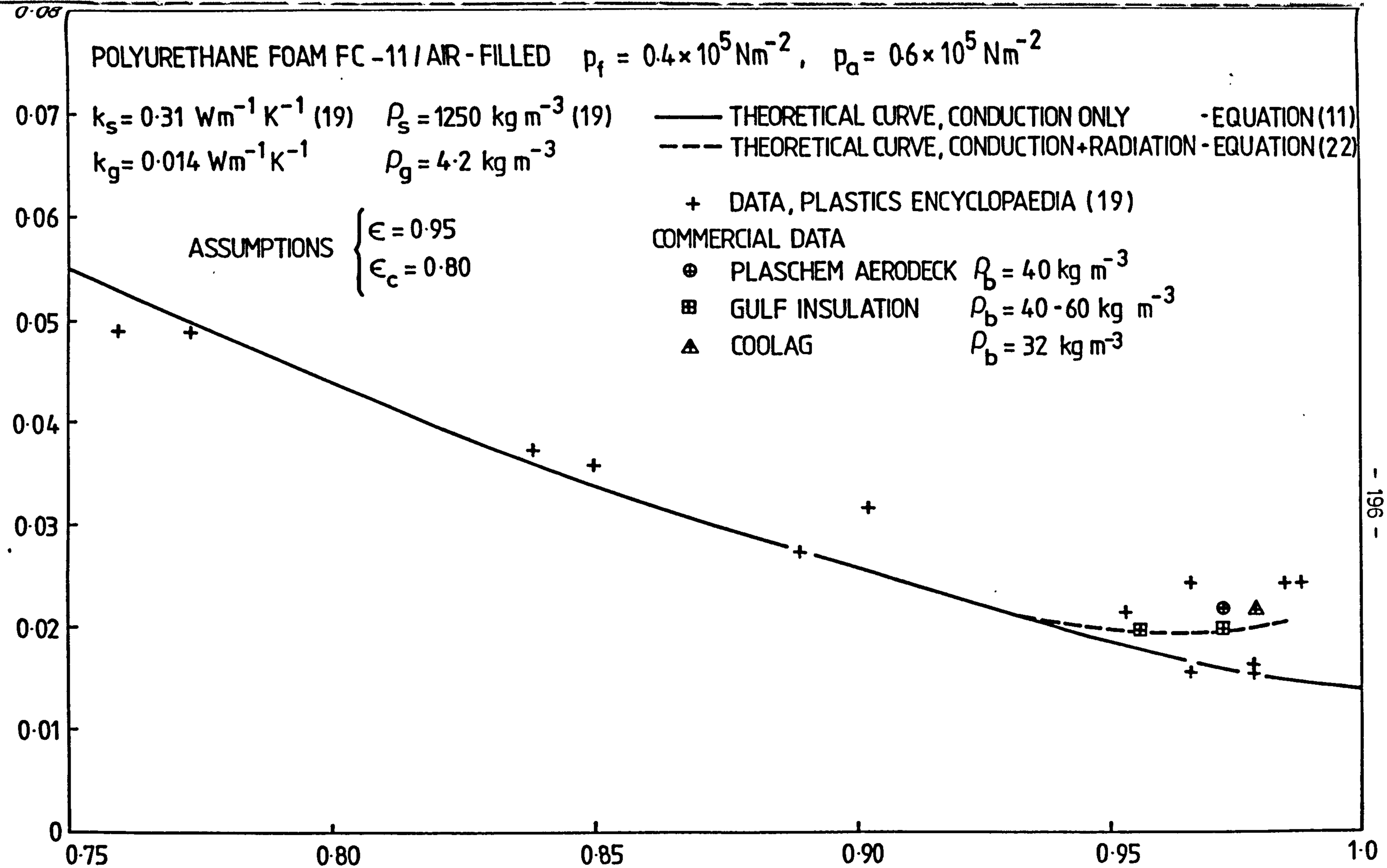

FIG. 10. THERMAL CONDUCTIVITY OF POLYURETHANE FOAM AT 20°C.

These assumptions were not considered unreasonable as cell sizes for polyurethane foams of porosity 0.97 → 0.98 range from 0.4 to 0.8 mm.

Discussion

The theory developed agrees well with published experimental data. In the case of polyurethane foams, a good match occurs even for porosities as low as 0.75. At porosities exceeding 0.98, the theoretical model does not lead to predicted values of the same order as the experimental data unless large cell sizes are assumed. Although cell sizes would be expected to increase as the fraction of solid phase becomes very small, it is also possible that the proportion of open cells would also increase which would effectively increase the overall air content of the assumed gas mixture thus increasing the conductive component of the apparent thermal conductivity. The onset of convective effects is more likely if several cells join together to enclose a space of 5 mm or more nominal diameter. Such open spaces would also facilitate radiative heat transfer.

REFERENCES

1. J.C. Maxwell — "A Treatise on Electricity and Magnetism", Clarendon Press, Oxford, Vol. 1, 3rd Ed'n, pp. 435-441, 1904.

2. J.A. Reynolds and J.M. Hough — "Formulae for dielectric constant of mixtures", Proc. Phys. Soc. 70, 8, pp.769-775, 1957.

3. H.W. Russell — "Principles of heat flow in porous insulants", J.Amer.Chem.Soc., 18, 1, pp.1-5, 1935.

4. W. Woodside — "Calculation of the thermal conductivity of porous media", Canadaian Journal of Physics, 36, pp.815-823, 1958.

5. A. Sugawara and Y. Yoshizawa — "An investigation on the thermal conductivity of a porous material and its application to porous rock", Australian Journal of Physics, 14, pp. 469-480, 1961.

6. A. Sugawara and Y. Yoshizawa — "An experimental investigation on the thermal conductivity of consolidated porous materials" Journal of Applied Physics, 33, 10, pp.3135-3138, 1962.

7. W. Woodside and J.H. Messmer — "Thermal conductivity of porous media. I. Unconsolidated sands. II. Consolidated Rocks" Journal of Applied Physics, 32, 9, pp.1688-1706, 1961.

8. M.R.J. Wyllie and P.F. Southwick — "An experimental investigation of the S.P. and resistivity phenomena in dirty sands" Journal of Petroleum Technology 6, pp.44-57, 1954.

9. R.L. Hamilton and O.K. Crosser — "Thermal conductivity of heterogeneous two-component systems", Industr ial and Engineering Chemistry, 1, 3, pp.187-191, 1962.

10. A.D. Brailsford and K.G. Major — "The thermal conductivities of aggregates of several phases, including porous materials", British Journal of Applied Physics, 15, pp. 313-319, 1964.

11. D.R. Flynn — "Thermal conductivity of ceramics" N.B.S. Special Publication 303, Mechanical and Thermal Properties of Ceramics Symposium, Gaithersburg, Maryland, pp. 63-113, 1968.

12. C.G. Bankvall — "Heat transfers in fibrous materials" National Swedish Building Research, Document, D4, Lund Institute of Technology, 1972.

13. H.M. Strong, F.P. Bundy and H.P. Bovenkerk — "Flat panel vacuum thermal insulation" J. Applied Physics, 31, 1, pp.39-50, 1960.

14. A.V. Luikov, A.G. Shashkov L.L. Vasilev and YU.E. Fraiman — "Thermal conductivity of porous systems", Int. J. of Heat and Mass Transfer, 11, pp. 117-140, 1968.

15. G. T-N. Tsao — "Thermal conductivity of two-phase materials" Industrial & Engineering Chemistry, 53, 5, pp. 395-397,

16. S.C. Cheng and R.I. Vachon — "The prediction of the thermal conductivity of two- and three-phase solid heterogeneous mixtures", Int. J. Heat Mass Transfer, 12, pp. 249-264, 1969.

17. S.C. Cheng and R.I. Vachon — "A technique for predicting the thermal conductivity of suspensions, emulsions and porous material" Int. J. Heat Mass Transfer, 13, pp.537-546, 1970.

18. J, Agranoff (Editor) — "Modern Plastics Encyclopaedia" 1976-77, Volume 53, No.10, McGraw Hill, New York, 1976.

19. K. Raznjevie — "Handbook of Thermodynamic Tables and Charts" Hemisphere Publishing Corporation, Washington, 1976.

20. ANON — "Insulation Handbook" Comprint Ltd., Watford, 1981.

21. F.J. Norton — "Thermal conductivity and life of polymer foams", Journal of Cellular Plastics, 3, pp.23-37, 1967.

22. Anonymous — "Freon Fluorocarbons Properties and Applications", Dupont Freon Product, Information Bulletin B-2E.

23. D.A. Brandreth and H.G. Ingersoll — "Accelerated ageing of rigid polyurethane foam", European Journal of Cellular Plastics, pp. 134-143, 1980.

24. D.A. Brandreth — "Factors influencing the ageing of rigid polyurethane foam", J. of Thermal Insulation, 5, pp. 31-39, 1981.

CONCLUSIONS

The thermal properties of building materials in use differ widely from those quoted by manufacturers. Therefore, the procurement of reliable thermal data is of the utmost importance if computer predictions of the thermal behaviours of structures are to be realistic.

The thermal-probe technique has been shown to be a reliable, rapid and accurate method for the measurement of both dry and moist materials.

It is essential that care is taken when designing the instruments to ensure that potential errors due to heat losses along the probes' axes are reduced to acceptable levels. The theoretical assessment of these losses, as derived by Blackwell (Chapter 4-(8)) has been shown to be adequate for probe designs in the materials studies.

The hot-wire technique in its present form is inadequate for the measurement of the apparent thermal conductivities of fibrous insulants. This is due to the inhomogenous nature of the material and its transparency to thermal radiation at high porosities (i.e. > 95%).

The view that the measured thermal conductivities of insulants are constant has been shown to be incorrect. Studies of the temperature distributions through loose-fill insulants show that the temperature gradient is not constant throughout the insulant depth. Experimental results demonstrate that the thermal conductivity of a horizontal layer of loose-fill insulant heated from below increases with the insulant thickness. Convection was seen to occur in the top surface layers of the insulant, thus explaining the disturbance of the temperature gradient in this region of the insulant thickness.

It is essential that further work continues to establish the accuracy of the apparatus used to study these temperature gradients and to extend the range of materials investigated. Such data would then allow more realistic assessments to be made for the economic thickness of horizontal insulant layers.

A model to predict the apparent thermal conductivity of cellular insulants which includes the effects of radiant heat transfers has been shown to describe adequately the values of this parameter for air-filled polystyrene foams and air/fluorocarbon-filled polyurethane foams.